Soft Open Points for the Operation of Medium Voltage Distribution Networks

Wanyu Cao

School of Engineering

Cardiff University

A thesis submitted for the degree of

Doctor of Philosophy

October, 2015

Acknowledgement

I would like to express my heartfelt gratitude to my supervisor, Prof. Jianzhong Wu, for being the source of inspiration, advice and encouragement throughout my research study. In addition, his patience and continuous guidance in improving my writing ability is of great value to me and my future academic life.

I would like to express my sincere gratefulness to my supervisor Prof. Nick Jenkins, CIREGS' leader, for his invaluable assistance, guidance and constructive criticism in conducting my research and developing this thesis.

I would like to thank Dr. Jun Liang and Sheng Wang for their kind support and suggestions during the research study, especially in the power electronics filed.

I would like to thank Dr. Chao Long, Dr. Cheng Meng and Dr. Lee Thomas who proofread my thesis and also suggested many improvements to the content.

I thank Cardiff University for giving the opportunity to pursue my research studies for a PhD. I thank, North China Electric Power University, Cardiff University, EPSRC and OPEN project, UK for funding my research study.

I thank all my friends and colleagues who helped in many ways during my stay in Cardiff.

Finally, I would like to express my deepest thanks to my family for their endless encouragement, understanding, patience and support all the while.

Declaration

This work has not previously been accepted in substance for any degree and is not concurrently submitted in candidature for any other higher degree.

Signed:……..(Candidate) Date:…….

Statement 1

This thesis is being submitted in partial fulfilment of the requirements for the degree of ……..(insert as appropriate PhD, MPhil, EngD)

Signed:……..(Candidate) Date:…….

Statement 2

This thesis is the result of my own independent work/investigation, except where otherwise stated. Other sources are acknowledged by explicit references.

Signed:……..(Candidate) Date:…….

Statement 3

I hereby give consent for my thesis, if accepted, to be available for photocopying, inter-library loan and for the title and summary to be made available to outside organisations.

Signed:……..(Candidate) Date:…….

Copyright

Abstract

Soft Open Points (SOPs) are power electronic devices installed in place of normally-open points in electrical power distribution networks. They are able to provide active power flow control, reactive power compensation and voltage regulation under normal network operating conditions, as well as fast fault isolation and post-fault supply restoration under abnormal conditions. The use of SOPs for the operation of medium voltage (MV) distribution networks was investigated. Three aspects were studied, which include the control of an SOP, benefit analysis of using SOPs and distribution network voltage control with SOPs.

Two control modes for the operation of an SOP, which is based on back-to-back voltage source converters (VSCs), were developed. The operating principle and performance of the back-to-back VSC based SOP under both normal and abnormal network operating conditions were analysed. It was found that during the change of network operating conditions, smooth transitions between the two controls modes were needed. Using soft cold load pickup and voltage synchronization processes can achieve the smooth mode transitions.

A steady state analysis framework to quantify the operational benefits of a MV distribution network with SOPs was developed, which considers feeder load balancing, power loss minimization and voltage profile improvement. The framework also considered traditional network reconfiguration and the combination of both SOP control and network reconfiguration to quantify the benefits. It was found that in the case study using only one SOP can achieve a similar improvement in network operation compared to the case of using network reconfiguration with all branches equipped with remotely controlled switches. The combination of both SOP control and network reconfiguration can achieve the optimal network operation.

A coordinated voltage control strategy for active distribution networks with SOPs was developed considering the control of SOP, the on-load tap changer (OLTC) and distributed generation (DG) units. Multiple objectives were considered, which include maintaining network voltages within the specified limits, mitigating DG active power curtailment, reducing the tap operations of the OLTC and the network power losses. The proposed control strategy is based on a distributed control framework where each control device is considered as a local control agent. A priority-based coordination method is applied on the local control agents to obtain a trade-off among the objectives based on their prioritisation. It was shown that, comparing with centralized control strategies, the proposed control strategy can provide reliable distribution network voltage control with less communication investments, reduced computation burden and fewer data exchanges. It was also found that the SOP played a key role of compensating for the OLTC control, avoiding unnecessary DG active power curtailment, reducing the number of tap operations and network power losses as well as reducing the amount of reactive power support from DG units for voltage control.

Contents

Acknowledgement ..... **ii**

Declaration ..... **iii**

Copyright ..... **iv**

Abstract ..... **v**

Contents ..... **vii**

List of Figures ..... **xi**

List of Tables ..... **xv**

Nomenclature ..... **xvi**

Chapter 1 - Introduction **1**

1.1 Background 2

1.1.1 Climate Change and Renewable Generation 2

1.1.2 Electricity Demand Growth 4

1.1.3 Emergence of Smart Grid Concept 5

1.2 Research Motivation 7

1.2.1 Control of an SOP 9

1.2.2 Benefits analysis of using SOPs 9

1.2.3 Distribution network voltage control with SOPs 10

1.3 Objectives and Contributions of this Thesis 11

1.4 Thesis Outline 12

Chapter 2 - Literature Review **14**

2.1 Challenges for Distribution Network Operation 15

2.1.1 Aging Assets and Lack of Circuit Capacity 15

2.1.2 Operational Constraints 16

2.1.3 Reliability and Efficiency of Supply 17
2.2 Network Operation Functions 18
2.2.1 Network Reconfiguration 19
2.2.2 Coordinated Voltage Control 20
2.2.3 Operation Functions Offered by Power Electronic devices 25
2.3 Soft Open Points 27
2.3.1 Benefits of Soft Open Points 27
2.3.2 Types of Soft Open Points 28
2.3.3 Previous Soft Open Points Studies 31
2.4 Summary 33
Chapter 3 - Control of a Back-to-Back VSC based SOP 35
3.1 Introduction 36
3.2 Back-to-Back VSC based SOP 36
3.3 Control Modes of the Back-to-Back VSC based SOP 38
3.3.1 Power Flow Control Mode 38
3.3.2 Supply Restoration Mode 40
3.4 SOP Operation in MV Distribution Networks 42
3.4.1 Normal Conditions 43
3.4.2 During Fault Conditions 45
3.4.3 Post-fault Supply Restoration Conditions 49
3.5 Summary 57
Chapter 4 - Benefits Analysis of SOPs for MV Distribution Network Operation .. 59
4.1 Introduction 60
4.2 Modelling of Soft Open Points 60

4.2.1 Physical Limitations of Back-to-Back Converters 62
4.2.2 Internal Power Losses of Back-to-Back Converter 63
4.3 Optimal Operation of the Soft Open Points 65
4.3.1 Problem Formulation 65
4.3.2 Method of Determining Optimal SOP Operation 67
4.4 Network Reconfiguration Considering SOPs 73
4.5 Case Study 74
4.5.1 Improve Network Performances Using SOPs 75
4.5.2 Improve Network Performance Considering both SOP and Network Reconfiguration 78
4.5.3 Impact of DG Connections 82
4.5.4 Impact of the SOP Device Losses 85
4.6 Summary 87
Chapter 5 - Voltage Control in Active Distribution Networks with SOPs 89
5.1 Introduction 90
5.2 Voltage Control Framework 90
5.2.1 Voltage Profile Estimation 91
5.2.2 Proposed Voltage Control Framework 96
5.3 Coordinated Voltage Control Strategy 99
5.3.1 Effectiveness of SOP on Voltage Control 99
5.3.2 Priority-Based Coordination 105
5.3.3 Implementation procedures of the information-sharing platform 115
5.4 Discussion: Benefits of the Proposed Control Strategy 116
5.5 Case Study 117

5.5.1 Voltage Profile Estimation 119

5.5.2 Coordinated voltage control using OLTC and SOP 121

5.5.3 Coordinated voltage control using OLTC, SOP and DG 125

5.6 Summary 130

Chapter 6 - Conclusions and Future Work 132

6.1 Conclusions 133

6.1.1 Control of a Back-to-Back VSC based SOP 133

6.1.2 Benefit Analysis of SOPs for MV Distribution Network Operation 134

6.1.3 Voltage Control in Active Distribution Networks with SOPs 135

6.2 Future 136

6.2.1 Use of other control strategies for the operation of the back-to-back VSC based SOP 136

6.2.2 Performances of the back-to-back VSC based SOP considering different load types 137

6.2.3 Impacts of SOPs on feeder automation 137

6.2.4 Use of SOPs in unbalanced three-phase distribution networks 138

6.2.5 Economic analysis of SOPs in MV distribution networks 138

Reference 140

Publications 148

Appendix A: Data for the Two-Feeder Test Network 149

Appendix B: Data for the Four-Feeder Test Network 151

List of Figures

Figure 1.1: The UK Renewable Energy Target [5] 3
Figure 1.2: World Electricity Consumption by Region [9] 4
Figure 1.3: Critical developments for UK smart grid routemap out to 2050 [17] 7
Figure 2.1: Three-feeder example network: (a) before network reconfiguration; (b) after network reconfiguration [27] 19
Figure 2.2: Cascaded control architecture for centralized coordination [48] 23
Figure 2.3: Coordination among three control agents via two ways communication [41] 25
Figure 2.4: Simple distribution network: option A representing a NOP connection and B representing an SOP [67] 27
Figure 2.5: Topologies of different types of SOPs [70] 29
Figure 3.1: (a) Basic configuration of a distribution network with an SOP; (b) Main circuit topology of the back-to-back VSC based SOP. 37
Figure 3.2: Control block diagram of the SOP for power flow control mode: (a) outer power control loop; (b) inner current control loop; (c) PLL controller 40
Figure 3.3: Control block diagram of the interface VSC for supply restoration control mode 41
Figure 3.4: Two-feeder MV distribution network with a back-to-back VSC based SOP 42
Figure 3.5: Transient response of the power flow control mode to step changes in active and reactive power references: (a) DC side voltage; (b) reactive power response of VSC1; (c) active power response of VSC2; (d) reactive power response of VSC2 44
Figure 3.6: SOP response for a three-phase fault at t=1s and blocked at t=1.2s: (a) output voltage (left) and current (right) on the faulted side VSC; (b) output voltage (left) and current (right) on the un-faulted side VSC; (c) power flow behaviour on both VSCs 47
Figure 3.7: SOP response for a single-phase to ground fault at t=1s and blocked at

t=1.2s: (a) output voltage (left) and current (right) on the faulted side VSC; (b) output voltage (left) and current (right) on the un-faulted side VSC; (c) power flow behaviour on both VSCs 49
Figure 3.8: Control mode transition system 50
Figure 3.9: Results of a hard transition to supply restoration mode at t=2.2s: (a) output voltage waveform of the faulted side VSC; (b) output current waveform 51
Figure 3.10: Output current waveforms of the faulted side VSC for a hard transition to supply restoration mode with: (a) an inductance connecting to Bus 17; (b) a capacitance connecting to Bus 17 52
Figure 3.11: Results of a smooth transition to supply restoration mode at t=2.2s: (a) output voltage waveform of the faulted side VSC; (b) output current waveform 53
Figure 3.12: Results of a hard transition to power flow control mode at t=3s: (a) output voltage waveform of the faulted side VSC; (b) output current waveform 54
Figure 3.13: Synchronisation controller 55
Figure 3.14: Voltage synchronisations for reconnection: (a) phase synchronisation; (b) magnitude synchronisation 56
Figure 3.15: Results of a smooth transition to power flow control mode: (a) output voltage waveform of the faulted side VSC; (b) output current waveform 57
Figure 4.1: (a) Simple distribution network with an SOP; (b) Power injection model of SOP for distribution network power flow control 61
Figure 4.2: Comparison between the quadratic and approximate loss estimation function 64
Figure 4.3: Flow chart of the proposed PDS method 68
Figure 4.4: Example of one SOP optimization by PDS method 71
Figure 4.5: Flowchart of proposed network reconfiguration considering SOPs 73
Figure 4.6: 33-bus distribution network [99] 74
Figure 4.7: Impact of different number of SOP installation on power loss minimization and voltage profile improvement 76
Figure 4.8: Impact of different number of SOP installation on load balancing and

voltage profile improvement 77
Figure 4.9: Voltage profiles of the network under normal loading condition 80
Figure 4.10: Results of load balancing capability and relevant voltage profile improvement under different methods 82
Figure 4.11: Voltage profiles of the network under different cases with DG connection 83
Figure 4.12: Results of load balancing capability and relevant voltage profile improvement under different cases with DG connections 85
Figure 4.13: Impacts of the SOP device losses on total network power losses 87
Figure 5.1: Voltage profiles of an MV feeder with and without DG..... 91
Figure 5.2: An MV feeder with segments for the minimum voltage estimation..... 92
Figure 5.3: A part of distribution feeder..... 93
Figure 5.4: Voltage estimation using simplified method..... 95
Figure 5.5: Distributed voltage control framework..... 96
Figure 5.6: Interior structure of a local control agent 97
Figure 5.7: Details of local measurements..... 98
Figure 5.8: Radial distribution feeder 99
Figure 5.9: Two-feeder MV distribution network..... 101
Figure 5.10: Voltage profiles of both feeder before voltage control 102
Figure 5.11: Voltage profiles with SOP voltage control: (a) active power control method; (b) reactive power control method 103
Figure 5.12: Comparison of the network active power losses 104
Figure 5.13: Priority-based coordination of the multiple local control agents 105
Figure 5.14: Prioritisation of the proposed objectives from high (H) to low (L)..... 106
Figure 5.15: Flow chart of the proposed priority-based coordination 107
Figure 5.16: The four-feeder MV test network..... 118
Figure 5.17: Normalized profiles of a weekend and weekday: (a) loads; (b) DGs..... 118
Figure 5.18: Per unit maximum and minimum voltage profile over the studied period at (a) feeder 1; (b) feeder 2; (c) feeder 3; (d) feeder 4 120

Figure 5.19: Per unit voltage profile at 11am in the first studied day along (a) feeder 1; (2) feeder 2; (3) feeder 3; (4) feeder 4 121
Figure 5.20: maximum and minimum voltage profiles at different control schemes .. 122
Figure 5.21: Change of the tap operation at different control schemes 123
Figure 5.22: Total network losses at different control schemes 124
Figure 5.23: Apparent power requirements for different SOP control schemes 125
Figure 5.24: maximum and minimum voltage profiles when increase DG penetration 126
Figure 5.25: maximum and minimum voltage profiles with increased DG penetration by coordinated control with and without involving SOP 127
Figure 5.26: Total active power generated with increased DG penetration by coordinated control with and without involving SOP 127
Figure 5.27: Change of the tap operation with increased DG penetration at different cases. 128
Figure 5.28: Total network losses with increased DG penetration 128
Figure 5.29: Power settings with increased DG penetration: (a) apparent power settings of the SOP, (b) reactive power settings of the PV DG unit 129

List of Tables

Table 3.1: Parameters of the Back-to-back VSC Based SOP 42

Table 4.1: System Load Balancing Index with Different Number of SOP Installation . 76

Table 4.2: Results of Computing Time for Optimal SOP Operation 78

Table 4.3: Results of Different Methods for System Power Loss 79

Table 4.4: Results of Different Methods for Load Balancing 81

Table 4.5: Results of Different Methods for Power Loss Minimization with DG Connections 83

Table 4.6: Results of Different Methods for Load Balancing with DG Connections 84

Table 5.1: Data of the Load and DG 118

Table A.1 Network Parameters for the SOP study in Chapter 5 149

Table B.1 Network Parameters for the Case study in Chapter 5 151

Nomenclature

List of abbreviations

AC	Alternative Current
CI	Customer Interruptions
CML	Customer Minutes Lost
DC	Direct Current
DG	Distributed Generation
DMS	Distribution Management System
DNO	Distribution Network Operator
DVR	Dynamic Voltage Restorer
d-q	Direct-Quadrature
EV	Electric Vehicles
FACTS	Flexible AC Transmission Systems
GA	Genetic Algorithm
GHG	Greenhouse Gas
HVDC	High-voltage DC Transmission System
ICT	Information and Communication Technologies
IGBT	Insulated Gate Bipolar Transistor
LBI	Load Balance Index
MPPT	Maximum Power Point Tracking
MV	Medium Voltage
NOP	Normally Open Point

OFGEM	Office for Gas and Electricity Market
OLTC	On-Load Tap Changer
PDS	Powell’s Direct Set
PI	Proportional Integral
PLL	Phase Locked Loop
PV	Photovoltaics
PWM	Pulse Width Modulation
SCADA	Supervisory Control and Data Acquisition
SOP	Soft Open Point
STATCOM	Static synchronous compensator
UPFC	Unified Power Flow Controller
VSC	Voltage Source Converter

Chapter 1

Introduction

THIS chapter introduces the background, motivation, objectives, and contributions of this thesis. An outline of the thesis is also provided.

1.1 Background

Electric power systems, after several years of slow development, are experiencing tremendous changes. In response to environmental and climate change, renewable generation is expected to play an important role in future power generation systems. The continuous development of economy as well as large-scale integration of electrified heating and transport are leading to increased demand for electricity. To tackle the inadequacies of current electricity grid, more intelligence is required in the grid for the sake of security, economy and efficiency thus allowing the emergence of the smart grid concept.

1.1.1 Climate Change and Renewable Generation

Global climate change resulting from greenhouse gas (GHG) emissions has had observable effects on the environment, such as loss of sea ice, frequent wildfires and more intense heat waves [1].

Over the past decades, worldwide efforts have been made in preventing the climate change. In 1997, more than 160 countries were gathered in Kyoto to discuss the solutions and signed an agreement, named ”Kyoto Protocol”, in order to reduce the emissions of GHG (carbon dioxide (CO2), methane (CH4), nitrous oxide (N2O)) to at least 5% below 1990 level during the commitment period of 2008 -2012 [2]. In 2012, a new deal to extend the Kyoto Protocol was agreed by nearly 200 countries, continuing cutting the GHG emissions during the 2013- 2020 period. In 2009, the European Commission ratified an agreement, named renewable Energy Directive, targeting a 20 % reduction of GHG emissions by 2020 compared with 1990 level for the European Union (EU) member countries. In addition, a long-term goal was established to cut its emissions substantially by 80-95% compared to 1990 by the end of 2050 [3].

The UK government has also committed to the reduction of GHG emissions targeting

at both international and EU level. The government has targeted a reduction of CO_2 emissions of 34% (below 1990 level) by 2020 and at least 80% by 2050. In order to meet these targets, a number of steps have been taken. The carbon budgets are used to make sure the UK is on track [4]. The impact of these regulatory schemes has been enhancing the use of renewable energy and the 'clean' generation technologies. Figure 1.1 presents an illustrative breakdown of the final shares of different types of renewable sources and technologies in the UK in 2020 [5].

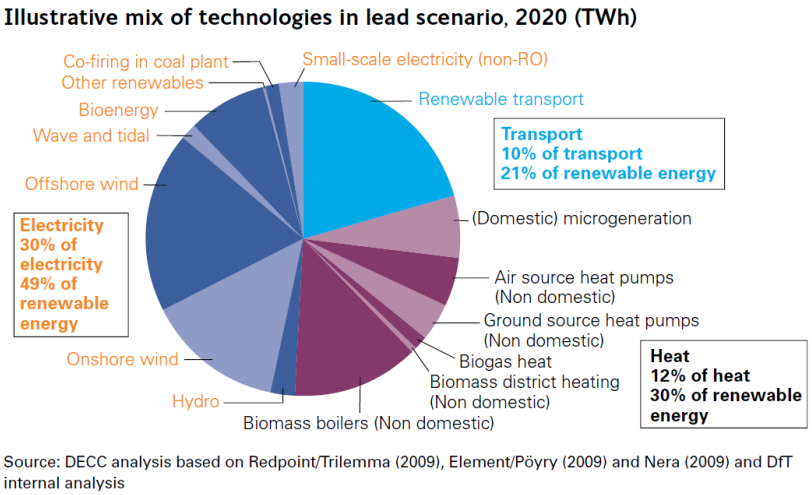

Figure 1.1: The UK Renewable Energy Target [5]

The overall targeted increase in the amount of energy generated from renewable sources will be from 2% to 15% by 2020. This target, as suggested in [5], could be achieved by the following renewable energy targets in each energy consumption sector:

- more than 30% of electricity generated from renewables;
- 12% of heat generated from renewables;
- 10% transport energy from renewables.

To assist the delivery of UK's ambitious targets, a substantial increase in using renewable energy, in the form of distributed generators (DGs), has emerged in the electricity sectors. DGs are small-size electricity power generation connected to a distribution network rather than the transmission network [6]. They have lots of economic and technique benefits for electric power networks, such as reducing network

losses, improving reliability and deferring network infrastructure reinforcement. [7]. Nevertheless, from the network operation perspective, problems are introduced by connecting a large capacity of DGs to the network, such as the reverse power flow, violation of voltage and thermal limits, increase of fault levels, harmonics and flickers etc.

1.1.2 Electricity Demand Growth

Electricity demand is the fastest-growing component of total global energy demand due to the increase of population, development of economy and the fact that electrical energy is the most suitable form of the energy with respect to human activities and environment [8]. As shown in Figure 1.2, the global demand of electricity increased by over 50% from 1990 to 2011, and is expected to increase by over 80% from 2011 to 2030 under current policies scenario. Among all the continents, Asia, as a developing area, has the most radical increase in electricity demand, projected to average around 5% per year respectively to 2035 [9].

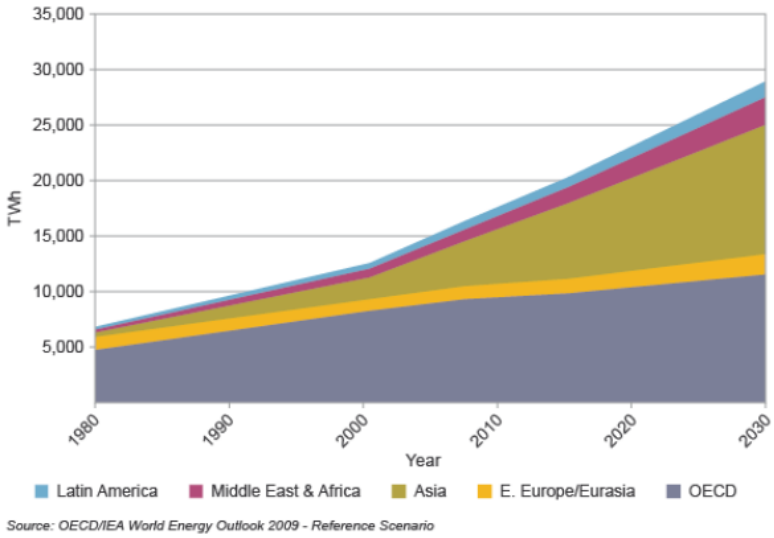

Figure 1.2: World Electricity Consumption by Region [9]

The UK's demand for electricity is expected to increase over the next a few decades [10]. A key reason is the transition to low carbon future. To meet government carbon

reduction targets, the UK's dependence on fossil fuels (e.g., gas and petrol) would be reduced and changed to renewable sources (e.g., wind and solar power). Examples include the large-scale integration of electrified transport (e.g., electric vehicles) and decarbonized domestic heating (e.g., electric heating pumps). Because of these, the UK's demand for electricity could double by 2050 [10].

To meet the growing demand for electricity, additional network capacity is needed. This would mean significant investments if using the conventional network reinforcement solution. Two direct consequences are anticipated [11]:

- **High cost to customers**

  According to the estimation made by Office for Gas and Electricity Market (Ofgem) [12]: the UK needs to invest as much as £53.4 billion in the electricity network between 2009 and 2025. This investment would be paid eventually by customers.

- **Impact on society and the environment**

  Reinforcing the electricity network will have a significant impact on carbon emissions [10]. Additionally, the reinforcement usually involves extensive excavations and disruption, while significant amount of time is inevitable due to the work scale (e.g. cable upgrades).

Under this circumstance, innovative solutions should be sought without or with reduced network reinforcement and expansion.

1.1.3 Emergence of Smart Grid Concept

Utility engineers across the globe are trying to address numerous challenges, e.g. the increasing integration of renewable generation, the continuing growth of electricity demand and the need for optimal deployment of expensive assets. It is evident that

these challenges cannot be solved based on the existing electricity grid. New generation of electricity grid, known as "Smart Grid", is being developed to address the major shortcomings of the existing electricity grid [13].

According to the US Department of Energy's Modern Grid Initiative:

"A smart grid is an electricity network that employs innovative products and service technologies together with advanced monitoring, control and communication technologies in order to:

- Enable and motivate active participation by consumers;
- Accommodate all generation and energy storage options;
- Enable new products, services, and markets;
- Run more efficiently;
- Provide higher quality of power required;
- Anticipate and respond to system disturbances in a self-healing manner;
- Operate resiliently against attack and natural disaster." [14, 15]

The UK's Electricity Networks Strategy Group (ENSG) published "A Smart Grid Vision" to outline what a UK smart grid should be and what challenges need to addressed. According to it, a Great Britain smart grid should be able to help the UK meet its carbon reduction targets, ensure energy security and wider energy goals while minimising costs to consumers. A "Smart Grid Routemap" was also published to deliver this vision [16]. It emphasizes the potential role of the smart grid as a key enabler to help UK power system accommodate a number of critical developments in the next 40 years. The detailed developments with an illustrative timeline are given in Figure 1.3 [17].

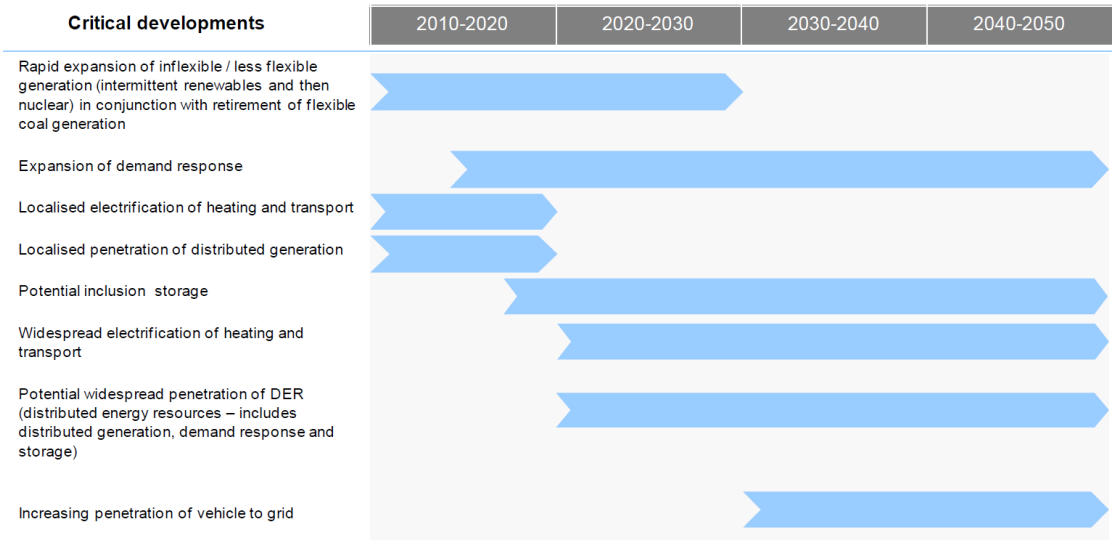

Figure1.3: Critical developments for UK smart grid routemap out to 2050 [17]

In the UK, Smart Grid has been primarily focused on the distribution networks where it is believed early action is needed. Firstly, the distribution network is the biggest component of electricity losses. It is most important that the distribution network operators (DNOs) can manage their carbon footprint. Moreover, the uptake of electric heat pumps and electric vehicles, investment in small wind generation, household and community micro-generation and other initiative to de-carbonize the energy use could have a profound impact on the nature and pattern of demand on the distribution networks. DNOs may need to actively manage the intermittent and bi-directional power flows of electricity, which requires significant changes in electricity generation and demand technologies [16]. Therefore, initially, the distribution network will have the greatest opportunity for smart interventions where mass investment is required, aligned with revised network operation and control paradigms, to ensure it can cope with the increasing demands and many new emerging requirements [16].

1.2 Research Motivation

Medium Voltage (MV) distribution networks are usually operated in a radial configuration. Normally Open Points (NOPs) are built, connecting adjacent feeders, to provide alternative routes of electricity supply in case of planned or unplanned power

outages. The unique benefit of this configuration is its inherent simplicity of operation and protection. However, this needs to be reconsidered under the new circumstance. With increasing penetration of intermittent renewables and growing electricity demand, distribution networks are facing the challenge of increasing power flows through existing networks. Although traditional network reinforcement is an option to deliver the additional network capacity, their high-cost and time-consuming features make this solution undesirable. Innovative solutions are therefore needed to increase the utilization of existing assets dynamically and reroute the power flow through less loaded circuits.

One way is to interconnect (or mesh) the conventional radial network, which enables the power delivery through a less heavily loaded feeder and hence relieves the stress on the heavily loaded feeders. Currently this configuration has been recognized by several DNOs in their development plans [18], achieved by closing the NOPs. Benefits of a closed loop network include balancing the loads between different feeders, improving the voltage profiles, reducing power losses and improving the reliability. However, the main problems of interconnection are:

- The rise in fault current, which could lead to the malfunction of the existing circuit breakers.
- The need of more complicated and expensive protection schemes.

An alternative solution between the radial and the mesh operation is to have a flexible mesh configuration. It is achieved by using a power electronic based device, named Soft Open Point (SOP), to replace the NOP. Instead of simply opening/closing the NOP, an SOP is able to provide the following functionalities:

- Flexible control of active power exchange between connected feeders;
- Flexible manipulation (absorbing and supplying) of reactive power on both interface terminals;

- Immediate fault isolation between interconnected feeders;
- Small and controllable contributions to fault current;
- Immediate post-fault supply restoration to support isolated loads on a feeder through power transfer from the adjacent feeder.

Therefore, the SOP offers further flexibility to current distribution networks. For network operation, it is envisioned to release capacity of existing feeders, enhance the efficiency and service quality to customers. This thesis is motivated to investigate the following three points, regarding the use of SOPs for MV distribution network operation.

1.2.1 Control of an SOP

The SOP is a multi-functional power electronic device, and hence its control strategy should be able to realize all the aforementioned functionalities. Previous studies (the detailed discussion is in Section 2.3) mainly focused on the use of SOP under normal network operating conditions, where the current-controlled strategy was used to achieve independent control of real and reactive power. However, this current-controlled strategy is not suitable to provide post-fault supply restoration (another functionality of the SOP) because it may result in voltage and/or frequency excursions that lead to either unacceptable operating conditions or instability. The operating principle of an SOP therefore needs to be investigated under both normal and abnormal network operating conditions.

1.2.2 Benefits analysis of using SOPs

It is urgently needed to quantify the benefits of SOPs for distribution network operation, which provides confidence for using SOPs in distribution networks. SOPs are effective in reducing power losses, balancing feeder loads, improving voltage profile, and thereby increasing network loadability and DG connections. A number of studies (the

detailed discussion is in Section 2.3) can be found for these purposes. However, they are mainly based on installing one or two SOP in a simple two-feeder network together with the controller design and simulation. Methodologies for the benefit quantification, i.e., steady state analysis of distribution networks with SOPs were not addressed and the advantages of a more widespread use of these devices in distribution networks have not been explored. In addition, distribution network reconfiguration has been intensively researched. It could achieve similar objectives as the SOP. However, unlike the SOP control, network reconfiguration is achieved by changing the network topology: closing some NOPs while opening the same number of closed switches to maintain a radial network structure. Extensive research has been conducted into network reconfiguration (the detailed discussion is in Section 2.2.1) for feeder load balancing, loss minimization and voltage profile improvement. It is needed to have a comparison between using SOPs and network reconfiguration to enhance the operation of a distribution network.

1.2.3 Distribution network voltage control with SOPs

Increasing DG capacity in the distribution network could cause the violation of voltage limits. SOPs are able to assist voltage control through changing the real and reactive power flow. Previous studies (detailed discussion is in Section 2.3) have reported the potential of using SOPs for network voltage control. However, the voltage control strategy considering the detailed operation of a SOP (determining the set points of the SOP) has not been investigated. In addition, coordination with other network controllable devices could achieve a better performance. There is a clear need to develop a coordinated voltage control strategy, in which the SOP and other voltage control devices are used together to achieve a better network voltage control.

1.3 Objectives and Contributions of this Thesis

The objectives and contributions of this work are outlined as:

- Investigate the operating principle of an SOP using back-to-back VSCs under both normal and abnormal network operating conditions.

  Two control modes were developed for the operation of a back-to-back VSC based SOP. The operating principle of the back-to-back VSC based SOP was investigated under both normal and abnormal network operating conditions. The performance of the SOP using two control modes has been analysed under normal conditions, during a fault and post-fault supply restoration conditions.

- Investigate the benefits of a MV distribution network with SOPs under normal network operating conditions, focusing on feeder load balancing, power loss minimization, and voltage profile improvement.

  A steady state analysis framework was developed to quantify the benefits of SOPs in MV distribution networks. The framework considers the network reconfiguration and the combination of both SOP and network reconfiguration.

- Investigate the use of the SOP for network voltage control and its coordination with OLTC and DG units in an MV distribution network. The coordinated voltage control strategy is able to maintain the network voltage while mitigating DG active power curtailment, reducing the tap operations and the network power losses.

  A novel coordinated voltage control strategy was proposed considering the SOP, the OLTC and multiple DG units. A distributed control framework was used, considering each of the controllable devices as a local control agent. A

priority-based control was developed, achieving the specified objectives in accordance with their prioritisation. Unlike centralised control strategies (detailed discussion in Section 2.2.2), which requires communication links with each network node and power flow solutions at each time step, this coordinated voltage control strategy achieves a trade-off among objectives with fewer communicational requirements and less computation burden.

1.4 Thesis Outline

The rest of this thesis is organized as follows:

Chapter two provides a literature review of challenges for distribution network operation. Available network operation functions in facing the emerging challenges are then introduced, with special attention paid to the network reconfiguration, coordinated voltage control and those functions offered by using power electronic devices in distribution networks. Last, the state-of-the-art of SOPs, including the benefits, possible device types and previous studies are presented.

Chapter three describes two control modes for the operation of a back-to-back VSC based SOP. The operating principle and performance of the back-to-back VSC based SOP using these two control modes were analysed under both normal and abnormal network operating conditions.

Chapter four describes a steady-state analysis framework to quantify the operational benefits of a distribution network with SOPs. A generic model of an SOP for steady-state analysis was developed. Based upon it, an improved Powell's direct set method was developed to obtain the optimal SOP operation. Distribution network reconfiguration algorithms, with and without SOPs, were developed and used to identify the benefits of using SOPs. Case studies have been conducted with promising

results obtained for using SOPs in MV distribution networks.

Chapter five describes a novel coordinated voltage control strategy, considering SOPs, OLTC and DG units, to maintain network voltages while mitigating DG active power curtailment, reducing the tap operations and the network power losses. A distributed based voltage control framework was developed which uses a simplified voltage profile estimation method. Followed by an analysis of using SOP for distribution network voltage control, a priority-based coordination, using the proposed voltage control framework, was developed to achieve a trade-off among the objectives. The effectiveness of the proposed coordinated control strategy was verified under various loading and DG penetration conditions.

Chapter six presents the conclusions drawn, main findings and recommendations for future work.

Chapter 2

Literature Review

THIS chapter presents a literature review on the challenges for distribution network operation, the network operation functions and the state-of-the-art of the SOP studies.

2.1 Challenges for Distribution Network Operation

Since the Carbon Emission Reduction Target (CERT) was introduced into the electric industry, electric power distribution networks have undergone dramatic changes. In this CERT context, distribution networks should not only be able to deliver electricity to customers with acceptable reliability and quality standards, but also to fulfil the tasks, such as accommodating increasing renewable energy sources and meeting the sustained high level of demand growth resulting from the electrified heating and transport, etc. These requirements impose great challenges to distribution networks, in particular in the operation perspective.

2.1.1 Aging Assets and Lack of Circuit Capacity

In many parts of the world (e.g., the USA and most European countries), the electric power system expanded rapidly in 1950s and 1960s [19]. The distribution equipment and cables installed then are now beyond its design life and in need of replacement. The capital costs of the like-for-like replacements will be very high [19]. The need to refurbish the transmission and distribution circuits is an obvious opportunity to innovate with new designs and operating practices. In addition, the introduction of intermittent DGs can increase the use of tap-changing devices (e.g., OLTC and switched capacitor banks) and therefore accelerate failure of the device [20]. A smarter operation is therefore needed to make effective use of existing assets and mitigate the wear and tear.

In many countries, constructing new overhead lines, needed to meet the load growth and to connect renewable DGs, has been delayed for up to 10 years due to the difficulties in obtaining rights-of-way and environmental permissions [19]. Therefore, some of the existing distribution line circuits are operating near their capacity, limiting DG integration and demand growth. This calls for intelligent methods, instead of traditional network reinforcement, to increase the power transfer capacity of circuits

dynamically and reroute the power flows through less loaded circuits.

2.1.2 Operational Constraints

Distribution networks have to operate within prescribed constraints in order to ensure secure electricity delivery. These constraints include [21]: voltage constraints, thermal constraints, frequency and short-circuit constraints, etc.

With the introduction of DGs and the continuous growth of demand, most distribution networks are experiencing constraint breaches. The large-scale integration of DGs can cause over-voltages at times of light load, and the demand growth can give rise to local low voltages. Hence, adequate voltage management requires a coordinated operation of the DGs, on-load tap changers and other equipment (e.g., voltage regulators and capacitor banks). Due to the local reverse power flow brought by the DGs, aligned with the increased demand, thermal limits of the existing transmission and distribution equipment and lines can be exceeded. Thus dynamic ratings that can increase circuit capacity in real-time are needed to address the thermal overloading. Some DG plants use directly connected rotating machines, for example, old wind turbines and small hydro turbines use induction generators while, large hydro turbines use synchronous generators [22]. The connection of these generators and new spinning loads can cause the maximum fault current to exceed the fault level rating of the distribution network. Thus effective fault current limiting technologies or services are required to maintain safe operation of the power system.

Therefore, distribution network operation has to be robust and flexible to address the constraint problems that are caused by the quantity, geography and intermittency of the DG integration as well as the new forms of load. Otherwise, traditional expensive network reinforcement has to be carried out.

2.1.3 Reliability and Efficiency of Supply

Morden society has increasing critical loads connected and power blackouts could result in enormous monetary loss and society chaos [23]. In the coming decades, the proportion of intermittent renewable generation in the energy mix will get higher, lowering the overall predictability of the electricity supply. In the meantime, the electricity capacity margin is reducing, which increases the risks to security of supply. To meet the requirement of the Government's reliability standard, UK's utilities had defined customer interruptions (CIs) and customer minutes lost (CMLs) as the indicator of each DNO's performance [24]. This calls for effective restoration strategies and other post-fault measures to retain or return the supply after the (inevitable) faults in the distribution networks.

Electrical power losses are an inevitable consequence of transferring electricity across distribution networks and they have significant environmental and financial impact on customers. For instance, the energy losses from the electricity distribution networks contribute to approximately 1.5 % of Great Britain's greenhouse gas emissions [25]. Moreover, present distribution networks usually have power losses in the range of 3% - 9% and this accounts for 80% of the total power losses in combined transmission and distribution networks [24]. Higher losses (dominated by the ohmic loss: I^2R terms) would be expected in 2030 due to the anticipated more heavily assets use [24]. All these losses are eventually paid for by customers and need to be mitigated. To encourage an efficient level of losses in distribution networks, Office for gas and electricity Market (OFGEM) has launched a losses incentive mechanism to be a part of their network price control since 2015 [26]. An improved operating efficiency is therefore needed for minimum energy losses.

2.2 Network Operation Functions

As discussed in the previous section, distribution networks need better control and supervision of distribution network facilities to support their operation in facing the emerging challenges.

Traditionally, there are well established operation functions available that enable control and supervision of distribution network facilities for desired network performance. Examples include the network reconfiguration, voltage and reactive power control, protection relay coordination and outage management, etc.

At present, the emergence of smart grid concept is a radical reappraisal of the functions of distribution networks. In response to the smart grid initiatives, various new technologies and applications are being introduced into distribution networks, such as the integration of distributed energy resources, active control of demand load and the progress of using distribution-level power electronics. These new technologies and applications are able to support network operation neither by adding to the effectiveness of existing operation functions (e.g., through a coordinated operation) or by offering new functions to the distribution network.

This thesis focused on the enhancement of distribution network operation through the use of power electronic based equipment - SOP - as well as its operation comparing and coordinating with traditional network reconfiguration and network voltage control. As background to the research that has been carried out, network reconfigurations, coordinated voltage control and the operation functions that can be offered by using power electronic devices in distribution networks will be introduced in subsequence sections.

2.2.1 Network Reconfiguration

Distribution networks are normally designed as meshed networks but are operated in a radial manner with normally open points [27]. Network configurations can be changed during the operation by changing the open/close status of switchgears, manually or automatically [27]. Figure 2.1 gives an example of network reconfiguration, which is based on a three-feeder network with three NOPs (dash lines). The configuration of the network is changed by closing NOPs 15 and 26 while opening closed switches 12 and 13.

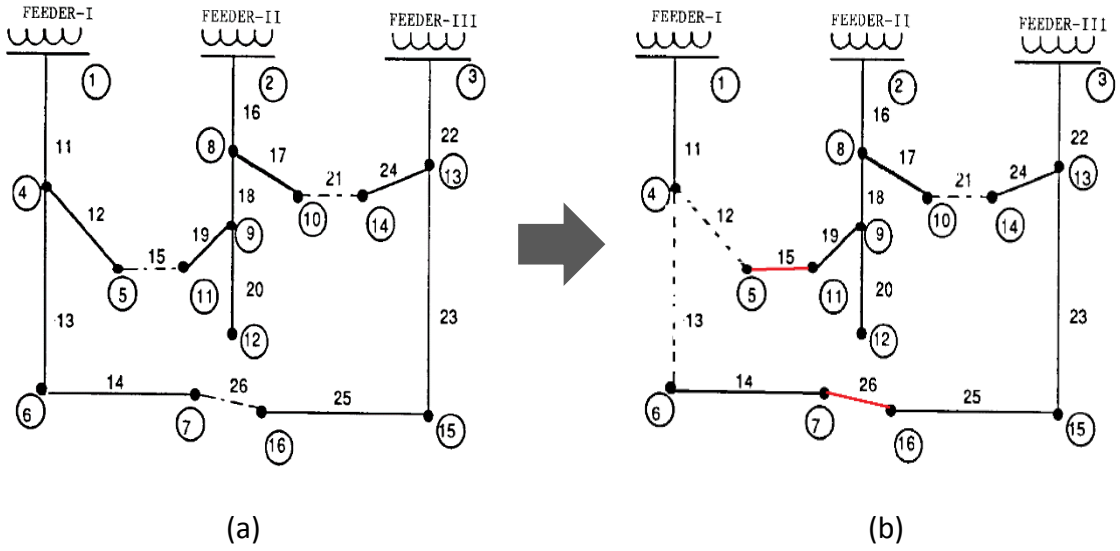

Figure 2.1: Three-feeder example network: (a) before network reconfiguration; (b) after network reconfiguration [27]

The main objectives of network reconfiguration include [19, 28]:

1. Supply restoration：This optimally restores de-energized customers through alternative sources in the case of planned and unplanned power outages.
2. Load balancing among substation transformers or different feeders and equalising the voltages.
3. Active power loss minimization at a given time or energy loss minimization during a period.

The methods used to solve the above network reconfiguration problems include those based on practical experience and optimization techniques. The methods based on optimization techniques determine the optimal network configuration by solving a complicated combinatorial, non-differentiable constrained optimization problem [29]. Possible solutions include mathematical algorithms [27, 30], computational intelligent-based algorithms (for example, generic algorithm, simulated-annealing, fuzzy logic) [31-33], and hybrid algorithms which combine two or more above algorithms [34, 35].

Network reconfiguration and its significant benefits have been reported in the past decades. However, practical applications of automatic network reconfiguration is presently very limited due to excessive costs of remotely-controlled switchgear, associated ICT infrastructures and maintenance of hardware/software (e.g., excessive wear and tear of switches) [36, 37]. The protection coordination requirement for the reconfigurable network is also a hurdle [38].

It is possible to use SOPs to achieve the same aforementioned benefits (objectives) offered by network reconfiguration. In the meantime, changes of network topology and protection coordination are no longer needed when using the SOP. In the study reported in Chapter 4, the potential and benefits of using SOP, compared with traditional network reconfiguration, was discussed in further detail.

2.2.2 Coordinated Voltage Control

Voltage control refers to the technique of using available voltage control equipment to maintain acceptable voltage levels at all points in the distribution network under all loading conditions [39]. As discussed in Section 2.1, it is one of the most significant issues that limits DG penetration in distribution networks. When DGs units are connected to a distribution network, they can significantly change the network voltage profile and interfere with conventional local control strategies of the transformer

tap-changers, line voltage regulators and shunt capacitors (which are designed based on the assumption of unidirectional power flow [40]). This interference leads to [41]: 1) unexpected over- and under-voltage, 2) increase in power losses and 3) excessive wear and tear of voltage control devices.

In these circumstances, a coordinated operation of the voltage control devices is needed to provide adequate voltage management, meanwhile, eliminating the aforementioned problems. In the literature, numerous control devices has been conducted to support voltage control. Examples include [42-45]: on-load and off-load transformer tap-changers, line voltage regulators and switched capacitor banks, energy storage, power electronic devices and the control of DG.

These control devices are the key factors to realize the coordinated voltage control in distribution networks. However, the first milestone is to find a most effective control strategy to achieve the coordination among the control devices. In the literature, numerous voltage control strategies have been proposed to achieve a proper coordination. According to the control structure and communication links, they can be categorized as [46]:

i) Localized coordination: with no communication links,

ii) Centralized coordination: with a wide range of communication links,

iii) Distributed coordination: with a few communication links among control devices.

- **Localized coordination**

Localized coordination does not require communication links. Control devices determine their operating set points based on local signals [39]. The coordination between the localized control actions can be achieved based on the time delay operation [40]. Alternatively, the local control strategies for DG units can be modified to mitigate

their impacts on the voltage profile, without modifying conventional local control strategies. For example, the authors in [47] proposed a decentralized reactive power control approach for the DG units, which absorbs reactive power to compensate the effect of voltage rise caused by active power injection. Therefore, the convention local control strategy is not affected by the reverser power flow.

The localized coordination approaches are reliable and scalable due to their independency and simplicity of control structure. However, their control performances are not optimal. Examples include: 1) the high stress on the control devices is not relieved, 2) the energy capture from DG units is not maximized, and 3) the feeder power losses may increase.

- **Centralised coordination**

Centralized coordination is a fully-coordinated control approach that calculates the optimal operating set points for all available controllable devices and delivers the best performance possible by solving a multi-objective optimization problem [48]. It is usually achieved based on a distribution management system (DMS) to receive measurements of the distribution network (e.g., voltage, power flow, and equipment status), and, then, to estimate the network status before dispatching control devices using state estimation technologies [49].

Figure 2.2 shows an example of the cascaded control architecture for centralized coordination. The distribution management system solves the optimization problem by either following different objectives at different times or considering conflicting objectives together in a weighted manner [50-54]. The DMS then dispatches the control devices accordingly via the supervisory control and data acquisition (SCADA) systems.

The main downsides to the centralized coordination include [49, 55]: 1) The extensive investment in sensors and communication links; 2) The requirement for the accuracy of

the state estimator; 3) The use of power flow and optimization solution at each time step, which might cause a large computation burden and numerical convergence issues when X/R ratio is low; 4) The undesirable properties with respect to scalability and reliability (fragile to single point of failure).

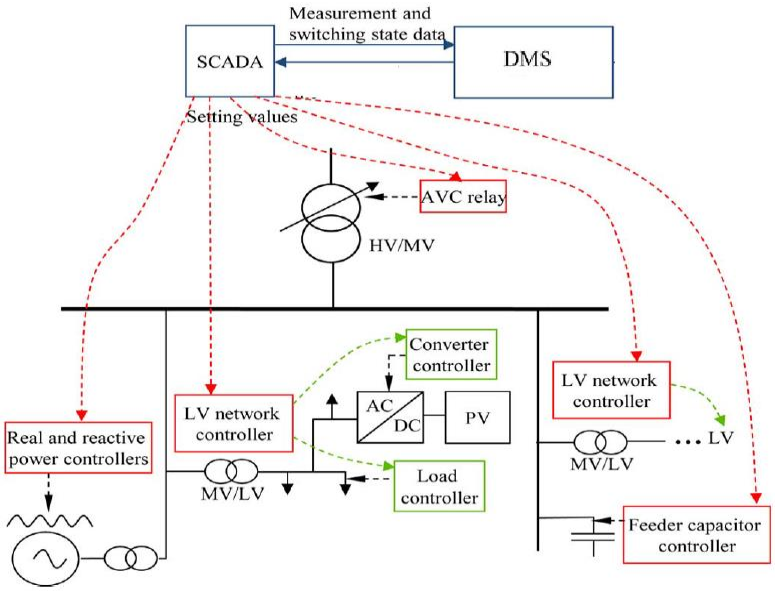

Figure 2.2: Cascaded control architecture for centralized coordination [48]

- **Distributed coordination**

Distributed coordination has been proposed recently to tackle the drawbacks of centralized and localised coordination [55]. It is usually accomplished by using a multi-agent framework. Each agent in the framework is an intelligent entity that can perceive its environment, create an action according to its own decision-making and communicate with other agents to achieve a common goal [46]. For voltage control problems, each control device is considered as an local control agent and communicates with other agents for improved control performance [46].

Compared with the centralized coordination, distributed coordination can reduce the communication requirements and computation burden as well as avoid the reliability issue (for example, single point of failure) because the dispatching is implemented in a

distributed manner, i.e., the original problem is decomposed into smaller sub-problems and each is assigned to a particular agent [56]. In addition, the implementation of centralized coordination becomes difficult with the increase of uncertainties due to DG integration and the efforts to achieve a "plug and play" property. Distributed coordination is expected to deal or at least relieve these issues [56]. In this thesis, the distributed coordination was employed to provide coordinated voltage control in an active distribution network with SOPs.

Numerous efforts have previously been made to achieve distributed coordination for network voltage control using the multi-agent framework [41, 46, 55-57]. In [56], a multi-agent reactive power dispatching scheme was proposed for voltage support of DG units in a single feeder. But the utility voltage control devices (for example, OLTC, shunt capacitors) were not considered. The authors in [57] proposed a coordinated voltage control for the OLTC control, where the remote terminal units were treated as local control agents and provide distributed state estimation. However, the OLTC was assumed as the only control devices. In [41] and [55], multi-agent frameworks were proposed for coordinated voltage control between both DG units and utility control devices. Figure 2.3 shows an example of the coordination among three control agents via two ways communication [41]. All three control agents have a common objective and each agent also has its own objective (see the circles). The control agent can take local measurements, make control decisions and negotiate with other agents when there is a need. In these studies, the control performances highly depend on their control design since the control optimality tends to be degenerated by the negotiation process among agents.

Another coordinated control strategy using a multi-agent framework was proposed in [46] to achieve both autonomy and optimal control. The use of "blackboard" memory data combined with the multi-agent framework can eliminate unnecessary negotiation process among agents and minimize data communications. However, the extensive

investment on sensors, the computation burden and the convergence issues due to running power flow were not addressed in this study.

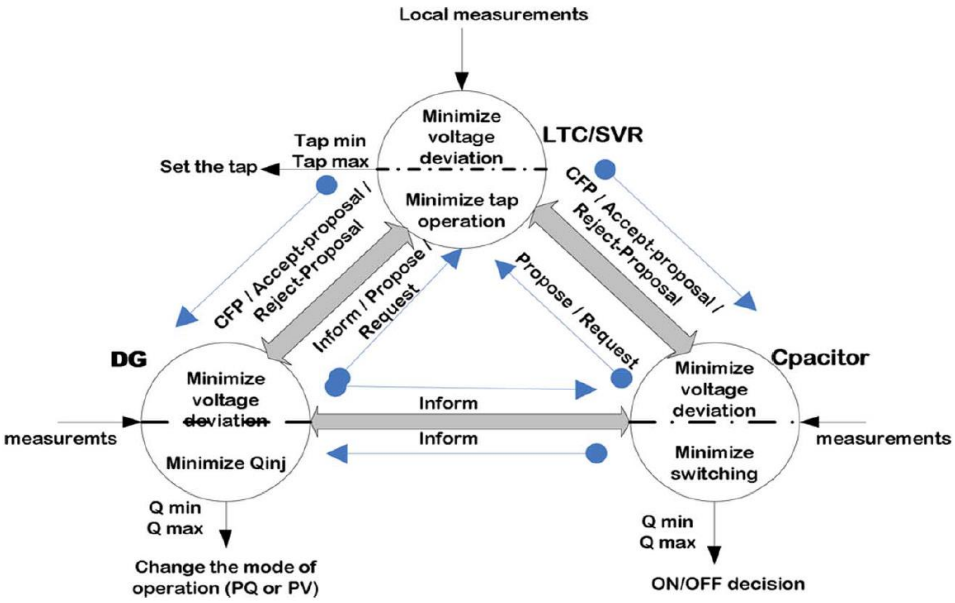

Figure 2.3: Coordination among three control agents via two ways communication [41]

In this thesis reported in Chapter 5, based on the proposed distributed coordination, a simplified voltage estimation method was used to reduce the number of sensors in the network. In addition, a coordination method was applied on the control agents (SOP, OLTC and DGs), which can eliminate unnecessary negotiation process among the agents and provide improved control performance without running power flow.

2.2.3 Operation Functions Offered by Power Electronic devices

Power electronics, in forms of the high-voltage DC transmission system (HVDC) and flexible AC transmission systems (FACTS), has played a visible and key role in power-gird control for over 60 years, mainly on the transmission network for bulk power transfer [58]. The use of power electronics at the distribution network level has been much more limited. At present, under the smart grid concept, visibility, controllability, and flexibility will be essential features throughout the future distribution network where power electronics can play a key role [19]. Several DNOs in the UK have already initiated to offer power electronics solutions to address their

network issues [59-61] and, hence, delay or eliminate the need of traditional network reinforcement. Further literature on the advantages of power electronic solutions over traditional network reinforcement is available in [18].

A wide variety of network operation functions can be offered by using power electronic devices in distribution networks. Examples include voltage control, phase rebalancing, active power filtering, fault current limiting and power flow control, etc.

Power electronics can support distribution network voltage control in forms of power electronic transformers [62], transformers with electronic tap changers [63] and reactive power compensation. Power electronic transformers and transformers with electronic tap changers can be installed in place of classical transformers, providing the competitive advantages of enabling fast and smooth voltage regulation as well as little wear and tear. The reactive power compensation, such as using the STATCOM [64], dynamic voltage restorer (DVR) [65] and SOP [61], can tackle the voltage problem either at the substation, path-way along the feeder or at the point-of-load.

Phase imbalance, as a result of differences in consumption patterns of consumers, can cause higher conduction losses and lower network utilization. It is also considered as a major cause of capacity limitation [66]. Power electronic devices that contain a common DG bus, such as the unified power quality conditioner, DVR, STATCOM and SOP, allow exchange of instantaneous power between the phases and, hence, can be used to rebalance current flow on a feeder.

Active power filters for harmonic elimination and power quality improvement have been applied within customer premises but not as network elements compensating a group of consumers [18]. In recent years, the need for filtering in networks with power electronic compensation has been recognized by DNOs, such as filtering in the locations with a high penetration of PV [18].

Power flow control are traditionally achieved through network reconfiguration with existing switchgear (discussed in Section 2.2.1), aiming to increase the power transfer capacity of circuits dynamically and reroute the power flows through less loaded circuits. At present, an alternative solution, that makes use of power electronics in the form of SOP to facilitate power flow in a dynamic and continuous manner, is attracting the interest of the DNOs. A Low Carbon Networks Fund (LCFN) project has already initiated to install the SOP in UK's distribution network to verify its effectiveness [61].

This thesis focuses on the new power electronics application. Details on the introduction of SOP benefits, types and previous work are presented in the following section.

2.3 Soft Open Points

2.3.1 Benefits of Soft Open Points

As shown in Figure 2.4, SOPs are multi-functional power electronic devices (discussed in Section 1.2) installed in place of the NOPs in distribution networks. They are also referred to as 'loop power flow controllers', 'series controllers' and 'DC links' in some literatures.

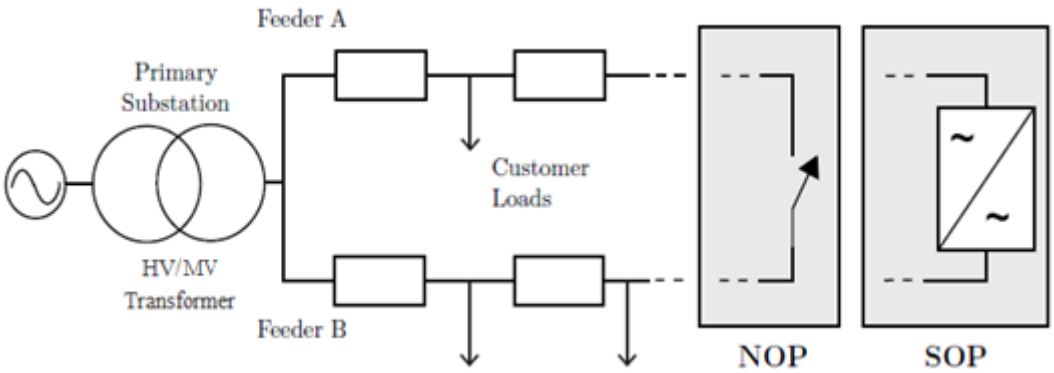

Figure 2.4: Simple distribution network: option A representing a NOP connection and B representing an SOP [67]

The most significant advantageous provided by these power electronic devices, compared with mechanical switches, are

- The power flow between the connected feeders can be regulated in a continuous and dynamic manner.
- The reactive power is able to be independently injected or absorbed at both interface terminals. Therefore, SOP can be used for dynamic voltage support.
- The SOP can be used to improve the power quality of the distribution networks [68], such as mitigating voltage imbalance, sags, flickers, and low-order harmonics, etc.
- The SOP can be used to connect any feeders regardless of the angular or rated voltage difference between them, particularly when the feeders are supplied by different substations. This is not possible with the mechanical switches.
- The short-circuit currents on the radial feeders (without SOPs) are not changed with the use of SOPs, owning to the capability of instantaneous fault current control. This indicates that this intervention would not require modifications of existing network protection assumptions or upgrades of protection devices (this is usually the case for a close-loop operation). [69]

2.3.2 Types of Soft Open Points

The functionalities of an SOP were descripted in Section 1.2. Possible SOP types, enable to realize these defining functionalities, include:

- Back-to-back VSCs
- Multi-terminal VSCs
- Unified power flow controller (UPFC)

An overview of the topologies of these types of SOPs is shown in Figure 2.5. Each is

made from an arrangement of VSCs with varying rating and quantity. The VSC is suitable for SOPs due to: 1) the freedom to operate with any combination of active and reactive power, 2) the ability to limit (or control) fault current and 3) the possibility to supply isolated areas of a network or even provide the black-start ability.

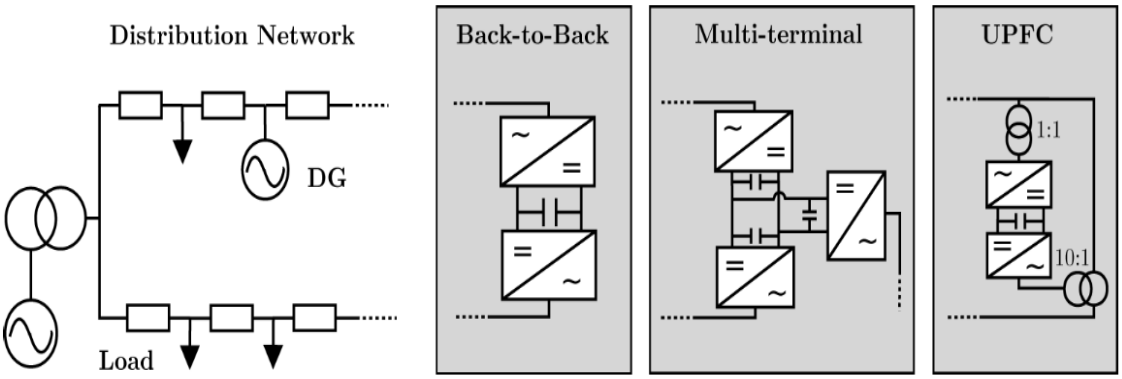

Figure 2.5: Topologies of different types of SOPs [70]

- **Back-to-back VSCs**

This thesis focused on the back-to-back VSC based SOP. It consists of two VSCs connecting via a common DC link to form an asynchronous AC/AC conversion device. Coupling transformers are usually equipped, interfacing each VSC with the connected feeder. However, transformerless topologies are possible [71], which reduces the size and weight of the device. This arrangement allows active power exchange between the AC front ends as well as independent reactive power manipulation at each interface terminal.

Under abnormal network conditions, the fault on one feeder can be isolated from the other feeder by the DC link. The fault current on the faulted side interfacing VSC can also be limited (and controllable) by appropriate control strategy [68]. Post-fault restoration is achievable, supplying the isolated loads on one feeder by power transfer from the adjacent feeder via the VSCs [68].

- **Multi-terminal VSCs**

The multi-terminal VSC based SOP is an extension of the back-to-back VSC based SOP, in which additional VSCs are connected to a common DC-link. The number of VSCs associated with a multi-terminal VSC based SOP is defined as 3 or greater. The same features discussed for the back-to-back VSC based SOP are applicable to the multi-terminal VSC based SOP.

- **Unified power flow controller (UPFC)**

The UPFC based SOPs, also known as shunt-series VSCs, consists of two VSCs with a common DC link. Unlike the configuration of the aforementioned two types, one VSC in UPFC is connected in series and the other is connected in shunt with the interconnected feeders. The series connected VSC injects a series voltage with controllable magnitude and phase angle, thereby controlling the power flows between interconnected feeders [72]. The shunt connected VSC supplies the active power demanded by the series VSC through the DC link. It can also provide reactive power manipulation independent of the operation of the series connected VSC.

The primary advantage of the UPFC based SOPs, compared with the aforementioned two types, is the potential to induce power flows greater than VSC rating (for example, 10 MVA transferred using 1 MVA VSCs). However, this ability is determined not only by the device ratings themselves, but also by the network topology, constraints, and operating point as well as the device placement [70]. An inherent drawback to the UPFC is the fact that the feeders connected with a UPFC are not isolated by a DC-link, and, hence, disturbances or faults on one connected feeder will affect the other unless a control strategy is developed to reject or compensate for disturbances. The instantaneous fault current limitation (or blocking) is possible [73], at the cost of higher device ratings. The interconnection is also not asynchronous and therefore the two electrical network connected via a UPFC based SOP must be synchronous.

2.3.3 Previous Soft Open Points Studies

Previous work on SOPs is discussed with the research gaps identified in terms of the control strategy, benefits analysis and their use for distribution network voltage control.

- **Control strategy**

The control strategy of an SOP has been reported early in 2006 [71]. A current-controlled strategy was developed for the operation of a back-to-back VSC based SOP. In this control strategy, direct-quadrature (*d*-*q*) current components were used for each VSC to provide control of instantaneous active and reactive power exchange between the VSC and the AC network. The effectiveness of the control strategy for instantaneous power flow regulation has been verified by a factory test using 6.6kV 1MVA transformerless back-to-back VSCs. But the performance of this control strategy under abnormal network conditions, i.e., during a fault and post-fault supply restoration, was not investigated.

In [74], the same current-controlled strategy was applied to a multi-terminal VSCs based SOP and validated in an experimental way. The transient performance of the control strategy during a three-phase short-circuit fault was evaluated. This current limiting capability has been demonstrated important to 1) protect VSCs from over-currents and 2) limit fault current and therefore maintain the same short circuit current as the radial network operation (without VSCs). Nevertheless, the operation of the SOP for post-fault supply restoration was not considered.

When the SOP provides post-fault supply restoration to isolated loads, the frequency and voltage are not dictated from the grid. Hence, the aforementioned control strategy is not desirable because it may cause voltage and/or frequency excursions that can lead to either unacceptable operating conditions or instability [75]. The operating principle of an SOP under both normal and abnormal network operating conditions was not found in previous literatures and need to be investigated.

- **Benefits analysis**

The benefits of using SOPs in distribution networks have previously been reported for different objectives, such as: loss minimization [76-78], feeder load balancing [36, 37] and maximisation of network loadability and DG penetration [69, 79, 80]. The authors in [69] developed an optimization framework to compare the benefits of using DC links (which are also SOPs) with conventional network reinforcement measures. Using the framework, a thorough assessment of the most promising SOP type was reported in [79]. The benefits of the back-to-back VSC based SOP, UPFC based SOP and a series VSC were analysed and compared in terms of their capability to maximise DG penetration in distribution networks.

In these literatures, operational benefits of using SOPs were studied mainly based on two or three feeders connected by an SOP. Methodologies for benefit quantification and the advantages of more widespread use of SOPs in distribution networks have not been explored.

On the other hand, it is possible to maximise the benefits of an SOP by combining with traditional network reconfiguration (discussed in Section 2.2.1). An SOP is only able to regulate the power flow of its own connected feeders. Using network reconfiguration can change the feeders that are connected to the SOP dynamically and, hence, can benefit the whole network. The combination of network reconfiguration and SOP control and its benefits are discussed in further detail in Chapter 4.

- **Distribution network voltage control**

The potential to use SOPs for distribution network voltage control has been reported [67] [81] by changing active and reactive power flows on the connected feeders.

In [81], the minimum voltage deviation among multiple feeders was achieved by using a multi-terminal VSCs based SOP. The effectiveness of using an SOP to mitigate

voltage deviation was compared with that using a close-loop operation. Similar performance was observed while the later one requires more complicated protection system. However, in this study, the reactive power control ability of the SOP was not considered.

In [67], the use of SOPs, controlling both active and reactive power flow, has been proposed for network voltage control and, ultimately, higher DG penetration in distribution networks. A comparative analysis was conducted between using SOPs and conventional voltage control options (for example, OLTC). However, the operation of the SOP (set points of active and reactive power) was determined by merely satisfying constraints. Well-established voltage control strategies including suitable operation mechanisms of the SOP were not elaborated in this study. In addition, the coordination of SOPs and other available voltage control devices for improved control performance has not been investigated in previous work.

2.4 Summary

Challenges for distribution network operation were summarized. The network operation functions that enable to deal with emerging challenges were then introduced, with special attention paid to the network reconfiguration, coordinated voltage control and those functions offered by using power electronics in distribution network level. The power electronic applications can offer a variety of operation functions and, hence, will play a key role to enable visibility, controllability, flexibility features throughout the future distribution networks.

SOP is a power electronic application in distribution networks. The possible layout of SOP and its benefits were introduced. In addition, a review of the state-of-the-art of the SOP studies was presented and followed by identifying the corresponding research gaps.

The current-controlled strategy has been reported for SOP operation to achieve the defining functionalities. However, this control strategy is not suitable for post-fault supply restoration (which is another key functionality of SOP). The operating principle of an SOP under both normal and abnormal network operating conditions is yet to be explored. Therefore, in this study, operating principle of a back-to-back VSC based SOP was investigated under normal conditions, during a fault and post-fault supply restoration (discussed in Chapter 3).

The benefits that an SOP can provide have been identified. However, methodologies for benefit quantification and the advantages of more widespread use of SOPs in distribution networks were not explored. In addition, using SOP control could achieve the same objectives as traditional network reconfiguration, and a combination of both SOP control and network reconfiguration could maximize the benefits of an SOP as well as benefit the whole network. These issues have not been explored in previous studies. Therefore, in this study, the operational benefits of using SOPs, with and without considering network reconfiguration, were quantified and reported in Chapter 4.

Distribution network voltage control can be achieved by using SOP through both active and reactive power flow control. However, research conducted on suitable operation mechanism of SOPs for distribution network voltage control and the coordination with existing voltage control devices was not found. Therefore, in this study, a coordinated voltage control strategy in active MV distribution networks with SOPs was investigated (discussed in Chapter 5), which is based on the distributed coordination.

Chapter 3

Control of a Back-to-Back VSC based SOP

THIS chapter investigates the operating principle of a back-to-back VSC based SOP under both normal and abnormal network operating conditions

3.1 Introduction

In this chapter, the circuit topology of back-to-back VSCs and its suitability for the role of an SOP is presented. Two control modes were developed for the operation of a back-to-back VSC based SOP. The operating principle of the back-to-back VSC based SOP with these two control modes was investigated under both normal and abnormal network operating conditions.

Studies on a two-feeder MV distribution network showed the performance of the SOP under different network operating conditions: normal, during a fault and post-fault supply restoration. During the change of network operating conditions, a mode switch method was used to achieve the transition between the control modes. The role and importance of soft cold load pickup and voltage synchronisation processes, essential for a smooth transition during the switching of control modes, were also investigated.

3.2 Back-to-Back VSC based SOP

Figure 3.1a shows a two-feeder distribution network interconnected with a back-to-back VSC based SOP. Two VSCs are located between the feeder endpoints and connected via a common DC link. The main circuit topology of the back-to-back VSCs is shown in Figure 3.1b. It consists of a DC capacitor to provide an energy buffer and reduce DC side voltage ripple, two two-level three-phase insulated gate bipolar transistor (IGBT)-based VSCs to generate voltage waveforms using pulse width modulation (PWM), and two series inductances [82]. These inductances provide high-frequency harmonic attenuation, limit the rate of rise of short circuit current, and facilitate control of power flow.

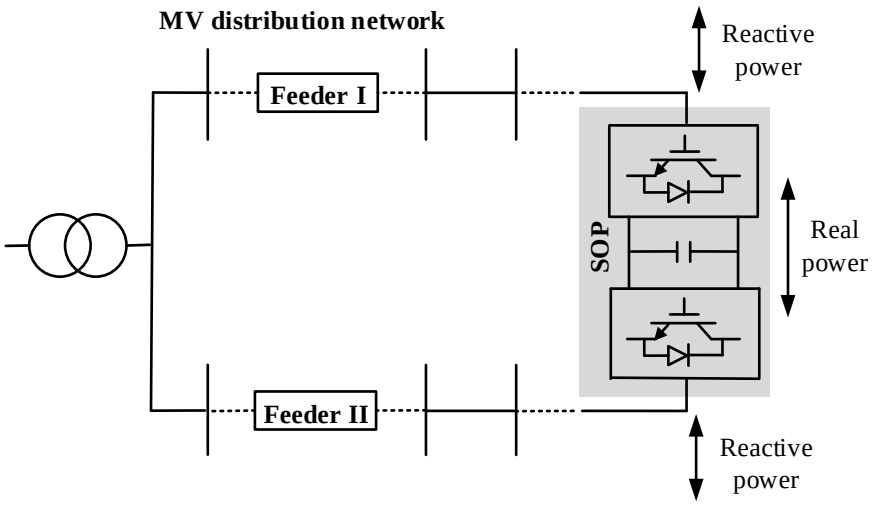

(a)

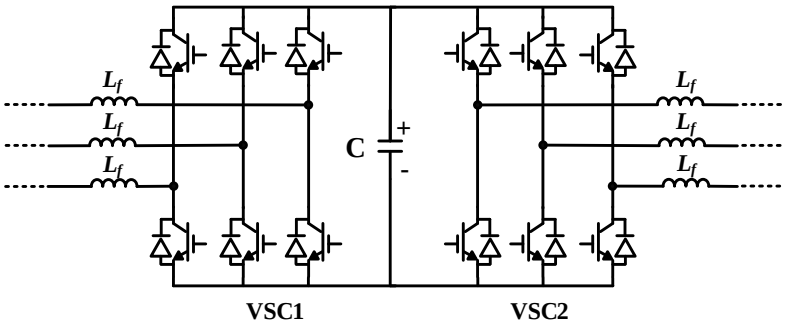

(b)

Figure 3.1: (a) Basic configuration of a distribution network with an SOP; (b) Main circuit topology of the back-to-back VSC based SOP.

The back-to-back VSCs are suitable for SOP operation due to the following characteristics:

- **Flexible active and reactive power control**

Both VSCs build their own voltage waveforms with desired amplitude and phase angle. This allows a full control of active power flowing through the DC link as well as independent reactive power supply or absorption at both interface terminals. This controllability enables SOP operation for normal network operating conditions, which includes feeder load balancing, power loss reduction and voltage profile improvement.

- **Instantaneous and independent voltage control**

The voltage waveform built by the VSCs can be controlled dynamically within milliseconds thus enabling transient control, e.g. dynamic Volt/VAR control and power oscillation damping [83]. In addition, the VSC can build its own voltage without the need of an active source at the receiving end. Hence cold load pick up for supply restoration is achievable using such device.

- **Disturbance and fault isolation**

Network disturbances and faults on one connected feeder can be isolated from the other side by the back-to-back VSCs since transient overvoltage and overcurrent are able to be limited by the control scheme [84].

3.3 Control Modes of the Back-to-Back VSC based SOP

Two control modes were developed to operate the back-to-back VSC based SOP under both normal and abnormal network operating conditions. The power flow control mode was used to 1) regulate both active and reactive power flow on the connected feeders under normal network operating conditions and 2) isolate fault between the interconnected feeders when a fault occurs on one feeder. The supply restoration mode was used under post-fault supply restoration conditions to provide power supply for the isolated loads on one feeder through the other feeder.

3.3.1 Power Flow Control Mode

A dual closed-loop current-controlled strategy [85] was used to operate SOP for the control of the feeder power flow under normal network operating conditions. Current-controlled strategy is advantageous because: 1) it provides de-coupled control of active and reactive power components; and 2) it inherently limits the VSC current

during network faults.

Figure 3.2 presents the overall control structure. The outer power control loop, the inner current control loop and the PLL are the three main components. In the outer power control loop (Figure 3.2a), one of the VSCs operates with the *P*-*Q* control scheme where the active and reactive power errors are transformed into the reference *d*-*q* current components, i_d^* and i_q^* through the proportional-integral (PI) controllers. Superscript asterisk denotes the reference values. The other VSC operates with the $V_{dc} - Q$ control scheme maintaining a constant DC side voltage for a stable and balanced active power flowing through the DC link. Dynamic limiters for i_d^* and i_q^* are inserted to enable overcurrent limiting during network faults and disturbances. In the inner current control loop (Figure 3.2b), the reference VSC *d*-*q* voltage, V_{dm} and V_{qm} are determined through the PI controllers considering the *d*-*q* current errors. The voltage feed-forward and current feed-back compensations are used to get a good dynamic response [86]. After transforming V_{dm} and V_{qm} into the VSC terminal voltage by the inverse of Park's transformation [87], the gate signals for the IGBTs are obtained through the PWM. The PLL is important for the connection of VSCs to the AC network in order to synchronize the phase of the output VSC voltage with the AC network voltage. A PLL control topology based on the *pq* theory was used [88], as shown in Figure 3.2c. By using the sum of the products of the feedback signals, f_α and f_β, and input $\alpha - \beta$ voltages (from Clark's transformation [87] of the phase voltages), the variation of the angular frequency $\Delta\omega$ is calculated as:

$$\Delta\omega = V_\alpha \cdot f_\beta + V_\beta \cdot f_\alpha \tag{3-1}$$

The PLL output angle θ is then obtained using a PI-controller, a feedback of the base angular frequency ω_b and an integrator.

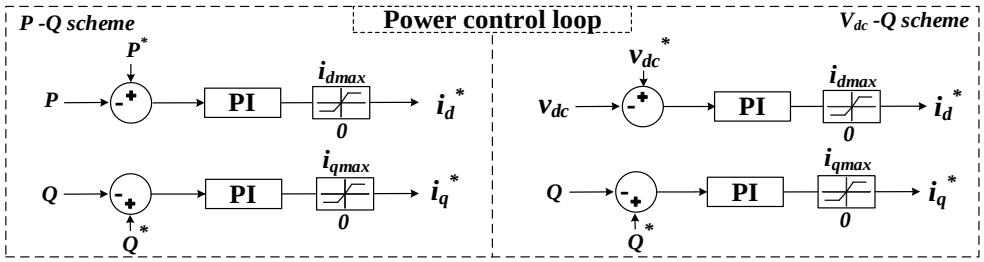

(a)

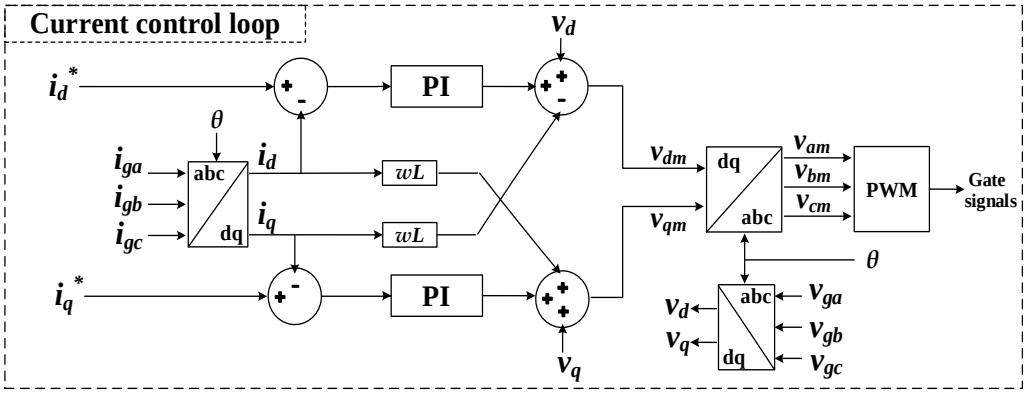

(b)

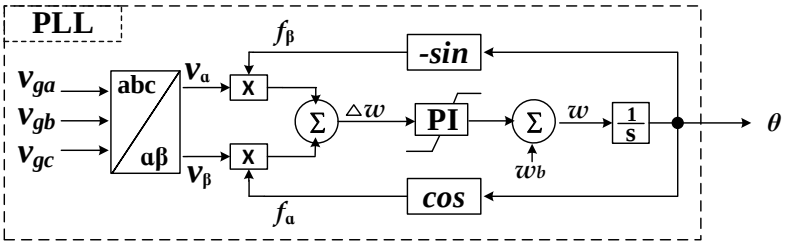

(c)

Figure 3.2: Control block diagram of the SOP for power flow control mode: (a) outer power control loop; (b) inner current control loop; (c) PLL controller

3.3.2 Supply Restoration Mode

When loads connected to one VSC of an SOP are isolated, the frequency and voltage of this VSC are no longer dictated by the grid. Using the previous current control strategy will cause voltage and/or frequency excursions and hence may lead to unacceptable operating conditions [75].

In such a case, the interface VSC (connected to the isolated loads) changes to act as a

voltage source in order to provide a desired load voltage with stable frequency. The other VSC still acts as a current source operating with the $V_{dc} - Q$ control scheme. Figure 3.3 shows the block diagram of the voltage and frequency control strategy for the interface VSC. For voltage control, the VSC output voltage is controlled directly in the *d-q* synchronous frame by holding $V_q{}^*$ to zero and controlling $V_d{}^*$ as:

$$V_d{}^* = \sqrt{2/3} \cdot V_{rms}{}^* \tag{3-2}$$

where $V_{rms}{}^*$ is the desired nominal line to line rms voltage of the isolated loads. $\sqrt{2/3}$ is included because Park's transformation is based on the peak value of the phase voltage. The output VSC voltage is regulated by closed loop control and generated through the PWM scheme. For frequency control, a stable voltage frequency is generated by using the PLL. The input phase voltages of the PLL are assigned by transforming the reference *d-q* voltages, $V_d{}^*$ and $V_q{}^*$ ($V_q{}^*$=0) through Clarke's transformation. Thus, $\Delta\omega$, as shown in Figure 3.2c, is calculated as:

$$\Delta\omega = V_\alpha \cdot f_\beta + V_\beta \cdot f_\alpha = V_d{}^* \cdot \cos\theta \cdot (-\sin\theta) + V_d{}^* \cdot \sin\theta \cdot \cos\theta = 0 \tag{3-3}$$

Since $\Delta\omega$ remains zero, the phase angle θ with a fix frequency of 50 Hz can be generated by integrating only the base angular frequency $\omega_b = 2\pi \times 50$ Hz.

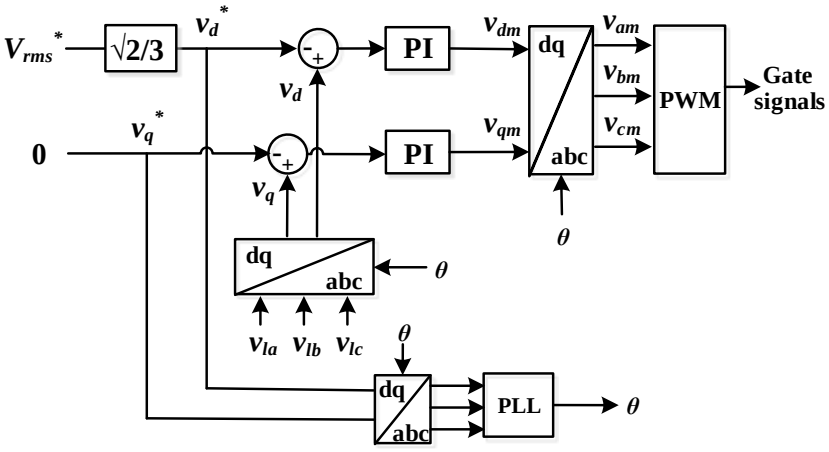

Figure 3.3: Control block diagram of the interface VSC for supply restoration control mode

3.4 SOP Operation in MV Distribution Networks

The operating principle and performance of the back-to-back VSC based SOP under different network operating conditions was analysed using a test system shown in Figure 3.4. It consists of two MV feeders with constant impedance loads extracted from an IEEE 33-bus distribution network [20] and a back-to-back VSC based SOP placed between the feeders. This test system was modelled in EMTDC/PSCAD. The parameters of the SOP device are shown in Table 3.1. An average model was used to represent the SOP device, where losses, harmonics and fast switching transients of the converters were neglected [89] [90].

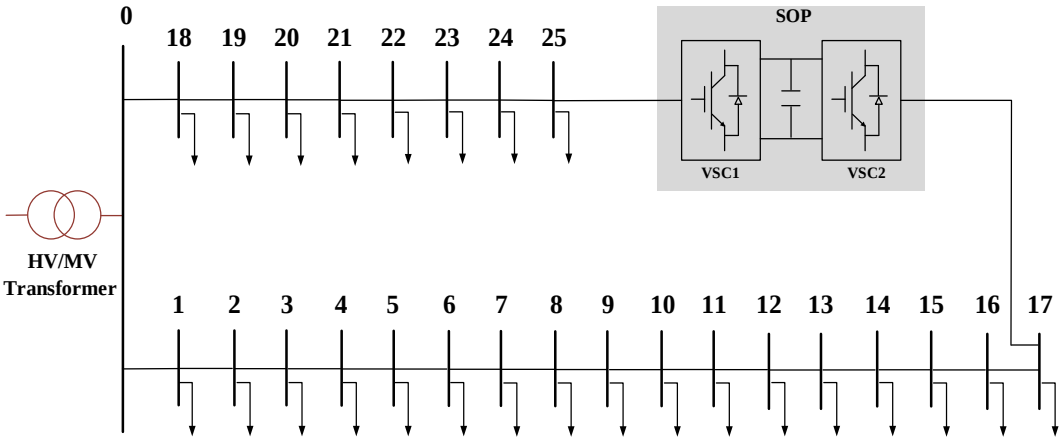

Figure 3.4: Two-feeder MV distribution network with a back-to-back VSC based SOP

Table 3.1: Parameters of the Back-to-back VSC Based SOP

Parameters	Value
DC link voltage V_{dc}	35 kV
Filter inductor L_f	5 mH
DC link capacitor *C*	600 μF
Rated power	1 MVA
Rated VSC voltage (line to line)	12.66 kV/ 50 Hz
Rated VSC current	0.08 kA

3.4.1 Normal Conditions

The feasibility of the control strategy for the power flow control mode was verified. Step changes on the active and reactive power reference signals were simulated. It was assumed that VSC1 is operated in V_{dc}-Q and VSC2 is operated in P-Q mode, as shown in Figure 3.4. The reference step changes were simulated as follows: positive and negative step changes on VSC1 reactive power ${Q_1}^*$ at 1s and 2s; on VSC2 reactive power ${Q_2}^*$ at 1.5s and 2.5s and active power ${P_2}^*$at 1.5s and 2s; the DC side voltage ${V_{dc}}^*$ remained a constant value.

Figure 3.5 shows the transient responses of the output power with respect to the step changes in reference signals. Good tracking performance was observed with accurate and rapid attainment of the steady state condition, i.e., attainted the steady state value within a few milliseconds without either an under damped response or variation. These results suggest the capability of the SOP to provide both instantaneous and longer duration power flow regulation as well as dynamic Volt/VAR control under normal network operating conditions. In addition, the DC link voltage remained a constant value except transient variations occurring upon the step change in the active power, as shown in Figure 3.5a. This is due to the step change of the active power which can cause instantaneous imbalance of power exchange at the DC link.

Such undesired transient variations are usually damped by increasing the DC link capacitance. However, it was found that when the step change in the active power decreased, the variation in the DC voltage reduced. As shown in Figures 3.5a and 3.5c, the DC voltage variation at t=2s caused by a step change of 0.5 MW was much smaller than the variation at t=1.5s caused by a step change of 1 MW. This indicates that tuning the active power controller (PI controller) for a slower transient (or step) response is viable to alleviate undesirable DC voltage variation without enlarging the DC capacitor.

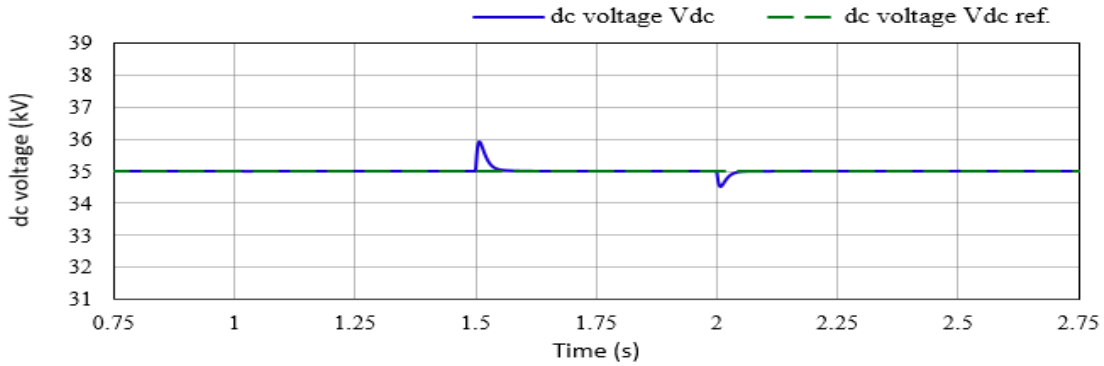

(a)

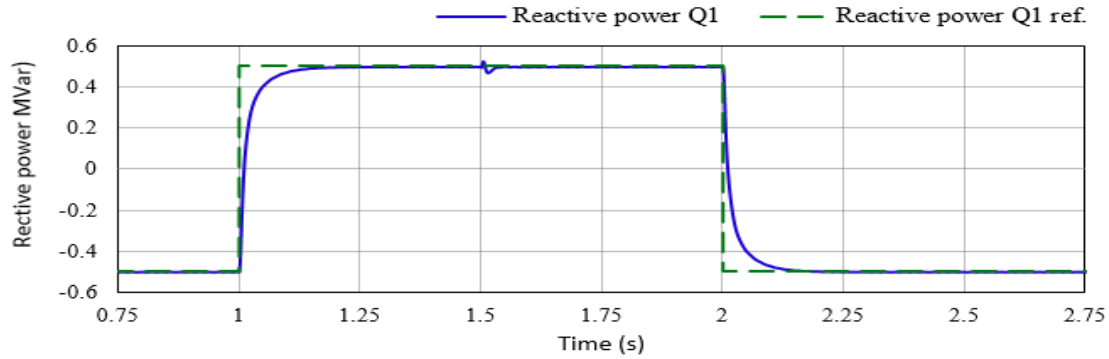

(b)

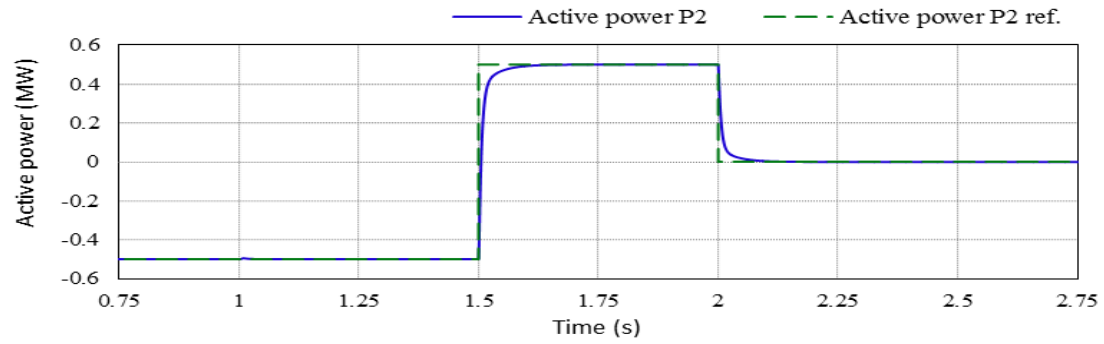

(c)

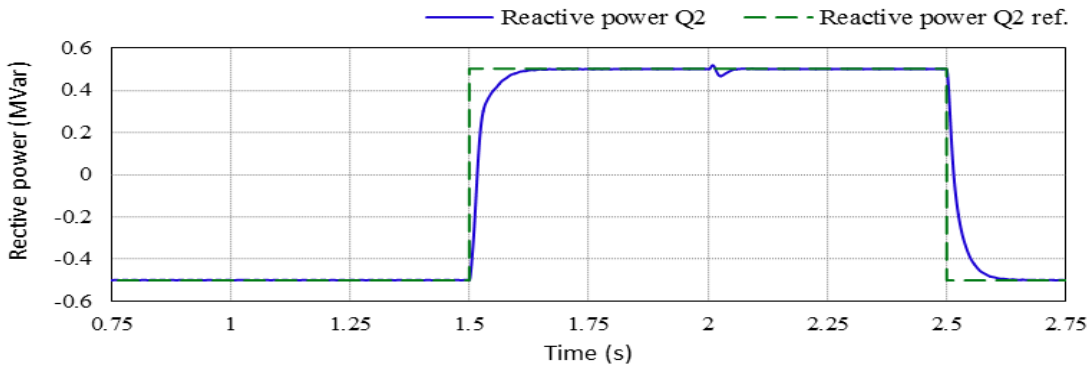

(d)

Figure 3.5: Transient response of the power flow control mode to step changes in active and reactive power references: (a) DC side voltage; (b) reactive power response of VSC1; (c) active power response of VSC2; (d) reactive power response of VSC2

3.4.2 During Fault Conditions

The behaviour of the SOP device and its controllers (power flow control mode) was investigated under both balanced and unbalanced network faults. All simulations presented in this section were conducted by assuming a fault occurs at Bus 13 (see Figure 3.4). VSC1 is operated in V_{dc}-Q and VSC2 is operated in P-Q mode.

- **Balanced fault on distribution network**

A three-phase fault was simulated at *t*=1s with a fault impedance of 3 Ω. Such a high impedance fault was chosen to avoid triggering the internal protection of the SOP device that is typically designed to limit the VSC current to 2-3 times the full load current [91]. It was assumed that the pre-fault direction of power flow is from the un-faulted side to the faulted side feeder and the circuit breaker of the faulted side VSC is tripped after 200ms.

Figure 3.6 presents the simulation results including the voltage, current and power flow on both faulted and un-faulted side VSCs. Power was flowing from the un-faulted side feeder to the faulted side feeder before the fault occurred. As seen in Figure 3.6a, the faulted side VSC had a limited contribution to the fault current before tripping the circuit breaker. The fault current became zero after tripping the circuit breaker. However, as expected its output voltage dropped to 2kV (line to ground) and thus an under-voltage protection scheme is sufficient to detect such a fault.

In contrast to the faulted side VSC, the un-faulted side VSC had a regulated output current and voltage that were not affected by the fault, as shown in Figure 3.6b. This suggests that the SOP device can effectively isolate a fault between the interconnected feeders. A reduction in the output current is observed after the fault occurred. This is due to the decrease of active power flow between the interconnected feeders.

Figure 3.6c shows the real and reactive power flow of both VSCs. Both active and reactive power outputs on the faulted side VSC (dashed line) decreased during the fault, and then became zero after tripping the circuit breaker. Nevertheless, the reactive power output on the un-faulted side VSC (solid line) remained at the pre-fault value due to the de-coupled controllability of active and reactive power.

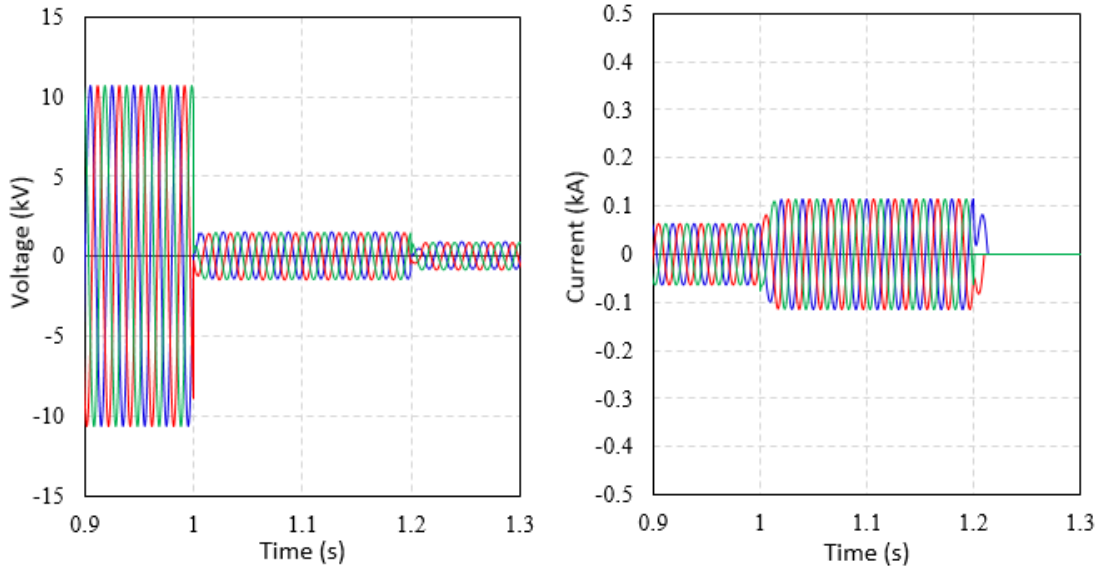

(a)

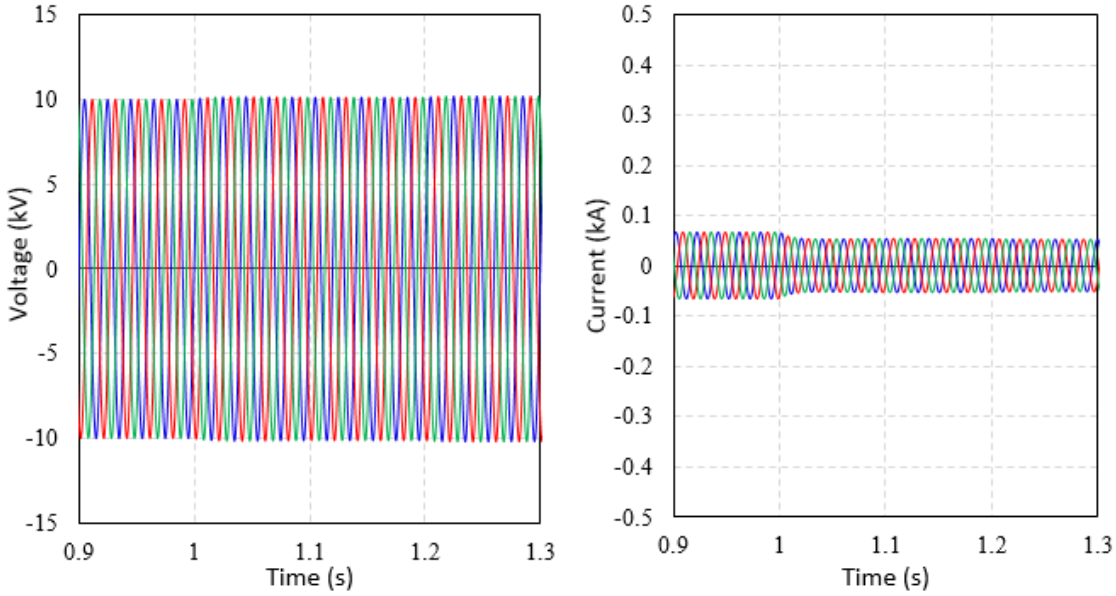

(b)

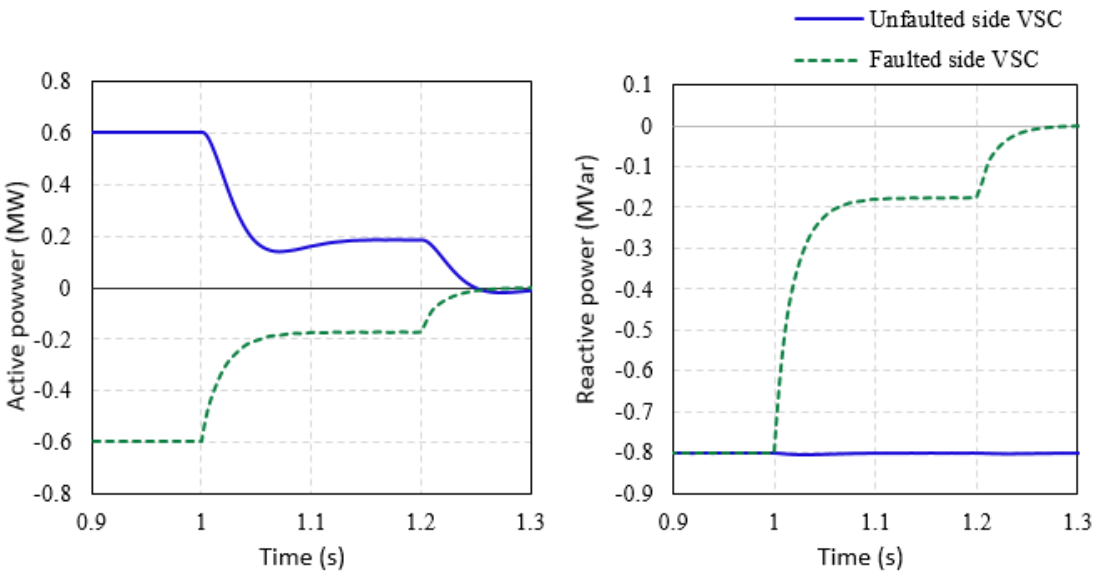

(c)

Figure 3.6: SOP response for a three-phase fault at t=1s and blocked at t=1.2s: (a) output voltage (left) and current (right) on the faulted side VSC; (b) output voltage (left) and current (right) on the un-faulted side VSC; (c) power flow behaviour on both VSCs

When the pre-fault active power was flowing from the faulted side to the un-faulted side feeder, a similar SOP response as shown in Figure 3.6 was observed

- **Unbalanced fault on distribution network**

A single-phase to ground fault was simulated at *t*=1s and cut off by tripping the circuit breaker after 200ms. The results are depicted in Figure 3.7. The faulted side VSC gave a greater contribution to the fault current than in the balanced fault case. Therefore, the network overcurrent protection is likely to react more quickly. Protection mechanisms based on negative sequence current and voltage are sufficient to protect feeders with SOP for this fault type. With respect to the un-faulted side VSC as shown in Figure 3.7b, it can be seen that both output current and voltage remained at the pre-fault values despite the large fault current on the other side VSC.

Regarding the power flow during the unbalanced fault, the output active and reactive power on the faulted side VSC remained at the pre-fault values but with notable ripple,

as depicted in Figure 3.7c. They became zero after the circuit breaker tripped. In contrast, the reactive power supplied by the un-faulted side VSC was barely affected by the fault, which remained at the pre-fault value. When the pre-fault active power flows from the faulted side to the un-faulted side feeder, the SOP performance is similar to those shown in Figure 3.7

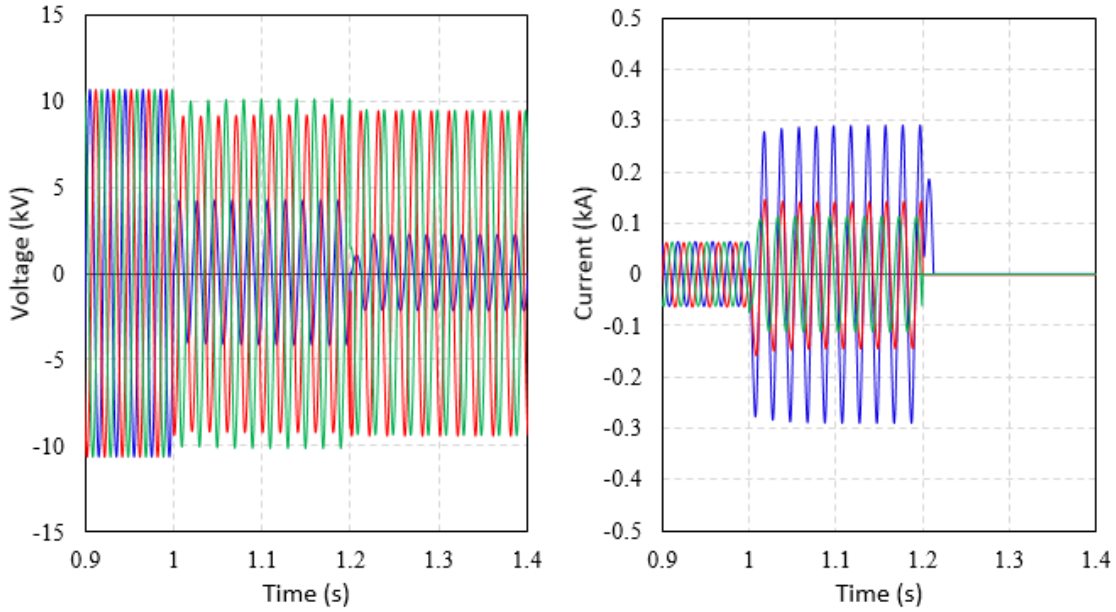

(a)

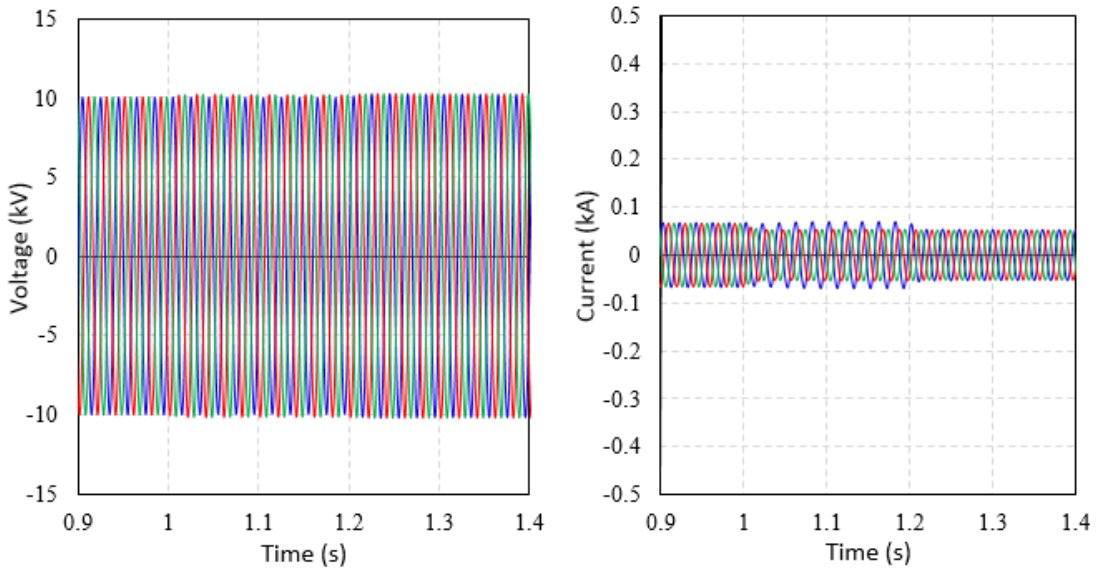

(b)

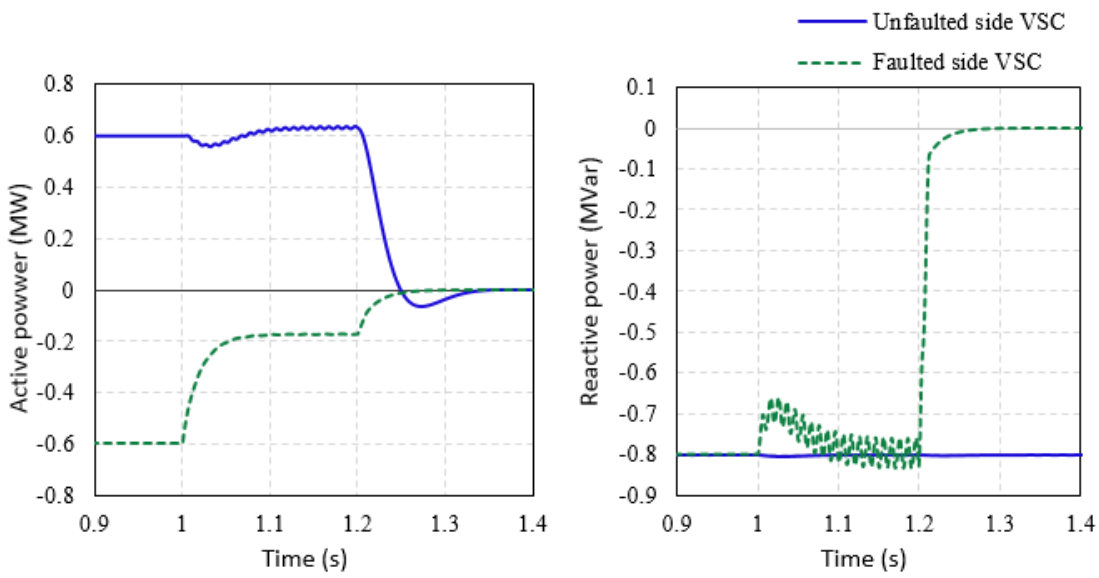

(c)

Figure 3.7: SOP response for a single-phase to ground fault at t=1s and blocked at t=1.2s: (a) output voltage (left) and current (right) on the faulted side VSC; (b) output voltage (left) and current (right) on the un-faulted side VSC; (c) power flow behaviour on both VSCs

Simulations have also been conducted when the faulted side VSC operates using the V_{dc}-Q scheme. Similar SOP performance was obtained to that shown in Figure 3.6 and Figure 3.7. From the results obtained, it is concluded that the SOP device and its controllers are effective in isolating the connected feeders during a fault, thus limiting both the fault propagation on the network and the increase of short-circuit current. In addition, despite the occurrence of a fault, the reactive power controllability on the un-faulted side VSC remains.

3.4.3 Post-fault Supply Restoration Conditions

Under this condition, the SOP is required to provide a smooth transition between different control modes: 1) from the power flow control mode to the supply restoration control mode to resume power supply to the un-faulted out-of-service loads; and 2) transfer back to the normal operation control mode when the isolated loads reconnect to the original feeder. Figure 3.8 shows the transition system based on the control modes proposed in Section 3.3. The *d*-*q* reference voltages input to the PWM modulation and

the input voltages of the PLL controller are changed by two switches 'S_1' and 'S_2'. The controllability of the transition system under the post-fault supply restoration conditions was investigated. All simulations presented in this section follow the fault occurrence described in Section 3.4.2. The feeder terminal units (FTUs) were assumed to be installed in each branch and the total power of isolated loads were within the capacity of the SOP device. Note that for a cold load pickup that exceeds the capacity of the SOP device, more complicated restoration procedure should be considered. However, this is beyond the scope of this work and will be considered as future research.

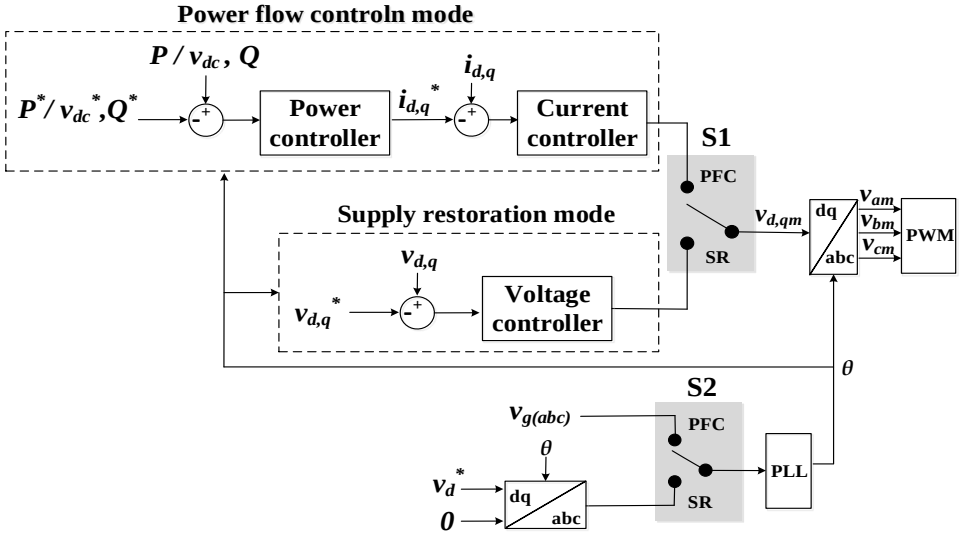

Figure 3.8: Control mode transition system

- **Transition from power flow control mode to supply restoration mode**

When a fault occurs at Bus 13 and is isolated by the network protection. The SOP is changed to supply restoration mode to support the un-faulted out-of-service loads, which is from Bus 14 to Bus 17. Once the supply restoration requirement is confirmed, switches 'S_1' and 'S_2' simultaneously change from the power flow control mode, 'PFC' to the supply restoration mode, 'SR'. It is assumed that the restoration requirement is confirmed at t=2.2s, i.e., 1s after the fault was isolated. This response delay represents

the time used by the distribution automation to isolate a permanent fault and confirm the requirement of supply restoration.

Figure 3.9 depicts the simulation results under a hard transition, i.e., directly connecting 'S_1' and 'S_2' to 'SR'. It is observed that when the output voltage waveform of the faulted side VSC was initiated from the desired reference value, a DC component was produced in the output AC current, as illustrated in Figure 3.9b. This is due to the inductive isolated loads.

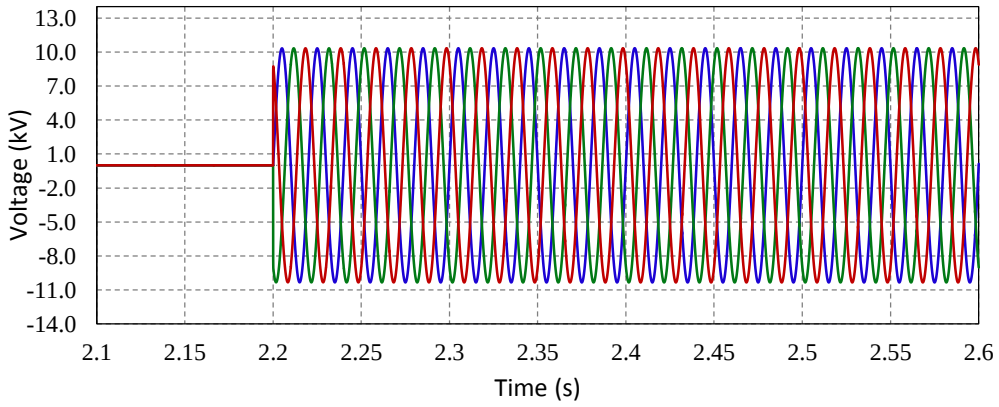

(a)

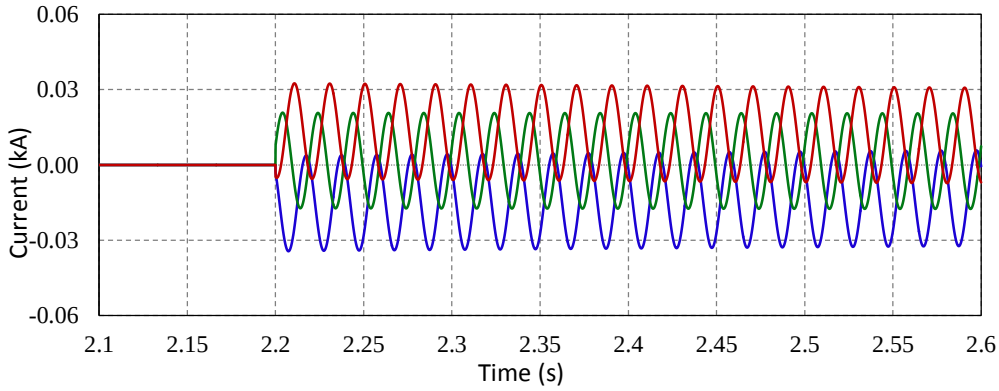

(b)

Figure 3.9: Results of a hard transition to supply restoration mode at t=2.2s: (a) output voltage waveform of the faulted side VSC; (b) output current waveform

In a highly inductive circuit, the current (sum of AC and DC currents) attempts to remain the same upon an instantaneous change in the applied voltage [92]. Therefore, when there is an instantaneous voltage change, the DC current component is produced

to compensate the change of AC current and thus lead to current DC offsets. As shown in Figure 3.10a, the current DC offsets became more severe when an inductance was connected in parallel with the isolated load (at Bus 17). Moreover, when a capacitance was connected in parallel with the isolated load (at Bus 17), a transient impulse was observed in the output current waveform, as shown in Figure 3.10b. The capacitive loads such as power factor correction and voltage support capacitors connected to the distribution network are normally not automatically disconnected from the network during fault isolation. Both of these current DC offset and transient impulse cannot be ignored due to the probability of triggering the inverter internal protection as well as the feeder protective relays.

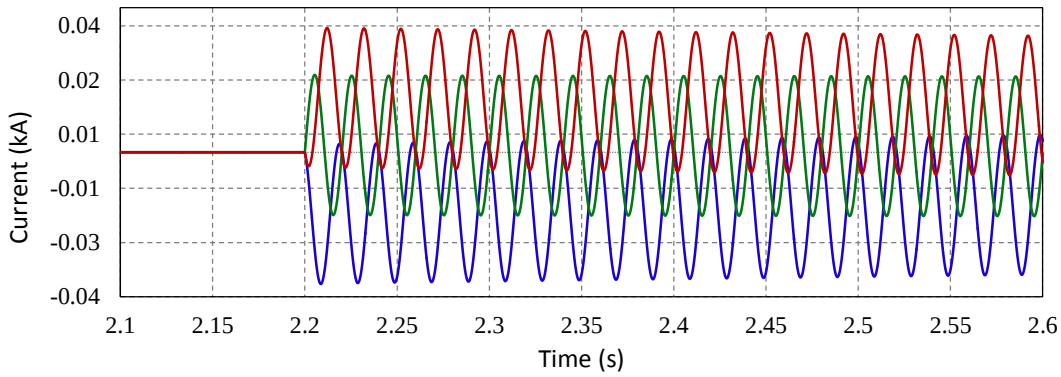

(a)

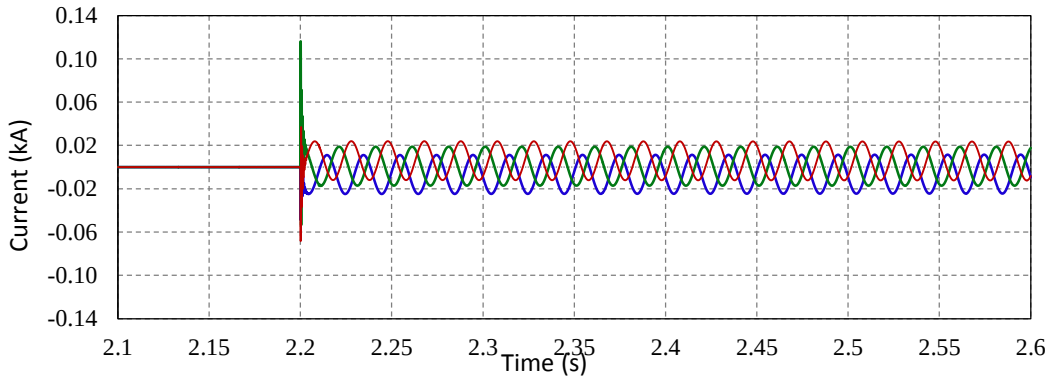

(b)

Figure 3.10: Output current waveforms of the faulted side VSC for a hard transition to supply restoration mode with: (a) an inductance connecting to Bus 17; (b) a capacitance connecting to Bus 17

A soft cold load pickup process to solve the current DC offset or inrush problems was proposed:

1) To avoid a sudden jump of the terminal voltage, at the instant of connecting switches 'S_1' and 'S_2' to 'SR', the initial values of both PLL angle and output voltage of the voltage controller are set to the values of the PLL angle and voltage magnitude just before switching to 'SR'.
2) The voltage controller (PI controller) is set for a slower transient response, i.e., a larger time constant to achieve a soft increase in the output voltage.

Figure 3.11 shows the output voltage and current waveforms after using the soft cold load pickup process. It can be seen that the output voltage was increased smoothly without a sudden jump to the reference value. The DC offset in the output current was successfully removed.

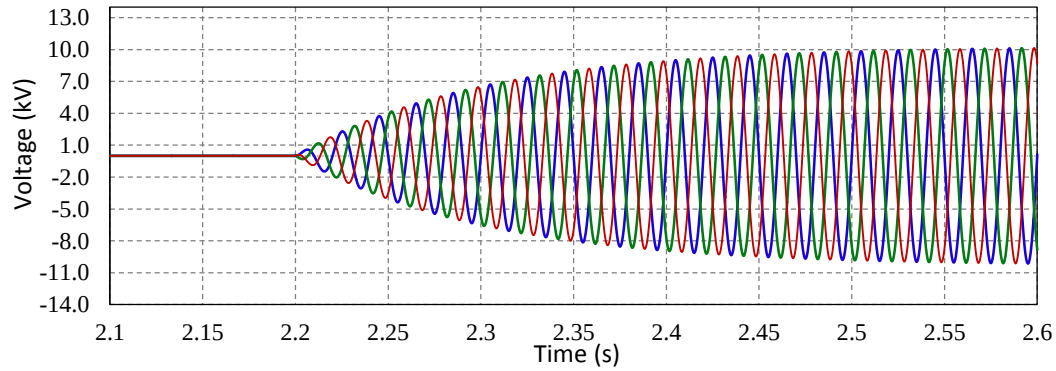

(a)

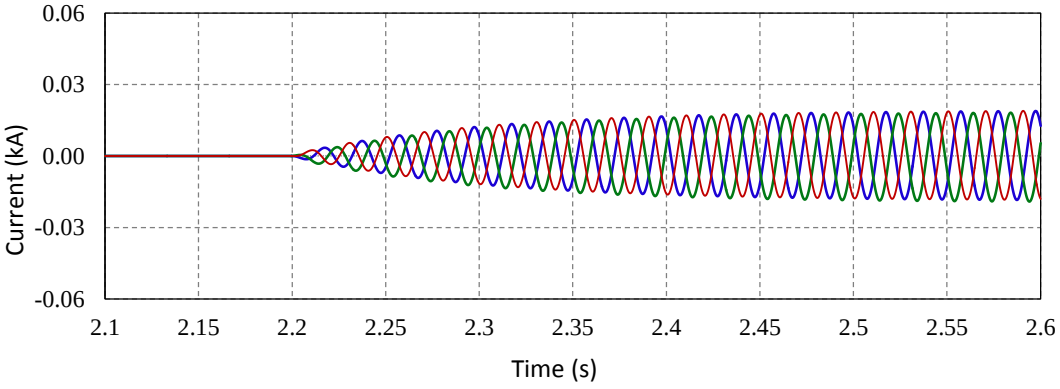

(b)

Figure 3.11: Results of a smooth transition to supply restoration mode at t=2.2s: (a) output voltage waveform of the faulted side VSC; (b) output current waveform

- **Transition from supply restoration mode to power flow control mode**

After the fault clearance, the isolated loads supplied by the SOP are reconnected to the original feeder. The SOP has to be changed from the supply restoration mode to the power flow control mode by switching 'S_1' and 'S_2'. The reconnection was assumed to occur at t=3s. Figure 3.12 depicts the simulation results under a hard transition, i.e., directly connecting 'S_1' and 'S_2' to 'PFC'. There was a current spike and voltage sag upon the transition, which may result in unexpected operation of the protection relays.

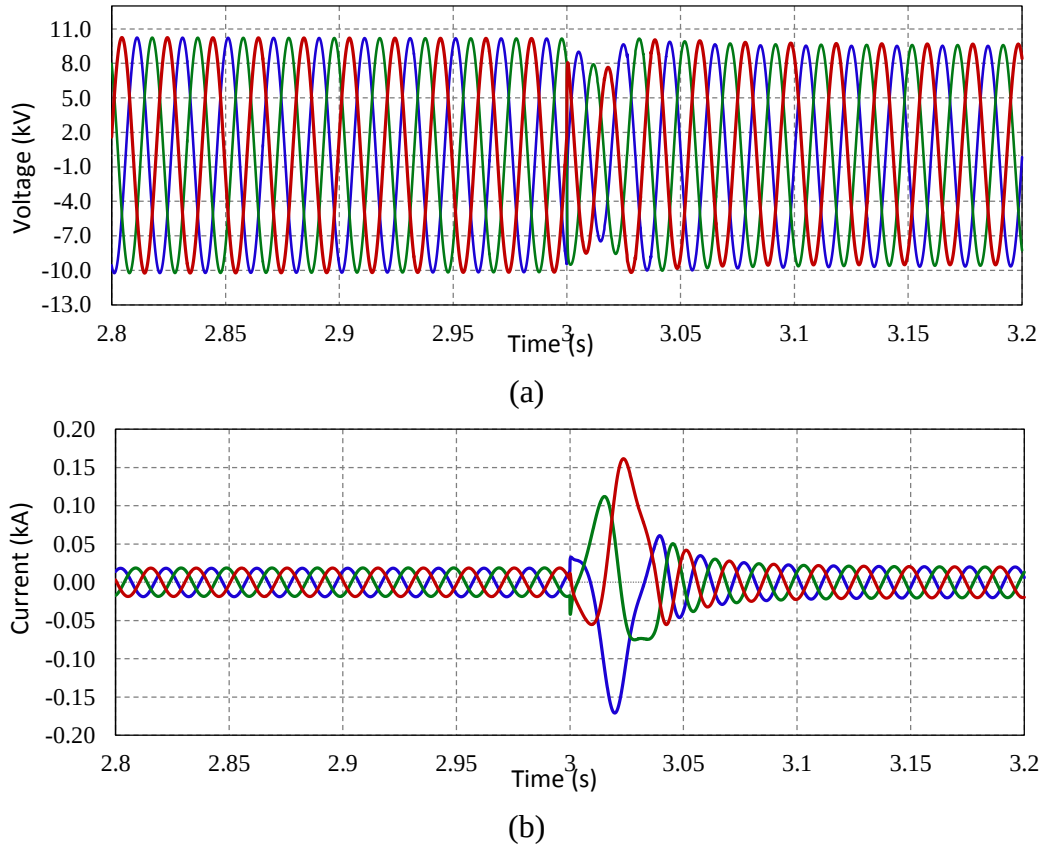

Figure 3.12: Results of a hard transition to power flow control mode at t=3s: (a) output voltage waveform of the faulted side VSC; (b) output current waveform

The reconnection is carried out after both voltage phase angle and magnitude are synchronized with the original feeder in order to avoid excessive transients. The detailed procedure for a seamless transition from the supply restoration mode to the power flow control mode is illustrated as follows:

1) Confirm that reconnection is required after the network fault has been removed.

2) The phase of the load voltage, $\angle V_{f\_r}$ at the reconnection point, i.e., at Bus 14, is synchronized with that of the original feeder voltage at Bus 13, $\angle V_{l\_r}$:

   - The phase difference between the original feeder and the reconnection point voltage is obtained by

$$\Delta\theta = \angle V_{f\_r} - \angle V_{l\_r} \tag{3-4}$$

   - Two sets of voltage values are used to obtain the information $\Delta\theta$

$$a = V_{f\_ra} \cdot V_{l\_ra} + V_{f\_rb} \cdot V_{l\_rb} + V_{f\_rc} \cdot V_{l\_rc} = \frac{3}{2}\cos\Delta\theta \tag{3-5}$$

$$\begin{aligned} b &= V_{l\_ra} \cdot V_{f\_rb} + V_{l\_rb} \cdot V_{f\_rc} + V_{l\_rc} \cdot V_{f\_ra} \\ &= \frac{3}{4}[-\cos\Delta\theta + \sqrt{3}\sin\Delta\theta] \end{aligned} \tag{3-6}$$

   Combining (3-5) and (3-6), $\sin\Delta\theta$ can be found as

$$\sin\Delta\theta = \frac{\sqrt{3}}{3} \cdot \left(\frac{4}{3}b + \frac{2}{3}a\right) \tag{3-7}$$

Figure 3.13 shows an overview of the phase synchronisation process. 'S_2' is switched to 'PFC' after the phase synchronisation is completed.

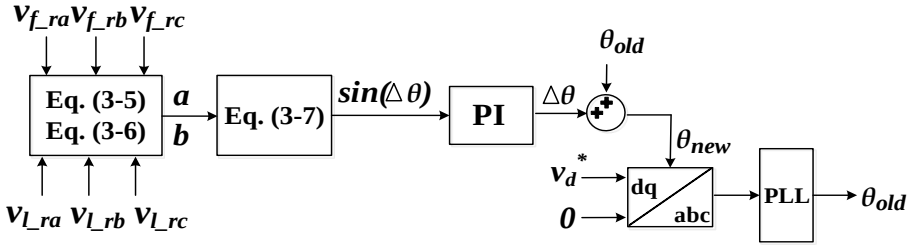

Figure 3.13: Synchronisation controller

3) The d–q feeder voltages are assigned as the d–q voltage references of the voltage controller in order to adjust the magnitude of the load voltage to that of

the grid voltage.

4) When both phase and magnitude of the output voltage match the original feeder voltage, 'S_1' is switched to 'PFC', and the isolated loads are reconnected to the original feeder. To prevent large transient flows of real and reactive power, the integers in both power and current controllers are reset and the reference values of real and reactive power are set as the value before transfer to the power flow control mode.

Figure 3.14 shows the synchronisation of the voltages when the synchronisation algorithm started to work in the supply restoration mode. As can be seen, the synchronisation process successfully forced the voltage at the end of the isolated area to track the voltage at the original feeder.

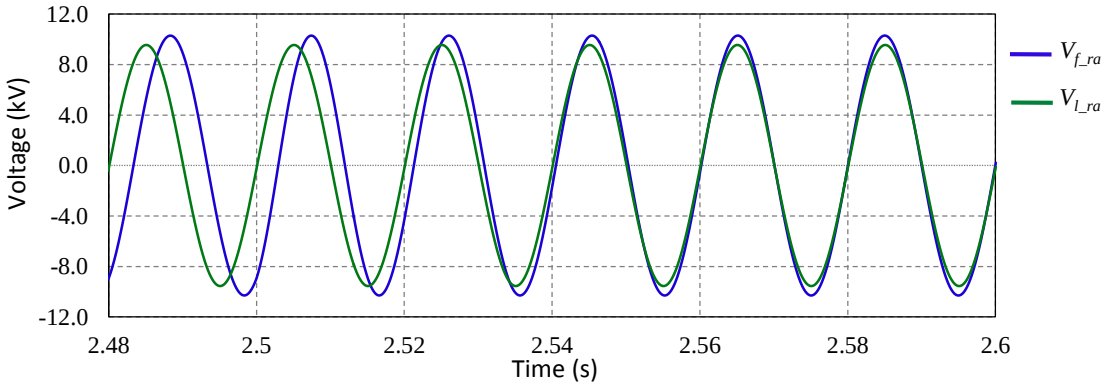

(a)

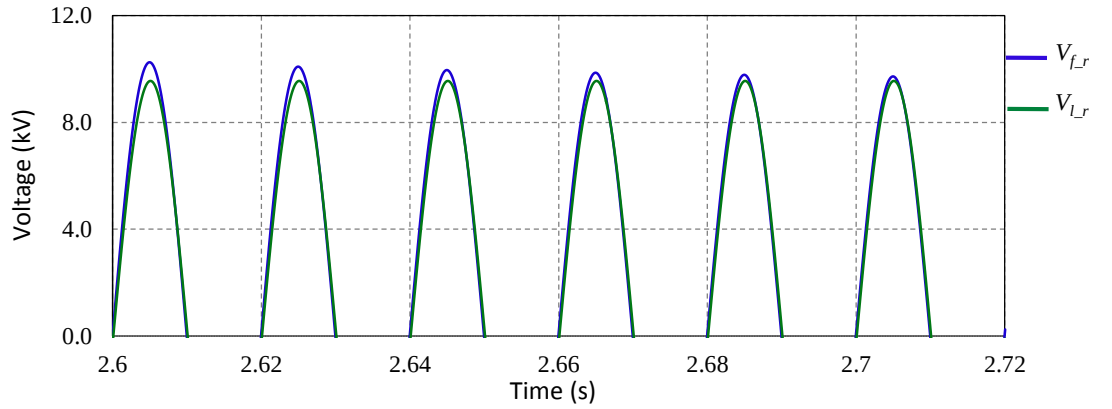

(b)

Figure 3.14: Voltage synchronisations for reconnection: (a) phase synchronisation; (b) magnitude synchronisation

Figure 3.15 depicts the output voltage and current waveforms of the faulted side VSC after using the synchronisation process. The current spike and voltage sag were successfully reduced.

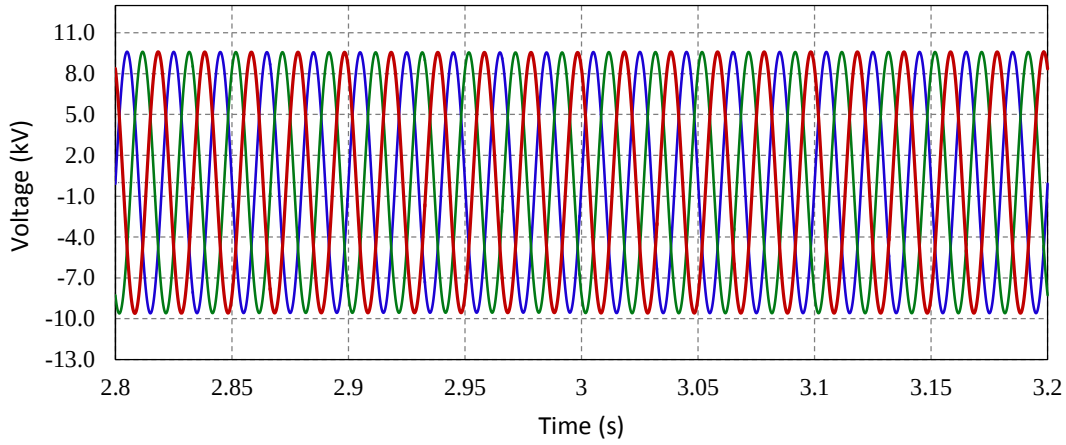

(a)

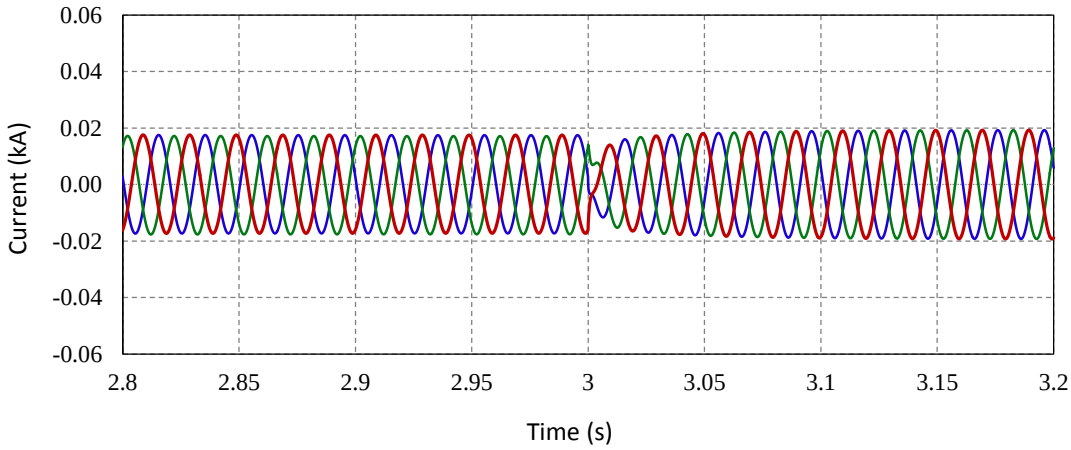

(b)

Figure 3.15: Results of a smooth transition to power flow control mode: (a) output voltage waveform of the faulted side VSC; (b) output current waveform

3.5 Summary

Two control modes were developed for the operation of a back-to-back VSC based SOP. For the power flow control mode, a dual closed-loop current-controlled strategy was used to regulate both active and reactive power on the connected feeders. For the supply restoration mode, a voltage and frequency control strategy was proposed to

provide fast power supply restoration when the loads connected to one side of SOP are isolated due to network faults. The operational principle of the back-to-back VSC based SOP was analysed under both normal and abnormal network operating conditions. Case studies based on a two-feeder MV distribution network evaluated the performance of the SOP device with the two control modes under normal, faults and post-fault supply restoration conditions.

Under normal conditions, the proposed SOP controller provides both instantaneous and longer duration power flow regulation between the interconnected feeders and dynamic Volt/VAR support on both terminals.

During fault conditions, the SOP controller (power flow control mode) is able to isolate both balanced and unbalanced network faults between interconnected feeders. The SOP is therefore capable of limiting both the fault propagation on the network and the increase of the short-circuit current.

Under post-fault supply restoration conditions, the SOP device was demonstrated to be effective in providing fast supply restoration through a smooth transition between the power flow control and the supply restoration modes. For the transition from the power flow control mode to the supply restoration mode, a soft cold load pickup process was preferred over the hard transition. The soft cold load pickup process removed the DC offset and inrush problems of the output current which may trigger unexpected protection operations. For the transition from the supply restoration mode to the power flow control mode, the undesirable current impulse and voltage drop were reduced after the use of the voltage synchronisation procedure and the reset of current and power controllers.

Chapter 4

Benefits Analysis of SOPs for MV Distribution Network Operation

THIS chapter investigates the operational benefits of SOPs for MV distribution network operation including power loss minimization, feeder load balancing and voltage profile improvement.

4.1 Introduction

In this chapter, a steady state analysis framework was developed to quantify the operational benefits of a MV distribution network with SOPs.

A generic power injection model of an SOP for steady state analysis was developed, which takes into account both physical limitations and internal power losses of the SOP device, using back-to-back VSCs. Based on the SOP model, an improved Powell's direct set method was developed to obtain the optimal SOP operation. Distribution network reconfiguration algorithms, with and without SOPs, were also developed and used to identify the benefits of using SOPs.

The performance of using SOPs, traditional network reconfiguration and the combination of both was compared and analysed based on a 33-bus distribution network. The impact of DG connections and the impact of SOP device losses were also evaluated through quantitative and sensitive analysis.

4.2 Modelling of Soft Open Points

Figure 4.1a shows a typical location of an SOP which allows power electronic devices to control active power flow between connected feeders and to supply or absorb reactive power at its interface terminals under normal network operating conditions. A generic power injection model of SOP was developed. This model considers SOP terminal power injections and hence enables the incorporation of SOPs into existing power flow analysis algorithms without considering the detailed controller design.

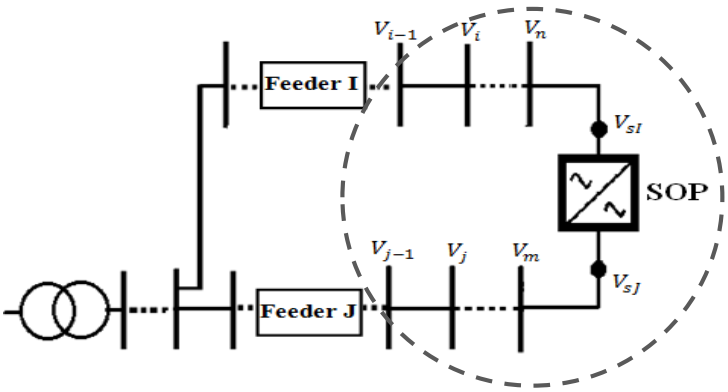

(a)

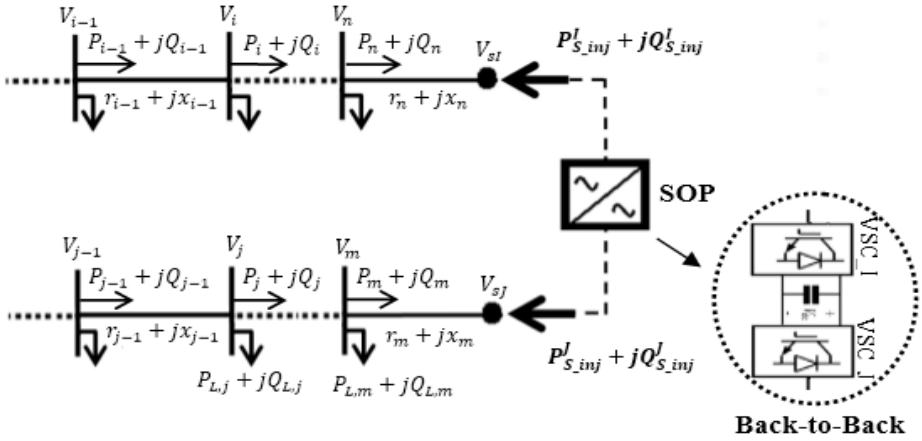

(b)

Figure 4.1: (a) Simple distribution network with an SOP; (b) Power injection model of SOP for distribution network power flow control

Figure 4.1b shows the representation of an SOP model with real and reactive power, injecting into feeders *I* and *J* through both terminals. Taking these power injections as decision variables, the power flow in feeder *I* is calculated by the following set of recursive equations [93]:

$$P_i = P_{i-1} - P_{Loss\,(i-1,\ i)} - P_{L,i} = P_{i-1} - \frac{r_{i-1}}{|V_{i-1}|^2} \cdot (P_{i-1}{}^2 + Q_{i-1}{}^2) - P_{L,\mathrm{i}} \qquad (4\text{-}1)$$

$$Q_i = Q_{i-1} - Q_{Loss\,(i-1,\ i)} - Q_{L,i} \quad = Q_{i-1} - \frac{x_{i-1}}{|V_{i-1}|^2} \cdot (P_{i-1}{}^2 + Q_{i-1}{}^2) - Q_{L,\mathrm{i}} \qquad (4\text{-}2)$$

$$|V_i|^2 = |V_{i-1}|^2 - 2 \cdot (r_{i-1}P_{i-1} + x_iQ_i) + \frac{(r_{i-1}{}^2 + x_{i-1}{}^2)}{|V_{i-1}|^2} \cdot (P_{i-1}{}^2 + Q_{i-1}{}^2) \qquad (4\text{-}3)$$

with boundary conditions:

$$\left|P_n + P^I_{S\_inj}\right| = P_{Loss\,(n,\ sI)} \tag{4-4}$$

$$\left|Q_n + Q^I_{S\_inj}\right| = Q_{Loss\,(n,\ sI)} \tag{4-5}$$

where P represents active power, Q reactive power, V nodal voltage, r resistance and x reactance. Subscript $Loss$ denotes line losses, and L denotes load. The variables and parameters are shown in Figure 4.1b. Similar recursive power flow equations with boundary conditions are applied to feeder *J*.

To consider the internal losses of the SOP equipment, the following equality constraint of power balance is used:

$$P^I_{S\_inj} + P^J_{S\_inj} + P_{SOP,Loss} = 0 \tag{4-6}$$

where $P_{SOP,Loss}$ denotes the internal power losses of the whole SOP device.

Various types of power electronic devices can be implemented as an SOP, such as UPFC, back-to-back VSCs and multi-terminal VSCs. In this work, back-to-back VSCs were used. Constraints of such device due to the physical limitations and the internal power losses are formulated as follows.

4.2.1 Physical Limitations of Back-to-Back Converters

As described in Section 2.3, back-to-back VSCs consist of two VSCs connected via a DC link. Both VSCs are able to provide fast and independent control of active and reactive power in all four quadrants of the P-Q plane. The terminal power injections of back-to-back VSCs operated as a SOP are controlled directly by each VSC, the operational limits of VSC capacity and terminal voltage are considered as:

$$\sqrt{{P_{S\_inj}^{I}}^{2} + {Q_{S\_inj}^{I}}^{2}} \leq S_{VSC,rate}^{I} \tag{4-7}$$

$$V_{sI} \leq V_{VSC,rate}^{I} \tag{4-8}$$

where $S_{VSC,rate}^{I}$ is the power rating of the VSC connected to feeder *I*; V_{sI} and $V_{VSC,rate}^{I}$ denote the actual and maximum AC terminal voltage. Similar constraints are applied to the other side VSC connected to feeder *J*.

4.2.2 Internal Power Losses of Back-to-Back Converter

Internal power losses of the back-to-back device are made up of the losses of its individual components, including the semiconductors (conduction and switching losses), passive components (DC link capacitor, filter, AC line choke), transformers and the cooling system.

As suggested in [94], these losses can be categorized into three components: no load losses, linear and quadratic losses depending on the converter current, which is a function of the active and reactive power exchanged with the AC network:

$$P_{VSC,Loss}^{I} = a^{I} \cdot {I_{VSC}^{I}}^{2} + b^{I} \cdot I_{VSC}^{I} + c^{I} \tag{4-9}$$

$$I_{VSC}^{I} = \frac{\sqrt{{P_{S\_inj}^{I}}^{2} + {Q_{S\_inj}^{I}}^{2}}}{|V_{sI}|} \tag{4-10}$$

where $P_{VSC,Loss}^{I}$ and I_{VSC}^{I} represent the power losses and the AC current of the VSC connecting to feeder *I*. Similar equations are applied to the other side VSC. Thus all equations shown in the following section only illustrate the VSC connected to feeder *I*.

As shown in (4-9), the total losses are determined by the coefficients, a^{I}, b^{I} and c^{I}. These coefficients are difficult to obtain due to the limited information from the open literature or manufacturers. Usually only the internal power losses (or efficiency) under

nominal conditions (rated power) and the no load loss, c^I are given.

A linear function is used to approximate the quadratic one in (4-9):

$$P^I_{VSC,Loss} = k^I \cdot I^I_{VSC} + c^I \tag{4-11}$$

$$k^I = (P^I_{VSC,Loss,rate} - c^I)/I^I_{VSC,rate} \tag{4-12}$$

where $P^I_{VSC,Loss,rate}$ and $I^I_{VSC,rate}$ are power losses and AC current of the VSC connected to feeder *I* under nominal condition.

Comparing the internal power losses derived from (4-9) and (4-11), as shown in Figure 4.2, it is noted that when $I^I_{VSC} \leq I^I_{VSC,rate}$, the device power losses using the approximate model are higher than those using the quadratic one, i.e., more conservative conclusions are drawn. Therefore, the approximate model was used in this work.

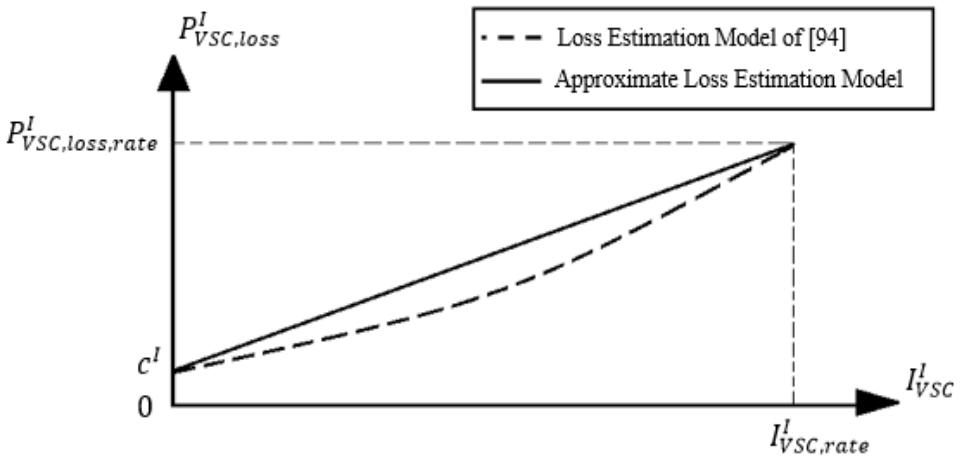

Figure 4.2: Comparison between the quadratic and approximate loss estimation function

4.3 Optimal Operation of the Soft Open Points

The benefits of SOPs for both system loss reduction and feeder load balancing were investigated. To quantify these benefits, the amounts of real and reactive power injections of the SOPs were determined through solving a combinational nonlinear constrained optimization problem.

4.3.1 Problem Formulation

Two objective functions are used separately to quantify the optimality of the SOP operation.

- **Active power loss minimization**

The active power losses consist of two components: the feeder losses and the internal power losses of the SOP devices. The active power loss minimization problem is formulated as:

$$Minimize \quad P_{T,Loss} = \sum_{k=1}^{n_l} r_k \cdot \frac{{P_k}^2+{Q_k}^2}{|V_k|^2} + P_{SOP,Loss} \tag{4-13}$$

where r_k, P_k, Q_k, V_k are resistance, active power, reactive power, and voltage of branch *k*; and n_l is the total number of branches in the network.

- **Feeder load balancing**

A branch loading index LI_k is used to measure the loading level of each branch in the network, which is expressed as:

$$LI_k = \left(\frac{I_k}{I_{k,rate}}\right)^2 \quad \forall\, k \in n_l \tag{4-14}$$

where I_k and $I_{k,rate}$ are the actual and the rated branch current of branch *k*.

Feeder load balancing is achieved by minimizing the load balance index LBI, which is defined as the sum of branch load balancing indices, as shown in (4-15):

$$Minimize \quad LBI = \sum_{k=1}^{n_l} LI_k \tag{4-15}$$

- **Constraints**

Constraints of the distribution network and the SOP devices are considered. The device constraints of each SOP are shown in (4-6)-(4-8). The network constraints are expressed as follows:

$$g(x, s) = 0 \tag{4-16}$$

$$\left|V_{i,min}\right| \leq |V_i| \leq \left|V_{i,max}\right| \ \forall\, i \in n_b \tag{4-17}$$

$$|S_k| \leq \left|S_{k,max}\right| \ \forall\, k \in n_l \tag{4-18}$$

where $g(x, s), V_{i,min}, V_{i,max}$ and $S_{k,max}$ are the power flow equations, the minimum and the maximum voltage of bus i and the maximum capacity allowed in branch k. n_b are the total number of buses of the network.

- **Penalty function**

Constrains of mentioned above are included into the objective function by using the penalty function method. In this way, unconstrained optimization methods are used directly by solving the transformed objective function (with penalty terms):

$$Minimize \quad F_{obj}(\boldsymbol{S}) = \{P_{T,Loss} \ or \ LBI\} + k_1 \cdot f_{SOP} + k_2 \cdot f_V + k_3 \cdot f_S \tag{4-19}$$

where k_1, k_2, k_3 are the penalty constants; $f_{SOP}, f_V,$ and f_S are the penalty functions for violations of the SOP device constraints, the network voltage and capacity constraints; $\boldsymbol{S}$ denotes the decision variable vector.

Based on the power injection model of SOP in Section 4.2, the real and reactive power injections at both terminals are specified as the decision variables: with one SOP installation, $\boldsymbol{S} = [P^I_{S_{inj}}, Q^I_{S_{inj}}, Q^J_{S_{inj}}]^{\mathrm{T}}$. $P^J_{S\_inj}$ is not included in $\boldsymbol{S}$ since it is determined if

$\boldsymbol{S}$ is specified according to the equality constraint equation of (4-6). Therefore, the coordinates of *n* SOPs are combined together sequentially to obtain a point of $\boldsymbol{s}$ in a *3n*-dimentional space, thus

$$\boldsymbol{S} = [P^I_{S\_inj,\ 1}, Q^I_{S\_inj,\ 1}, Q^J_{S\_inj,\ 1}, P^I_{S\_inj,\ 2}, Q^I_{S\_inj,\ 2}, Q^J_{S\_inj,\ 2},$$
$$\ldots, P^I_{S_{inj},\ n}, Q^I_{S_{inj},\ n}, Q^J_{S_{inj},\ n}]^{\mathrm{T}} \quad (4\text{-}20)$$

4.3.2 Method of Determining Optimal SOP Operation

Based on the Powell's Direct Set (PDS) method presented in [95], an improved PDS method to optimize the SOP operation was developed. The performance improvement is achieved by obtaining a good initial approximated SOP operation.

- **Powell's Direct Set method**

Most mathematical optimization methods require expressions of the derivatives to define the direction of movement, i.e. search the direction approaching to the optimum (from a starting point).

The Powell's Direct Set method is a direct search method proposed by Powell *et al.* [95]. It defines the search directions in a direct manner, i.e., solely depending on the objective function itself. Therefore, this method is easy to implement and is not limited by the existence of derivatives of the objective function. It has been successfully applied to solve problems for which it is difficult or impossible to calculate the derivatives [96-98].

A comprehensive review of PDS method as well as the mathematical proof of its convergence were given in [95]. Three key properties of this method are highlighted below:

i. For an *N*-dimensional problem, minimization is achieved by an iterative procedure that searches down *N* linear independent directions within each iteration, i.e. starting from the best known approximation to the optimum.

ii. Fast convergence to the optimum is achievable by only searching down *N* mutually conjugate directions. The optimal solution of a quadratic function has been proved achievable by searching along those mutually conjugate directions once only. Hence only *N* iterations are required to solve the *N*-dimensional quadratic problem [95]. The efficacy has also been demonstrated for any other function forms, as presented in [96, 97], but may require more iterations.

iii. The mutually conjugate directions are generated after each iteration, as illustrated in the following part.

- **PDS method for optimal SOP operation**

The process of determining optimal SOP operation using the PDS method is shown in Figure 4. 3.

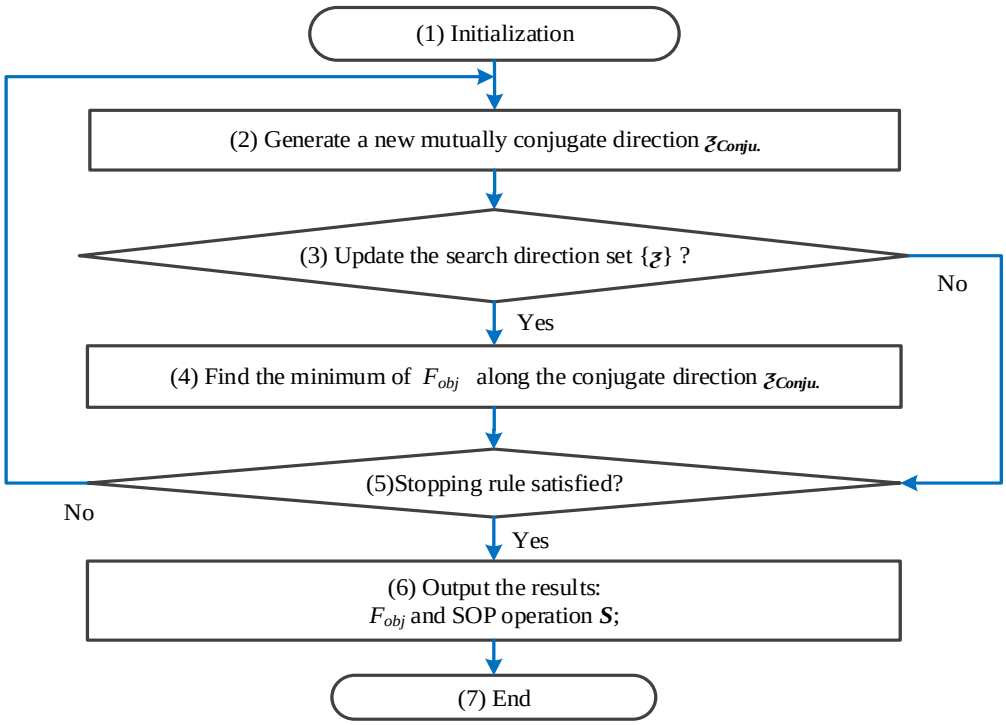

Figure 4.3: Flow chart of the proposed PDS method

STEP 1): Initialization. Based on (4-20), the initial approximate SOP operation $\boldsymbol{S_0^{(1)}}$, the initial search direction set with 3*n* linear independent search directions, $\{\boldsymbol{\xi}\}^{(\mathbf{1})} = \{\boldsymbol{\xi_1^{(1)}}, \ldots, \boldsymbol{\xi_i^{(1)}}, \ldots, \boldsymbol{\xi_{3n}^{(1)}}\}$ and the convergence criterion ε are specified. The 3*n* directions in $\{\boldsymbol{\xi}\}^{(\mathbf{1})}$ are initially chosen to be the co-ordinate directions (linear independent). This means only one decision variable in (4-20) will be changed when searching along one direction.

STEP 2): Generate a new mutually conjugate direction within one iteration. There are two sub steps:

i. Starting from $\boldsymbol{S_0^{(k)}}$, *k* indicates the iteration number (one iteration includes searching along 3*n* directions, *k*=1 initially), sequentially find $\boldsymbol{S_i^{(k)}}$ which gives the minimum of the objective function (4-19) along each search direction, $\boldsymbol{\xi_i^{(k)}}$ in $\{\boldsymbol{\xi}\}^{(\boldsymbol{k})}$, which is expressed as:

$$Min \quad F_{obj}\left(\boldsymbol{S_i^{(k)}}\right) = F_{obj}\left(\boldsymbol{S_{i-1}^{(k)}} + \lambda_i \cdot \boldsymbol{\xi_i^{(k)}}\right), \quad i=1, 2,\ldots, 3n \qquad (4\text{-}21)$$

In this work, a one-dimensional search method, the golden section search [95], was adopted to calculate the optimal step size, λ_i. The load flow analysis method introduced in [99] combined with the SOP injection model formulated in (4-1) - (4-6) was implemented as a subroutine to calculate the objective function $F_{obj}\left(\boldsymbol{S_i^{(k)}}\right)$ in (4-21).

ii. After searching down the 3*n* directions, a conjugate direction is generated by (4-22)

$$\boldsymbol{\xi_{conju.}^{(k)}} = \boldsymbol{S_{3n}^{(k)}} - \boldsymbol{S_0^{(k)}} \qquad (4\text{-}22)$$

STEP 3): Update the search direction set for the next iteration $\{\boldsymbol{\xi}\}^{(\boldsymbol{k+1})}$. Two scenarios are considered:

i. If n=1, discard the first direction $\boldsymbol{\xi}_{\mathbf{1}}^{(k)}$ in $\{\boldsymbol{\xi}_{\boldsymbol{i}}^{(k)}\}$ by adding $\boldsymbol{\xi}_{\boldsymbol{conju.}}^{(k)}$ to the end, as shown in (4-23):

$$\{\boldsymbol{\xi}\}^{(\boldsymbol{k+1})} = \left\{ \boldsymbol{\xi}_{\mathbf{2}}^{(k)}, \boldsymbol{\xi}_{\mathbf{3}}^{(k)}, \dots, \boldsymbol{\xi}_{\boldsymbol{3n}}^{(k)}, \boldsymbol{\xi}_{\boldsymbol{conju.}}^{(k)} \right\} \tag{4-23}$$

ii. If n>1, a 'smarter' updating procedure is required to ensure a reasonable rate of convergence, i.e., replace the direction in $\{\boldsymbol{\xi}\}^{(\boldsymbol{k})}$, which shows the worst performance. The general procedure is presented as follows [95]:

- Find $\boldsymbol{\xi}_{\boldsymbol{m}}^{(k)}$ that gives maximum reduction among the previous one-dimensional searching processes in Step 2, as shown in (4-24):

$$\Delta_{max} = \underset{\mathbf{1} \le \boldsymbol{m} \le \mathbf{3n}}{Max} \left\{ F_{obj}\left(\boldsymbol{S}_{\boldsymbol{m-1}}^{(k)}\right) - F_{obj}\left(\boldsymbol{S}_{\boldsymbol{m}}^{(k)}\right) \right\} \tag{4-24}$$

- Replace $\boldsymbol{\xi}_{\boldsymbol{m}}^{(k)}$ by $\boldsymbol{\xi}_{\boldsymbol{conju.}}^{(k)}$ to give more efficient convergence if the following two criterions are satisfied:

$$\left.\begin{array}{c} (w_1 - 2w_2 + w_3)(w_1 - w_2 - \Delta_{max})^2 < 0.5 \cdot \Delta_{max}(w_1 - w_3)^2 \\ w_3 < w_1 \end{array}\right\} \tag{4-25}$$

where $w_1 = F_{obj}\left(\boldsymbol{S}_{\mathbf{0}}^{(k)}\right)$, $w_2 = F_{obj}\left(\boldsymbol{S}_{\boldsymbol{3n}}^{(k)}\right)$, $w_3 = F_{obj}\left(2 \cdot \boldsymbol{S}_{\boldsymbol{3n}}^{(k)} - \boldsymbol{S}_{\mathbf{0}}^{(k)}\right)$. Thus,

$$\{\boldsymbol{\xi}\}^{(\boldsymbol{k+1})} = \{ \boldsymbol{\xi}_{\mathbf{1}}^{(k)}, \dots, \boldsymbol{\xi}_{\boldsymbol{m-1}}^{(k)}, \boldsymbol{\xi}_{\boldsymbol{conju.}}^{(k)}, \boldsymbol{\xi}_{\boldsymbol{m+1}}^{(k)}, \dots, \boldsymbol{\xi}_{\boldsymbol{3n}}^{(k)} \} \tag{4-26}$$

Otherwise$\{\boldsymbol{\xi}\}^{(\boldsymbol{k})}$is not updated in this iteration, let $\boldsymbol{S}_{\mathbf{0}}^{(k+1)} = \boldsymbol{S}_{\boldsymbol{3n}}^{(k)}$ and jump to Step 5.

STEP 4): Search down along the conjugate direction. Calculate λ as (4-21) so that $F_{obj}(\boldsymbol{S}_{\boldsymbol{0}}^{(k+1)})$ reaches its minimum along the conjugate direction generated in (4-22). Let $\boldsymbol{S}_{\boldsymbol{0}}^{(k+1)} = \boldsymbol{S}_{\boldsymbol{3n}}^{(k)} + \lambda \cdot \boldsymbol{\xi}_{\boldsymbol{conju.}}^{(k)}$.

STEP 5): *Convergence check.* If $\left\| \boldsymbol{S}_{\boldsymbol{0}}^{(k+1)} - \boldsymbol{S}_{\boldsymbol{0}}^{(k)} \right\| > \varepsilon$, let k=k+1 and then go to Step 2, else stop.

An example shown in Figure 4.4 illustrates the searching of the optimization process. As the red solid line shows, the optimization starts from an initial approximation $\boldsymbol{S}_{\boldsymbol{0}}^{(1)}$ and then reaches the minimum $\boldsymbol{S}_{\boldsymbol{1}}^{(1)}$, $\boldsymbol{S}_{\boldsymbol{2}}^{(1)}$, $\boldsymbol{S}_{\boldsymbol{3}}^{(1)}$along each of the coordinate directions in $\{\boldsymbol{\xi}\}^{(\boldsymbol{1})}$. The first conjugate direction $\boldsymbol{\xi}_{\boldsymbol{conju.}}^{(1)}$ is hence obtained, as shown by the blue dotted arrow. After searching along the conjugate direction, a new approximation $\boldsymbol{S}_{\boldsymbol{0}}^{(2)}$ is obtained for the second iteration.

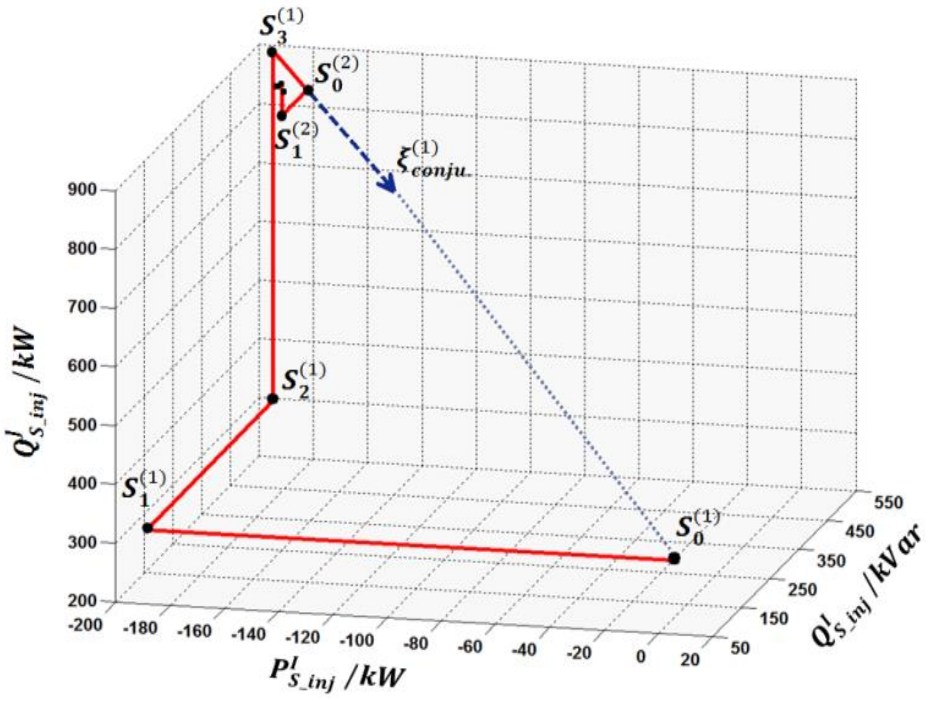

Figure 4.4: Example of one SOP optimization by PDS method

- **Determine the initial approximated SOP operation**

The PDS method is able to start from any initial point $\boldsymbol{S_0^{(1)}}$. A good approximation of SOP operation is obtained by running the PDS method once using the objective function of (4-21) with simplified power flow equations given by [99]:

i. All nodal voltage magnitudes are assumed to be 1 *p.u.*, equations (4-13) and (4-15) are reduced to

$$P_{Loss} \approx \sum_{k=1}^{n_l} r_k \cdot ({P_k}^2 + {Q_k}^2) + P_{SOP,Loss} \tag{4-27}$$

$$LIB \approx \sum_{k=1}^{n_l} \frac{{P_k}^2+{Q_k}^2}{{I_{k,rate}}^2} \tag{4-28}$$

ii. Ignoring all the quadratic terms (line losses) from the power flow equations in (4-1)-(4-3). The branch power P_k and Q_k are obtained by summing up the downstream power loads:

$$P_k \approx \sum_{i=k+1}^{n} P_{L,i} \tag{4-29}$$

$$Q_k \approx \sum_{i=k+1}^{n} Q_{L,i} \tag{4-30}$$

The constraints of nodal voltage and branch capacity are considered by:

$$|V_i|^2 \approx |V_0|^2 - 2\sum_{k=1}^{i}(r_k P_k + x_k Q_k) \leq {V_{max}}^2 \tag{4-31}$$

$$S_k \approx ({P_k}^2 + {Q_k}^2) \leq {S_{k,max}}^2 \tag{4-32}$$

Using the simplified equations, as shown in (4-27)-(4-32), the initial approximated SOP operation is able to be obtained directly without using the accurate load flow calculations.

4.4 Network Reconfiguration Considering SOPs

Reconfiguring distribution networks is used to achieve better network operation including power loss minimization, feeder load balancing and supply restoration. To investigate the performance of distribution network reconfiguration when SOPs are installed to replace some of the normally-open points, the proposed PDS method for optimal SOP operation was combined with the network reconfiguration method introduced in [34].

The procedure of the combined algorithm is given in Figure 4.5.

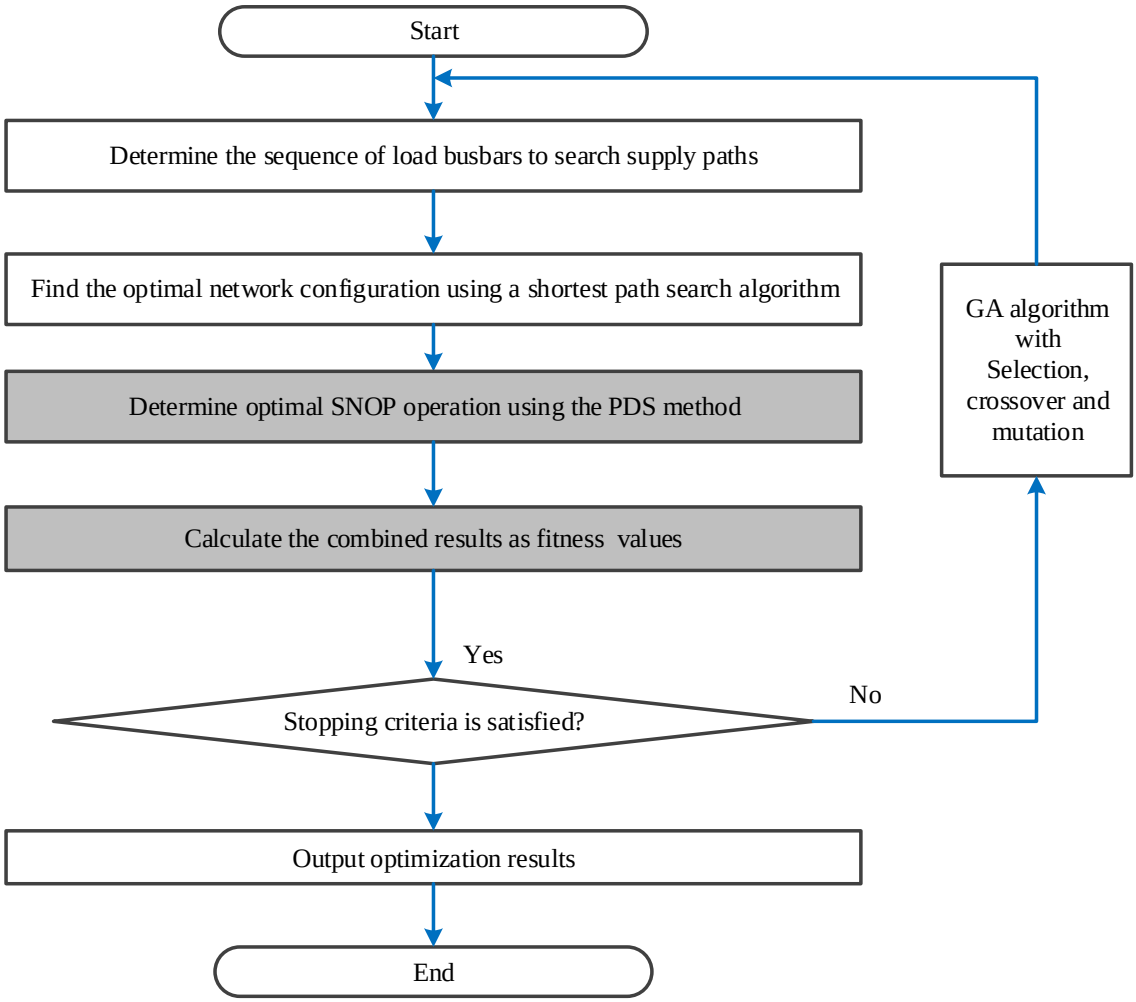

Figure 4.5: Flowchart of proposed network reconfiguration considering SOPs

According to [34], a shortest-path algorithm is used to find the optimal electricity supply path for each load busbar. A genetic algorithm (GA) with the selection, crossover and mutation operators is used to optimize the sequence of load busbars searching for the supply paths because the sequence affects the obtained network configurations. The improved PDS method for optimal SOP operation is integrated after the shortest path algorithm. The fitness functions are formulated in Section 4.3.1.

4.5 Case Study

A 33-bus distribution network, as shown in Figure 4.6, was used for case study [99]. This network has 32 normally-closed switches, 5 normally-open switches and the nominal voltage is 12.66 kV. The total real and reactive power loads are 3,715 kW and 2,300 kVar. Four normally-open switches, i.e., the switches between buses 25 and 29, 33 and 18, 8 and 21, 12 and 22, were chosen as candidate places for SOP installation. The size of each SOP unit was assumed to be 3 MVA. Such a large size is chosen to ensure enough capacity for SOP operations under all studied network conditions.

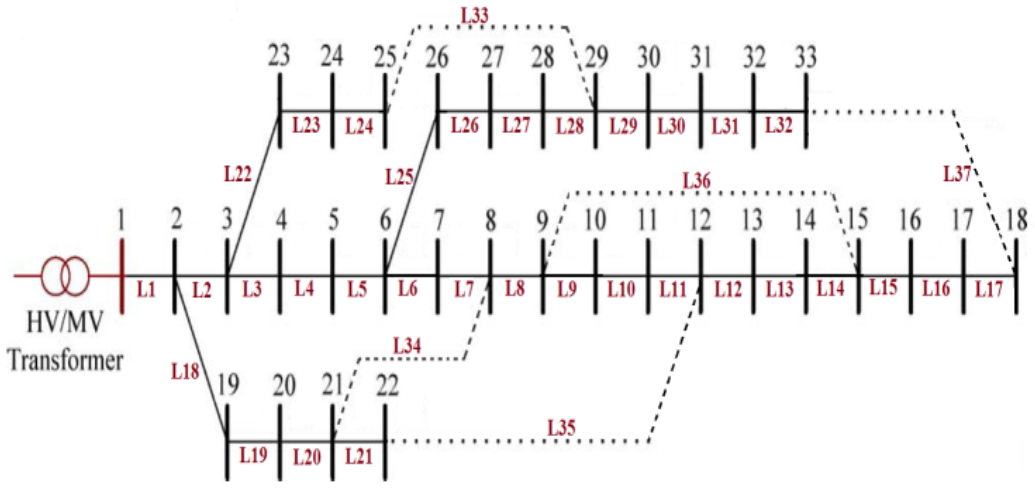

Figure 4.6: 33-bus distribution network [99]

Four cases were defined and used for quantifying the benefits of SOPs for improvement of network performance:

Case I: Improve network performance using SOPs;

Case II: Improve network performance considering both SOPs and network reconfiguration;

Case III: Impacts of DG connections;

Case IV: Impact of power losses of SOP devices.

4.5.1 Improve Network Performances Using SOPs

The impact of different number of SOPs installed in the network on both power loss minimization and feeder load balancing was investigated. The device power losses were ignored for this case.

- **Power loss minimization**

Figure 4.7a shows the results of minimized power losses with 1 to 4 SOPs installed in the network. There was a significant reduction (by 42%) of the system power loss with one SOP installation. With more SOPs installed in the system, the total power losses were further reduced (by 57%).The voltage profiles of the system were also improved with the SOP installations, as shown in Figure 4.7b.

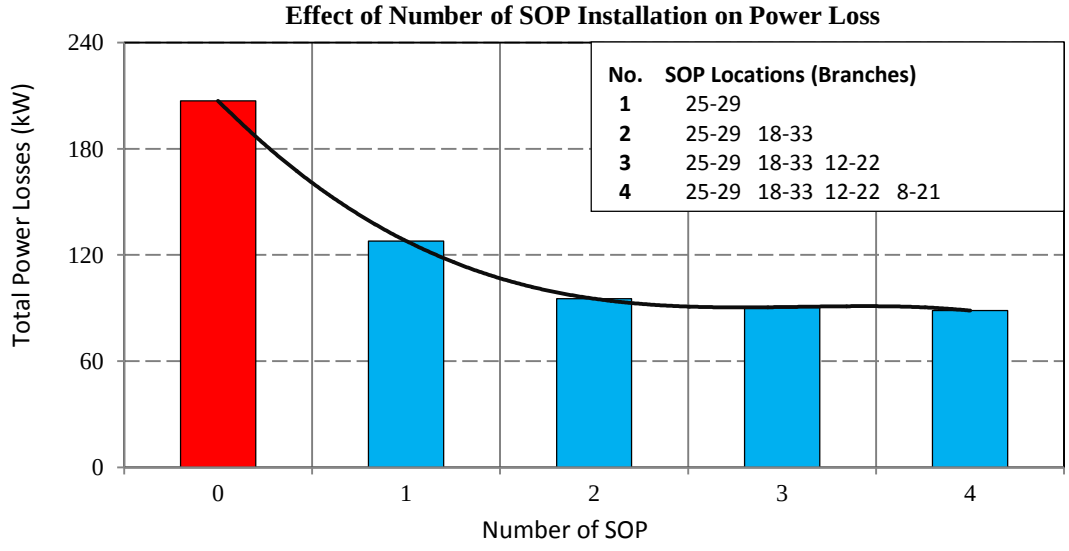

(a)

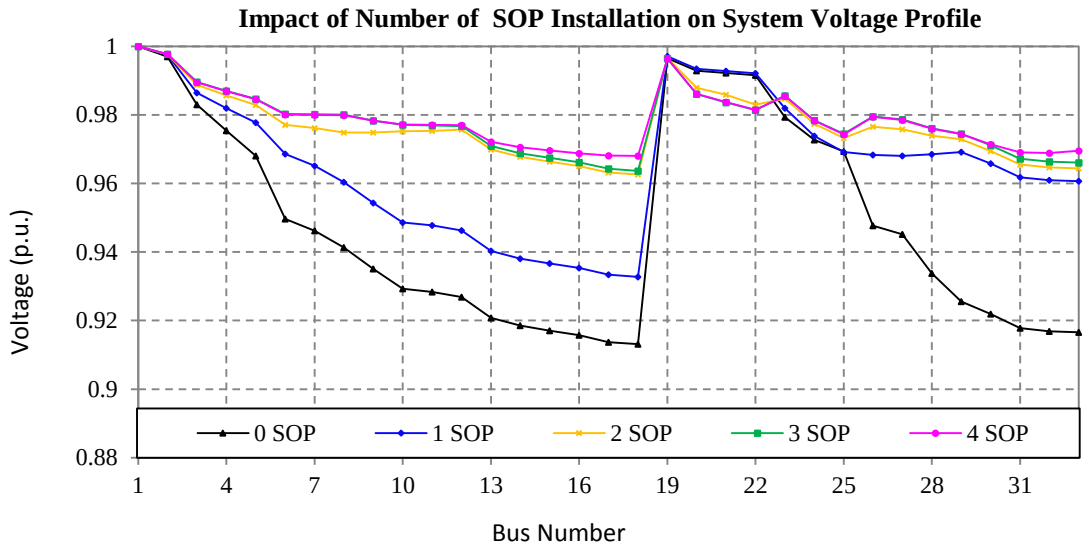

(b)

Figure 4.7: Impact of different number of SOP installation on power loss minimization and voltage profile improvement

- **Feeder load balancing**

One feeder of the network from branch L25 to branch L32 as shown in Figure 4.8 was assumed to be heavily loaded, i.e., 1.6 times higher than the loading under the normal condition. Table 4.1 shows the impact of different number of SOPs on feeder load balancing. It is observed that the system load balancing index *LBI* was reduced by 47.73% with one SOP. Although the *LBI* reduction was further improved with more SOPs installed, the rate of improvement was diminishing.

Table 4.1: System Load Balancing Index with Different Number of SOP Installation

Number of SOP Installed	0	1	2	3	4
SOP Locations (Branches)	–	25-29	25-29 18-33	25-29 18-33 12-22	26-29 18-33 12-22 8-21
System Load Balancing Index	6.156	3.218	2.566	2.428	2.389
% *LBI* Reduction	–	47.726	58.317	60.056	61.192

Figure 4.8a illustrates the branch loading profile of the network. By using SOPs, the loading of those heavily loaded branches (e.g. branches L1 to L6 and L25 to L30) was reduced dramatically by transferring loads to the lightly loaded branches via SOP control. As a consequence, the loading levels from branches L12 to L24 were increased. The voltage profile was also improved, as shown in Figure 4.8b. The minimum bus voltage (at bus 32) was 0.88 *p.u.* due to overloading, and it was improved by 9.09% after the system loading was balanced using SOPs.

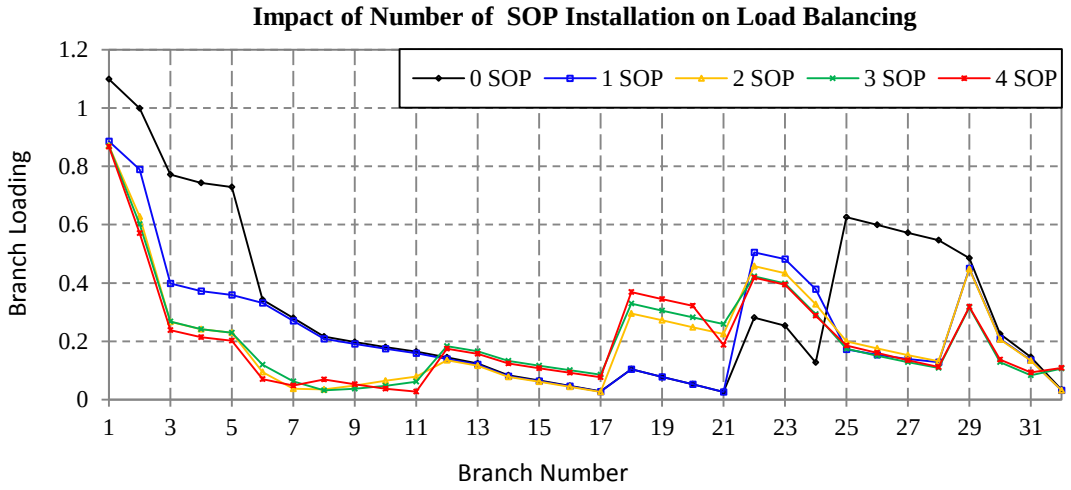

(a)

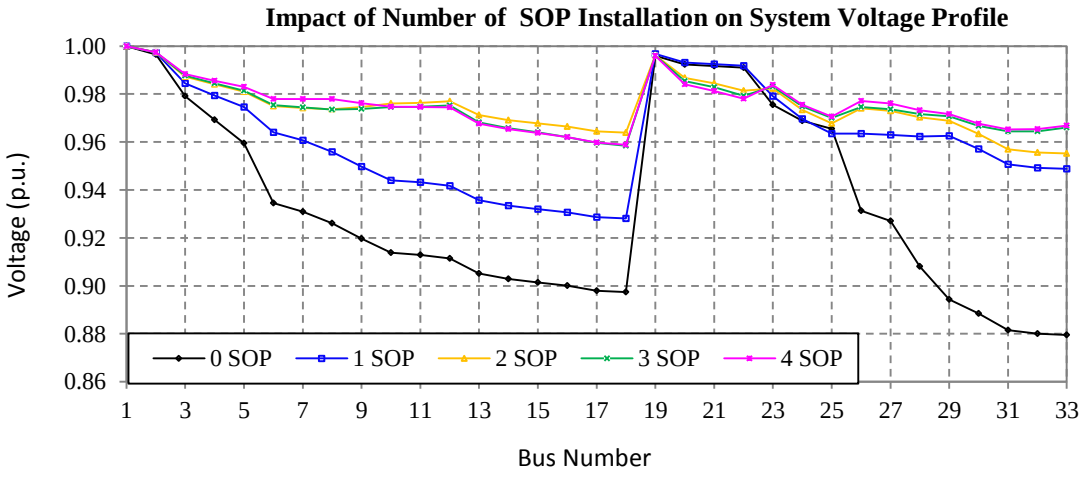

(b)

Figure 4.8: Impact of different number of SOP installation on load balancing and voltage profile improvement

- **Performance of the improved PDS method for optimal SOP operation**

Table 4.2 lists the computation time required for the calculation of above case studies considering only one SOP. The total time required by using the conventional PDS method (starting from an arbitrary point) and the proposed method with a good initial approximation were compared. It can be seen that for both power loss minimization and feeder load balancing there were significant reductions in computation time by using the improved PDS method. Especially for solving the feeder load balancing, the total CPU time was reduced by 68% (from 8.295s to 2.614s) after using the improved PDS method.

Table 4.2: Results of Computing Time for Optimal SOP Operation

Optimization technique	Power loss minimization			Feeder load balancing		
		PDS	Improved PDS		PDS	Improved PDS
CPU time (s)	Light Loading	4.565	1.998	Overload Condition	8.295	2.614
	Normal Loading	5.364	3.343			
	Heavy Loading	5.774	3.578			

4.5.2 Improve Network Performance Considering both SOP and Network Reconfiguration

The benefits of combining SOP and network reconfiguration for power loss minimization and feeder load balancing were evaluated. In this case, the SOP device was assumed to be located between buses 25 and 29 and its power losses were ignored. Another three case studies were also carried out for comparisons, which are

- Base case study with neither reconfiguration nor SOP;
- Case study considering only network reconfiguration;
- Case study considering only one SOP, which is located between buses 25 and 29.

- **Power loss minimization**

The network performance on power loss minimization was simulated under three loading conditions: light (50%), normal (100%), and heavy (160%). The simulation results are listed in Table 4.3.

Table 4.3: Results of Different Methods for System Power Loss

Case Studies			Load Level		
			Light (0.5)	**Normal (1.0)**	**Heavy (1.6)**
Base Case No reconfiguration No SOP installed	Switches with open status		8-21 12-22 25-29 9-15 18-33		
	Power Loss (kW)		47.118	202.876	575.966
	Minimum Voltage (p.u.)		0.958	0.913	0.853
Only network reconfiguration	Switches Opened		7-8 9-10 14-15 25-29 32-33		
	Power Loss (kW)		33.312	137.946	381.418
	% Loss reduction		29.301	32.005	33.778
	Minimum Voltage (p.u.)		0.970	0.938	0.897
Only SOP	Switches with open status		8-21 12-22 9-15 18-33		
	SOP Operation	$P^1_{S\_inj}$/ MW	0.230	0.605	0.998
		$Q^1_{S\_inj}$/ MVar	0.225	0.471	0.784
		$Q^2_{S\_inj}$/ MVar	0.610	1.239	2.017
	Power Loss (kW)		29.774	124.456	337.525
	% Loss reduction		36.810	38.653	41.398
	Minimum Voltage (p.u.)		0.967	0.933	0.890
Combined network reconfiguration with SOP	Switches with open status		7-8 9-10 14-15 18-33		
	SOP Operation	$P^1_{S\_inj}$/ MW	0.183	0.374	0.607
		$Q^1_{S\_inj}$/ MVar	0.215	0.424	0.697
		$Q^2_{S\_inj}$/ MVar	0.516	1.045	1.686
	Power Loss (kW)		22.758	93.915	250.179
	% Loss reduction		51.700	53.708	56.564
	Minimum Voltage (p.u.)		0.978	0.955	0.925

The percentages of total power loss reduction implies that using only one SOP achieved a similar power loss reduction to that of network reconfiguration under three loading conditions. The most significant power loss reductions and voltage improvement under all three loading conditions were obtained using the combined method. The SOP operation required to achieve power loss minimization indicates that the combined method contributed more to power loss reduction while requiring smaller SOP sizes.

Figure 4.9 illustrates the voltage profiles of all case studies under the normal loading condition. The shapes of the voltage profile under the other two loading condition were the same except minor change in magnitude, and hence are not illustrated.

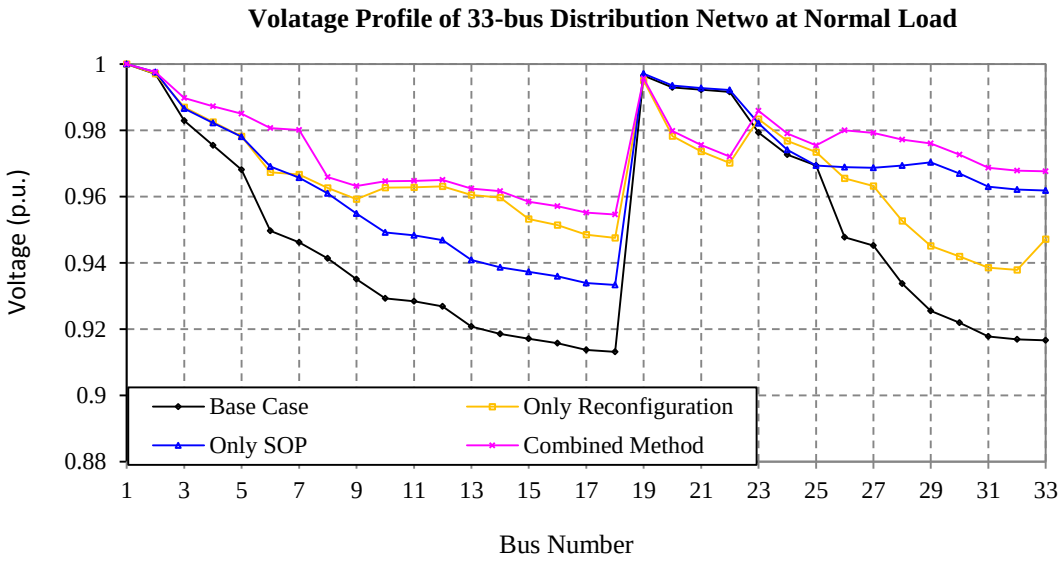

Figure 4.9: Voltage profiles of the network under normal loading condition

- **Feeder load balancing**

The same overloading condition described in the previous case study was simulated. Table 4.4 presents the load balancing index for the four case studies. The branch loading profiles and voltage profiles are shown in Figure 4.10. From these results, it is seen that by using only one SOP to control network power flows achieved better performance on load balancing than that of using network reconfiguration to change the

open/close status of a sequence of switches. The highest *LBI* reduction, i.e., the most well-balanced network, and the highest improvement on minimum voltage were achieved using the combined method.

Table 4.4: Results of Different Methods for Load Balancing

Case Studies		Base Case	Only network reconfiguration	Only SOP	Combined reconfiguration with SOP
System load balancing index		6.156	4.139	3.218	2.594
***LBI* reduction (%)**		-	32.765	47.726	68.337
Minimum Voltage (p.u.)		0.880	0.904	0.928	0.943
SOP Operation	$P^1_{S\_inj}$/ **MW**	-	-	0.916	1.142
	$Q^1_{S\_inj}$/ **MVar**	-	-	0.569	0.577
	$Q^2_{S\_inj}$/ **MVar**	-	-	1.791	2.417

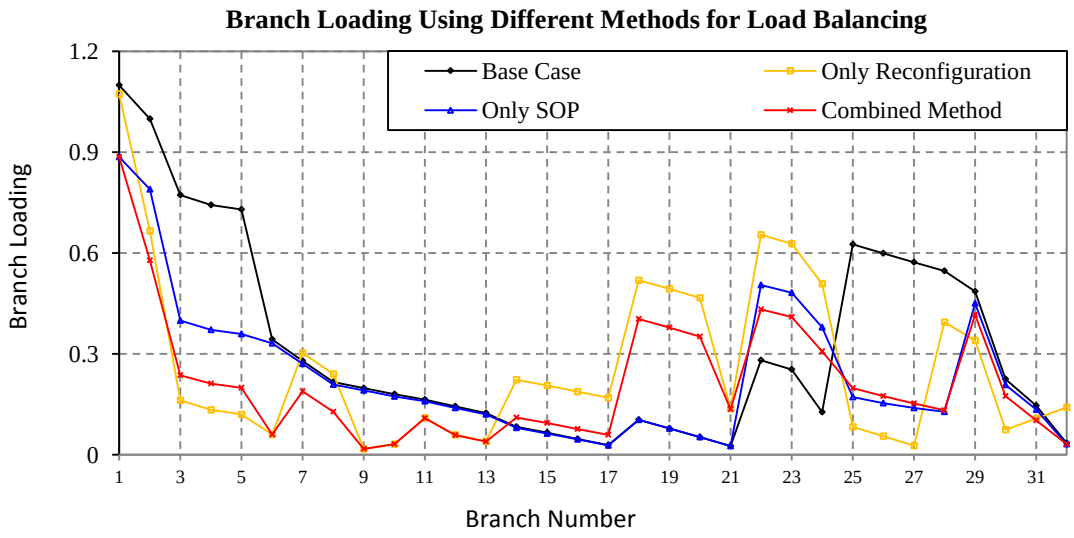

(a)

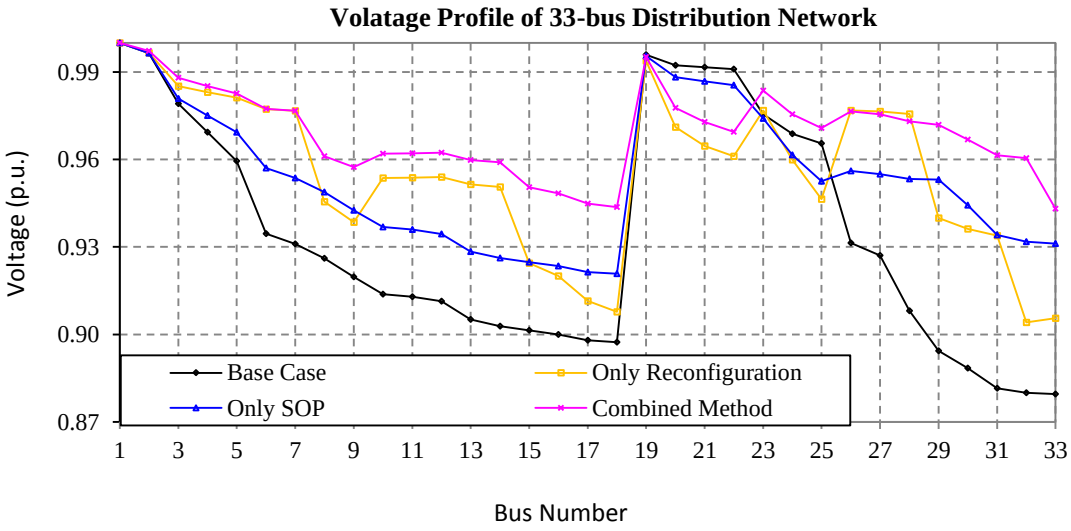

(b)

Figure 4.10: Results of load balancing capability and relevant voltage profile improvement under different methods

4.5.3 Impact of DG Connections

A large capacity of intermittent renewable energy in the distribution network can aggravate feeder loads unbalance and network power losses. To evaluate the benefits of using the SOP for power loss minimization and feeder load balancing with DG connections, three DGs were assumed to be connected to buses 16, 17 and 18. Each DG had a power production of 1 MW with a unity power factor and was modelled as a negative load in this study. An SOP was assumed to be located between buses 18 and 33 and its power losses were ignored. Five case studies were carried out for comparisons, which are

- Base case study with and without DG connections;
- Case study using only network reconfiguration;
- Case study using only one SOP;
- Case study using the combined network reconfiguration and SOP.

- **Power loss minimization**

Table 4.5 shows the network power losses for the five case studies under normal loading conditions. It can be seen that the network power losses were increased by 70% due to the DG connections. A significant power loss reduction (72%) was achieved by using only one SOP, which gave better performance than by using only network reconfiguration. The most significant power loss reduction was obtained by using the combined method while requiring smaller SOP size. Figure 4.11 shows the voltage profile of the network. There was a notable voltage rise due to the DG connections. The use of SOP (either with or without network reconfiguration) achieved much flatter network voltage profiles.

Table 4.5: Results of Different Methods for Power Loss Minimization with DG Connections

Case Studies		Base Case without DGs	Base Case with DGs	Only Network Reconfiguration	Only SOP	Combined Method
Total Power Losses (kW)		202.875	345.502	120.783	92.334	63.221
% Loss Reduction		-	-	65.044	73.275	81.702
SOP Operation	$P^1_{S\_inj}$/ MW	-	-	-	1.661	1.606
	$Q^1_{S\_inj}$/ MVar	-	-	-	0.376	0.381
	$Q^2_{S\_inj}$/ MVar	-	-	-	0.899	0.904

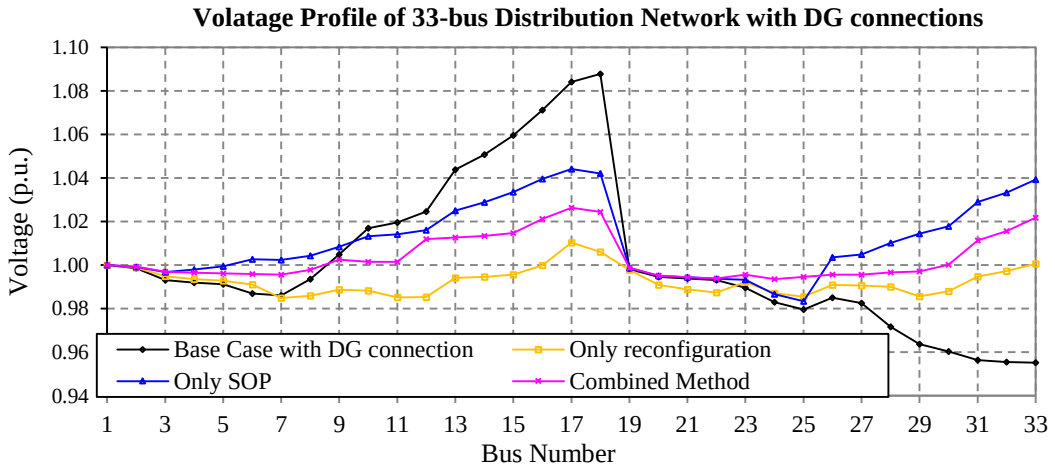

Figure 4.11: Voltage profiles of the network under different cases with DG connection

- **Feeder load balancing**

To evaluate the benefits of the SOP for feeder load balancing with DG connections, (especially when one feeder has high DG power generation while the other one is under a heavy loading condition,) the same overloading condition adopted previously was used again. Table 4.6 shows the load balancing index for the five case studies. It is observed that the network was more unbalanced (higher *LBI*) after connecting DGs. A significant reduction on *LBI* (77.51%) was achieved by transferring loads from the heavily loaded feeder to that with DG integration via the SOP, which gave much better performance than network reconfiguration. The most well-balanced network was achieved by using the combined method with smaller SOP size required.

Table 4.6: Results of Different Methods for Load Balancing with DG Connections

Case Studies		Base Case without DGs	Base Case with DGs	Only Network Reconfiguration	Only SOP	Combined Method
System Load Balancing Index		6.156	7.238	2.995	1.628	1.267
% *LBI* Reduction		-	-	58.621	77.507	82.495
SOP Operation	$P^1_{S\_inj}$/ MW	-	-	1.692	1.480	1.606
	$Q^1_{S\_inj}$/ MVar	-	-	0.457	0.523	0.381
	$Q^2_{S\_inj}$/ MVar	-	-	1.252	1.211	0.904

Figure 4.12 shows the branch loading profiles and voltage profiles. As shown in Figure 4.12a, the peak branch loading of the network was reduced from 72% to 50% by using only one SOP. It shows that the increase in peak currents in the feeders and branch loading was reduced effectively by using only one SOP. The combined method achieved the lowest peak branch loading. The voltage profile was also much flatter by using the SOP and the combined method, as shown in Figure 4.12b.

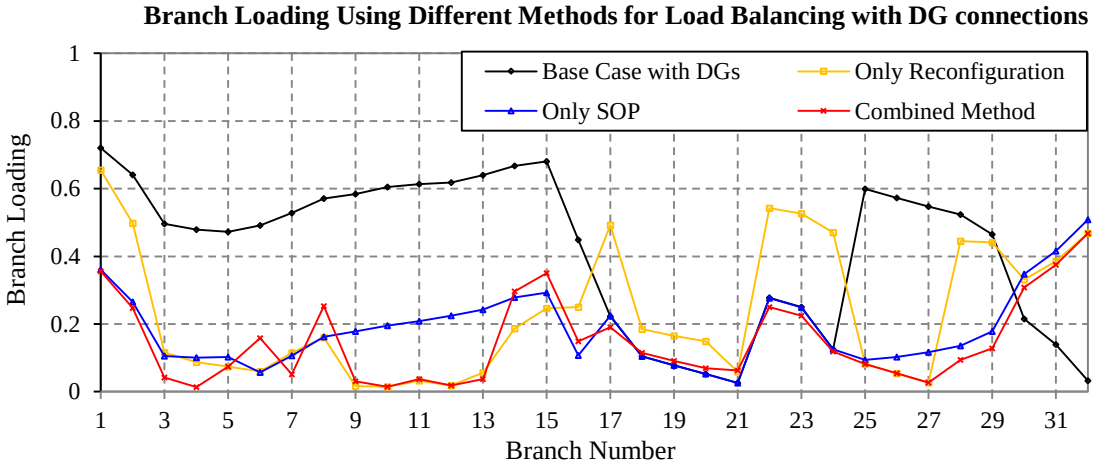

(a)

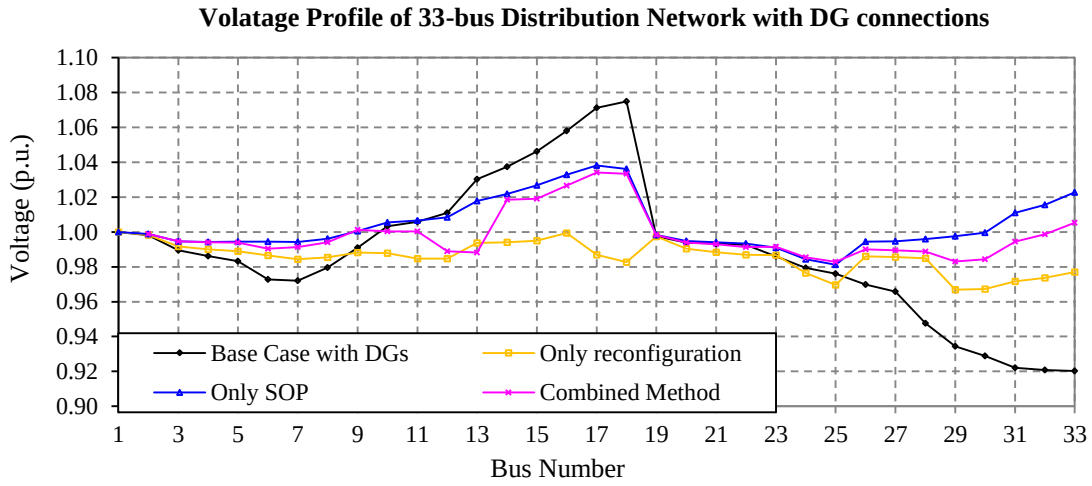

(b)

Figure 4.12 Results of load balancing capability and relevant voltage profile improvement under different cases with DG connections

4.5.4 Impact of the SOP Device Losses

A significant reduction on feeder power losses using SOPs has been demonstrated in the previous study, where the SOP device losses were not considered. Although the SOP device losses have minor impact on its power flow control, it may lower the economic benefits obtained from reducing the total network power losses. The impact of SOP device losses on the total network power loss reduction was investigated based on sensitivity analysis. Different VSC efficiencies at the rated power, i.e. the values of loss coefficients k^I and k^J in (4-11), were considered. For the VSCs in the back-to-back converters, it was assumed that k^I is equal to k^J. The constant power loss of the SOP

device was set as 0.2% of the rated power.

Figure 4.13a illustrates the total network power loss minimization (feeder losses and SOP device losses) under the normal loading conditions. One SOP, located between buses 25 and 29 (without DG connections), was considered in this case. Different device efficiencies of each VSC were considered from 93.5% to 100%. It is observed that the total network losses were reduced by using the SOP. However, the benefits were lowered when the device efficiency decreased. The SOP lost its capability in reducing network power losses when the device loss coefficients fell to 0.065, i.e., 93.5% VSC efficiency at the rated power. Figure 4.13b shows the performance on total network power losses for each percentage of system loading from 0 to 60%. The figure shows that SOP had a greater positive impact on the network power losses under higher system loading conditions. The requirements on SOP device efficiency for total network loss reduction were reduced when the system loading increases.

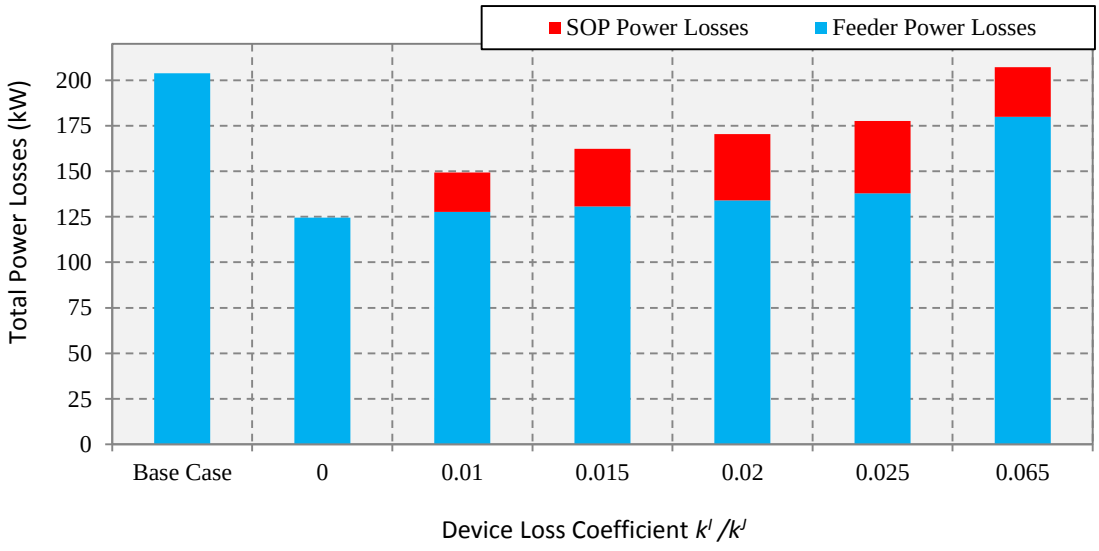

(a)

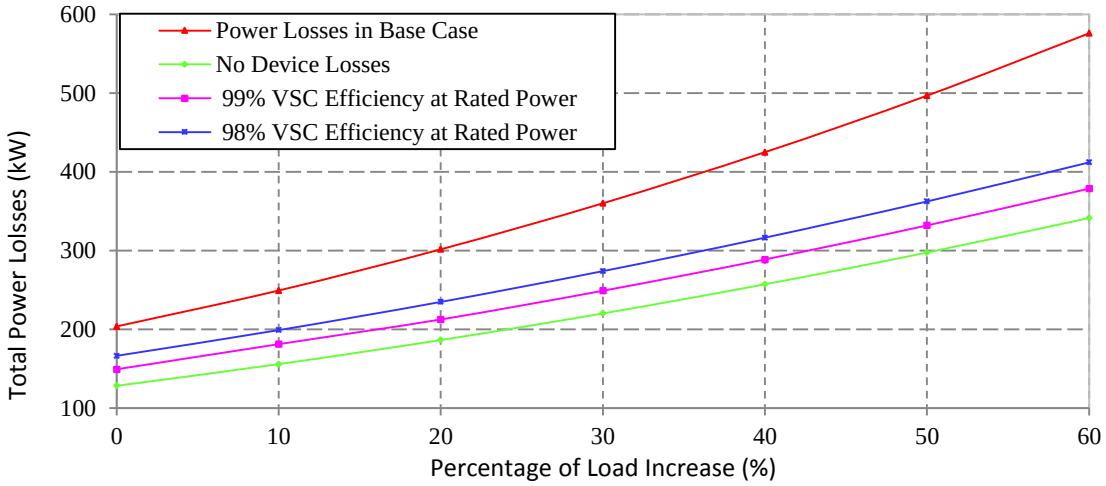

(b)

Figure 4.13: Impacts of the SOP device losses on total network power losses

4.6 Summary

The benefits of using SOPs for medium voltage distribution networks were investigated focusing on power loss reduction, feeder load balancing and voltage profile improvement. A generic power injection model of SOP that is suitable for steady state analysis was developed, taking into account both physical limits and internal power losses of a typical SOP device: back to back VSCs. The optimal SOP operation is obtained using improved Powell's Direction Set method. The combined method considering both SOP and network reconfiguration was proposed to demonstrate the superiority of using SOPs.

Different number of SOPs was considered. Results showed that SOPs significantly contributed to power loss reduction, feeder load balancing and voltage profile improvement. By comparing with network reconfiguration, using only one SOP achieved similar improvement on network power loss reduction and feeder load balancing. The greatest improvements were obtained when combining SOP and network reconfiguration where smaller SOP sizes were required.

The impact of the penetration of DGs was investigated. Results showed that SOPs are able to significantly reduce the peak currents in feeders and alleviate undesirable voltage excursions induced by the connection of DG and demand. Therefore SOPs can be used as an alternative to infrastructure upgrades in accommodating distributed energy resources.

The impact of SOP device losses was illustrated which shows that the economic benefit of SOP in reducing total network power losses was lowered with a decrease of device efficiency. However, a greater positive impact was obtained when system loading increased. In other words, the requirements on SOP device efficiency for total network loss reduction were reduced when the system loading increases.

Chapter 5

Voltage Control in Active Distribution Networks with SOPs

THIS chapter reports a novel coordinated voltage control strategy for active distribution networks considering the SOP, the OLTC and multiple DG units as the voltage control devices.

5.1 Introduction

Chapter 3 illuminated the excellent performance of an SOP in controlling real and reactive power flow under normal operating conditions using back-to-back VSCs. Although it is anticipated that SOPs will support distribution network voltage control by changing the real and reactive power flow of the network, the control strategy regarding the exact operation of the SOP and the coordination with other voltage control devices for distribution networks needs to be investigated.

In this chapter, a novel coordinated voltage control strategy was proposed considering the controllable devices of the OLTC, the SOP and multiple DG units. The performance of the control strategy (using single device or coordination among multiple devices) were assessed considering the voltage compliance, number of tap operations, daily DG energy integration and network energy losses as the key metrics. A distributed control framework was used, where each of the controllable elements is considered as a local control agent and operates based on the local measurements and the shared data through an information-sharing platform. This coordination was priority-based, where the local control agents, without losing the independence of each, can achieve an optimal voltage management with few information exchanges. In the case study of this work, the proposed control strategy was applied to an 11-kV example network considering different network operating conditions and DG penetrations.

5.2 Voltage Control Framework

In medium voltage (MV) networks, voltage control devices usually make control actions based on the adequate knowledge of the status of the network. Due to the limited visibility in MV networks, it is desirable to achieve a better voltage management based on some estimations of the voltage profile using the existing real-time measurements and advanced information and communication devices.

5.2.1 Voltage Profile Estimation

In an MV network, the voltage control actions can be taken base on the maximum and minimum voltages in the network. Figure 5.1 shows the voltage profiles of an MV feeder with and without DG. For a passive network without DG connections (assuming no SOP connection in this case), the voltage profile along the feeder decreases, as shown in Figure 5.1 (profile *a*). Therefore, the maximum and minimum voltages are located at the substation busbar (i.e., the secondary of the transformer) and the remote end of the feeder, respectively. For an active network with DG units, the voltage in the feeder can be higher than the substation busbar, as shown in Figure 5.1 (profile *b*). Moreover, SOPs is able to change the network power flow and thus change the voltage profile. Therefore, for a network with DG connections and/or SOPs, the maximum voltage can locate either at the substation busbar, the DG or SOP connecting buses whilst the minimum voltage point can locate at any bus including in and between the substation busbar, DG or SOP connecting bus.

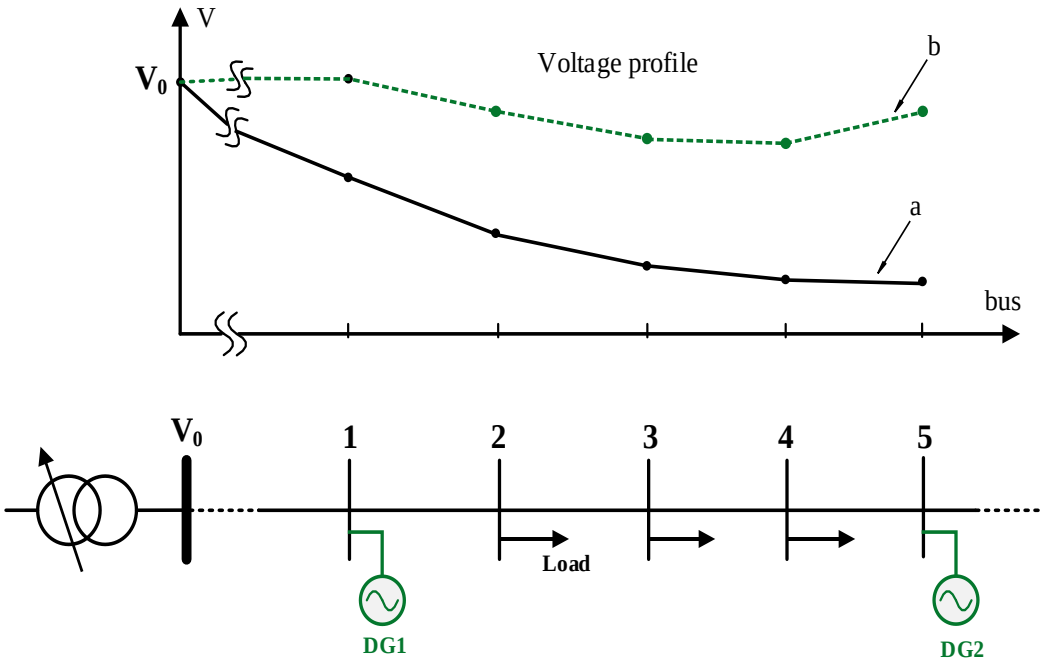

Figure 5.1: Voltage profiles of an MV feeder with and without DG

In this work, it is assumed that the maximum voltage of an MV feeder is obtained from

the meter readings at the substation busbar, DG and SOP connecting buses. A simplified estimation for the minimum voltage is carried out based on these meter readings and necessary calculations.

Figure 5.2 shows an MV feeder with several DG units and an SOP connected. Meters are placed at the substation busbar, the SOP point and each DG connecting bus. The feeder line between each two of them is considered as a segment.

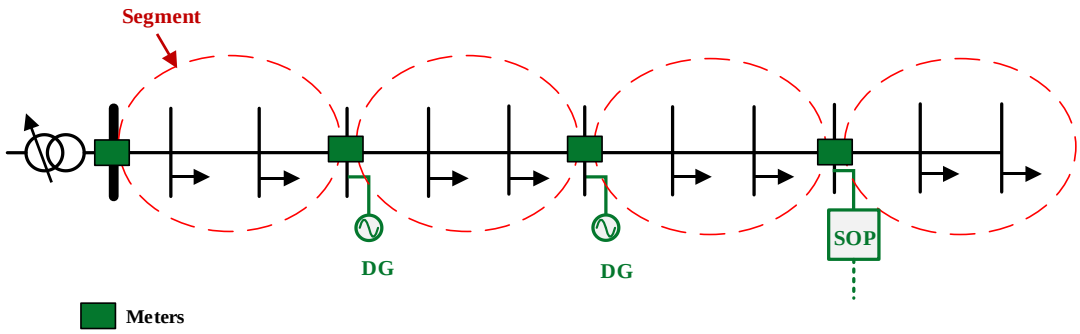

Figure 5.2: An MV feeder with segments for the minimum voltage estimation

The minimum voltage for each of these segments is first estimated by using the meter readings of the corresponding two terminals and necessary calculations (shown below), and then the minimum for the whole feeder is obtained by comparing all these values.

Mathematically, the estimation of the minimum voltage within a segment can be implemented through two steps:

1) Checking the existence of a minimum voltage point within a segment
2) Estimating the value of the minimum voltage if it exists.

Details of these two steps are presented as follows.

Step1) Checking the existence of a minimum voltage point within a segment

It is observed from Figure 5.1 that there is a minimum voltage point in between the two

DG connecting buses if and only if, for both DGs, the voltage of the DG connecting bus is higher than the voltage of its neighbouring bus (in the direction of the other DG). For instance, in Figure 5.1, there will be a minimum voltage point in between bus 1 and bus 5 if and only if the voltage of bus 1 is higher than the voltage of bus 2 while the voltage of bus 5 is higher than the voltage of bus 4. Equation (5-1) shows the mathematical condition for the existence of a minimum voltage point between DG 1 connecting bus and DG 2 connecting bus:

$$\begin{cases} V_1 - V_2 > 0 \\ V_5 - V_4 > 0 \end{cases} \tag{5-1}$$

To solve the above inequality equations, the power flow in the feeder, as shown in Figure 5.3, is calculated by the following set of recursive equations [93]:

$$P_i = P_{i-1} - P_{Loss\ (i-1,\ i)} - P_{L,i} = P_{i-1} - \frac{r_{i-1}}{{V_{i-1}}^2} \cdot ({P_{i-1}}^2 + {Q_{i-1}}^2) - P_{L,\mathrm{i}} \tag{5-2}$$

$$Q_i = Q_{i-1} - Q_{Loss\ (i-1,\ i)} - Q_{L,i} = Q_{i-1} - \frac{x_{i-1}}{{V_{i-1}}^2} \cdot ({P_{i-1}}^2 + {Q_{i-1}}^2) - Q_{L,\mathrm{i}} \tag{5-3}$$

$${V_i}^2 = {V_{i-1}}^2 - 2 \cdot (r_{i-1}P_{i-1} + x_i Q_i) + \frac{({r_{i-1}}^2 + {x_{i-1}}^2)}{{V_{i-1}}^2} \cdot ({P_{i-1}}^2 + {Q_{i-1}}^2) \tag{5-4}$$

where P represents active power, Q reactive power, V nodal voltage, r resistance and x reactance. Subscript $Loss$ denotes line losses, and L denotes load.

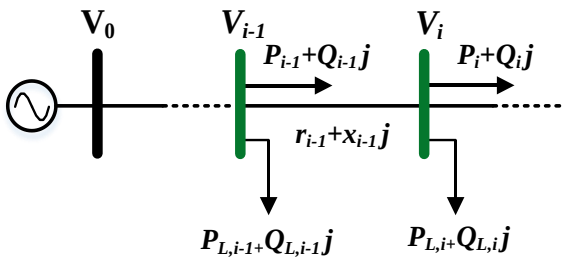

Figure 5.3: A part of distribution feeder

Ignoring the quadratic terms (line losses) since it is much smaller than the branch power [99], equation (5-2)-(5-4) can be written as

$$P_i = P_{i-1} - P_{L,\mathrm{i}} \tag{5-5}$$

$$Q_i = Q_{i-1} - Q_{L,\mathrm{i}} \tag{5-6}$$

$$V_i{}^2 = V_{i-1}{}^2 - 2 \cdot (r_{i-1}P_{i-1} + x_i Q_i) \tag{5-7}$$

Based on (5-7), (5-1) can be represented as follows:

$$\begin{cases} V_1 - V_2 = \frac{2\cdot(P_1\cdot r_1 + Q_1\cdot x_1)}{V_1+V_2} > 0 \\ V_4 - V_5 = \frac{-2\cdot(P_4\cdot r_4 + Q_4\cdot x_4)}{V_4+V_5} > 0 \end{cases} \tag{5-8}$$

After further simplification on (5-8), the condition for the existence of a minimum voltage point between DG 1 and DG 2 can be given as

$$\begin{cases} P_1 \cdot r_1 + Q_1 \cdot x_1 > 0 \\ P_4 \cdot r_4 + Q_4 \cdot x_4 < 0 \end{cases} \tag{5-9}$$

where the reactive and reactive power are measured locally by using meters at the DG locations. Note that (5-9) can be used as a generic condition for checking the existence of a minimum point within any segment, such as the segment between the substation busbar and one DG, one DG and one SOP, etc.

Step 2) Estimating the value of the minimum voltage within a segment

A simplified estimation method is used to obtain the value of the minimum voltage if it exists. This method gives a worst case value thus it is considered as a good lower bound for the voltage management purpose.

The loads in between the two DG connecting buses in Figure 5.1 are assumed to be concentrated and connected half way between the two DG connecting buses, as shown in Figure 5.4.

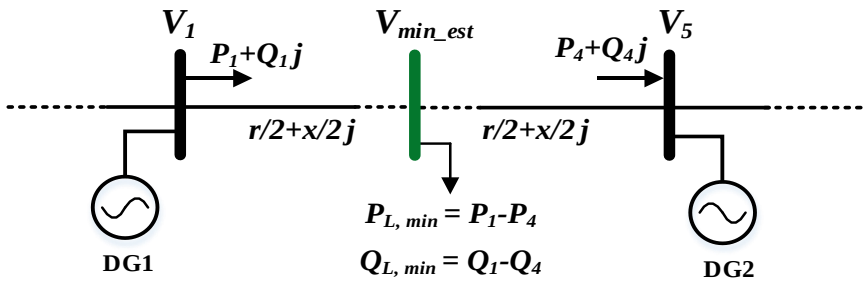

Figure 5.4: Voltage estimation using simplified method

Therefore, the minimum voltage between the DG 1 and DG 2 calculated from DG 1 using (5-7) is

$$V_{\min\_est,DG1} = \sqrt{V_1{}^2 - 2 \cdot (P_1 \cdot \frac{r}{2} + Q_1 \cdot \frac{x}{2})} \tag{5-10}$$

Similarly, the minimum voltage calculated from DG 2 is

$$V_{\min\_est,DG2} = \sqrt{V_5{}^2 + 2 \cdot (P_4 \cdot \frac{r}{2} + Q_4 \cdot \frac{x}{2})} \tag{5-11}$$

where r and x are the total value of the reactance and resistance between DG 1 and DG 2.

Taking the minimum value of $V_{\min\_est,DG1}$ and $V_{\min\_est,DG2}$ as the minimum voltage of the segment, V_{min}, as shown in (5-12).

$$V_{\min\_est} = min\{V_{\min\_est,DG1}, V_{\min\_est,DG2}\} \tag{5-12}$$

Equation (5-12) provides an estimation of the minimum voltage using the data measured at the substation, DG or SOP connecting buses.

Note that above calculation used to estimate the minimum voltage of an MV feeder did not consider feeders having long laterals or DGs connected in the lateral. In this work, the loads and DGs connected to the laterals are assumed to be lumped into the nearest main stream of the feeder and hence errors exist.

5.2.2 Proposed Voltage Control Framework

A distributed voltage control framework is proposed, as depicted in Figure 5.5. Each of the controllable elements, i.e. the OLTC, the SOP and DG units, is considered as a local control agent that operates based on the local measurements and the shared data through an information-sharing platform.

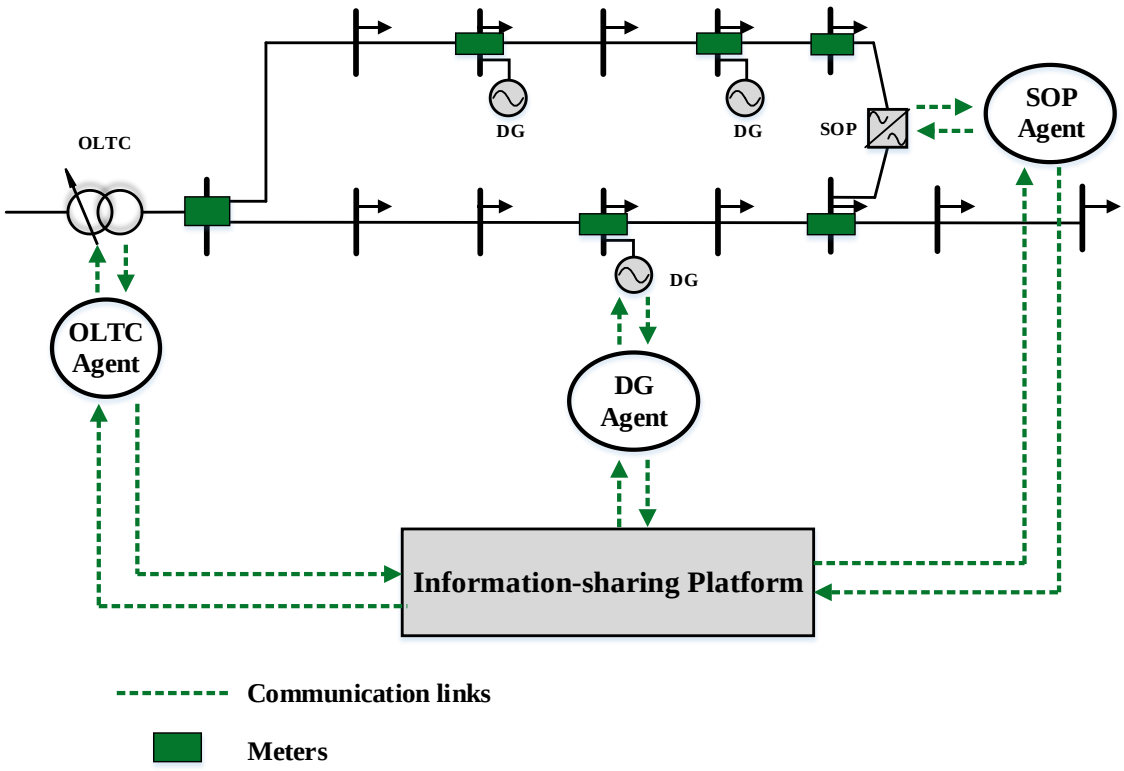

Figure 5.5: Distributed voltage control framework

- **Local control agents**

The local control agents carry out real-time control based on the local measurements but considering coordination with other local control agents via the information exchange through the information-sharing platform. Figure 5.6 shows the interior structure of each control agent.

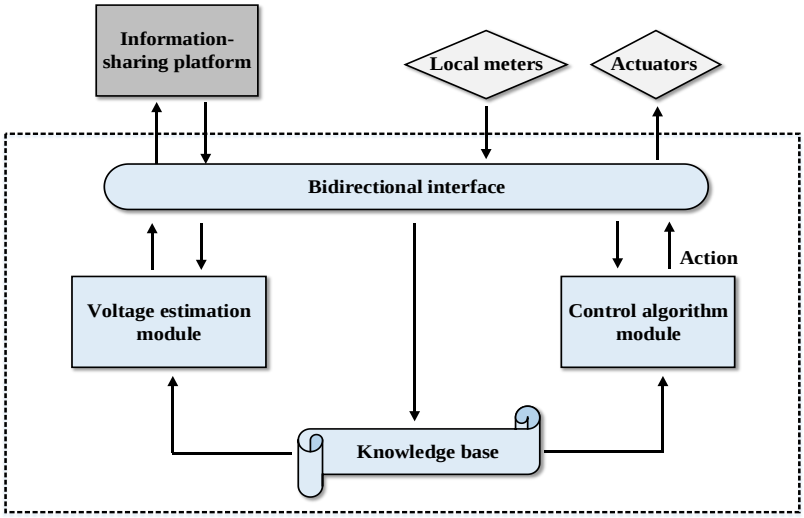

Figure 5.6: Interior structure of a local control agent

Details of the four blue blocks shown in Figure 5.6 are given as follows.

Bidirectional interface is responsible for 1) exchanging data with the *information-sharing platform*, 2) passing the measurements from the local meters and the information-sharing platform to the *voltage estimation module* inside the agent, and 3) passing the control commands issued by the *control algorithm module* to the actuator.

Voltage estimation module is responsible for performing the segment voltage estimation as described in 5.2.1. The detailed process is shown as follows.

1) The module receives the measurements from the local meter. Figure 5.7 shows a detailed view of the measurements by each local meter. It includes the voltage magnitude at the connecting bus, the real and reactive power flow in lines connected to the connecting bus. These measurements provide the measured potential maximum voltage and the data needed to estimate the minimum voltages within its corresponding segments, i.e., segments in between its agent and any neighbour agent.

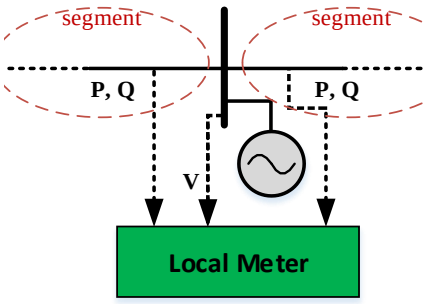

Figure 5.7: Details of local measurements

2) According to Step 1 in Section 5.2.1, the module checks one part of the condition for the existence of a minimum voltage point within a segment.
3) If the minimum voltage point is found exist, the module estimates the value according to Step 2 in Section 5.2.1. Otherwise, goes to 4).
4) The module sends voltage data to the *bidirectional interface* and finally to the *information-sharing platform*. Noted that only the critical data are sent to the *information-sharing platform*, i.e., the measured node voltage and estimated minimum voltages within the corresponding segments.

Control algorithm module provides local control commends using the corresponding control algorithm.

Knowledge base stores the knowledge information of the network, e.g. network topology, line parameters.

- **Information-sharing platform**

The Information-sharing platform works as a moderator: 1) determining the overall maximum and minimum voltages of each feeder and passing onto the local control agent if needed; and 2) perform the coordinated voltage control strategy, which are described in Section 5.3.

5.3 Coordinated Voltage Control Strategy

In this section, the voltage control using the SOP and its coordination with other control devices (i.e., OLTC and DG units) were investigated. The effectiveness of the SOP on voltage control and its impacts on networks was first examined. Then, a priority-based coordination using the proposed control framework described in Section 5.2 was developed.

5.3.1 Effectiveness of SOP on Voltage Control

- **Voltage change caused by an SOP**

Figure 5.8 shows a radial feeder of an MV network.

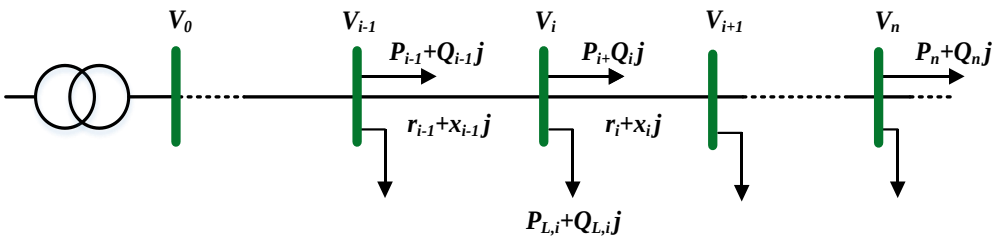

Figure 5.8: Radial distribution feeder

According to (5-5)-(5-7), the active and reactive power at node *i* and the voltage magnitude at node *i* can be given as follows:

$$P_i = P_n + \sum_{k=i+1}^{n} P_{L,k} \tag{5-13}$$

$$Q_i = Q_n + \sum_{k=i+1}^{n} Q_{L,k} \tag{5-14}$$

$$V_i^{\,2} = V_0^{\,2} - 2 \cdot \sum_{k=0}^{i-1} (r_k P_k + x_k Q_k) \tag{5-15}$$

Equations (5-13) to (5-15) show the change of the branch power flow and consequently the change of the voltage magnitude at bus *i* depends on the sum of power loads ($P_{L,k}$ and $Q_{L,k}$), the downstream active and reactive power flow (P_n and Q_n) and the

voltage magnitude at the initial upstream bus (V_0), i.e. the substation busbar.

Therefore, if an SOP is connected in the downstream of bus *i*. According to the generic power injection model of SOP developed in Chapter 3, the change of the branch power at bus *i* caused by the change of the power injection， ΔP_{S_inj} and ΔQ_{S_inj} at the SOP connecting bus can be estimated based on (5-13) and (5-14):

$$\Delta P_i = P_i^{new} - P_i^{old} = \Delta P_n = \Delta P_{S\_inj} \tag{5-16}$$

$$\Delta Q_i = Q_i^{new} - Q_i^{old} = \Delta Q_n = \Delta Q_{S\_inj} \tag{5-17}$$

Thus, the estimation on the change of the voltage magnitude at bus *i* using (5-15) can be obtained as

$$\Delta(V_i^2) = V_i^{new2} - V_i^{old2} = \left(V_0^{new2} - V_0^{old2}\right) - 2 \cdot \sum_{k=0}^{i-1} r_k \cdot \Delta P_{S_{inj}} - 2 \cdot \sum_{k=0}^{i-1} x_k \cdot \Delta Q_{S_{inj}}$$

$$= \Delta(V_0^2) - 2 \cdot \sum_{k=0}^{i-1} r_k \cdot \Delta P_{S_{inj}} - 2 \cdot \sum_{k=0}^{i-1} x_k \cdot \Delta Q_{S_{inj}} \tag{5-18}$$

where $\Delta(V_0^2)$ is the change of the substation voltage; $2 \cdot \sum_{k=0}^{i-1} r_k$ and $2 \cdot \sum_{k=0}^{i-1} x_k$ are the sensitivity factors of bus *i*. These sensitivity factors constants determined by the line parameters only.

While, for bus *i* in the downstream of SOP connecting bus, the change of the voltage at bus *i* equals to the change of the voltage at the SOP connecting bus *j*, which is written as follows:

$$\Delta(V_i^2) = \Delta(V_0^2) - 2 \cdot \sum_{k=0}^{j} r_k \cdot \Delta P_{S\_inj} - 2 \cdot \sum_{k=0}^{j} x_k \cdot \Delta Q_{S\_inj} \tag{5-19}$$

Note that the change of the substation voltage, i.e., $\Delta(V_0^2)$ is calculated based on the transformer impedance and the system input impedance at the primary side of the

substation. It is assumed that this change is small and thus ignored in this study. Equations (5-18) and (5-19) also applies to the DG unit for voltage control in this work.

- **The impacts of the SOP on MV networks for voltage control**

According to the UK statutory instruments, the Distribution Network Operator (DNO) is obligated to maintain the voltages on MV networks within ± 6% of nominal [100]. In this work, voltage limits of ± 5% of nominal, i.e. 1.05 and 0.95 p.u. were considered so as to leave some headroom for unexpected voltage violation due to the errors of measurements, estimations and communication delays.

An SOP controls network voltage by either supplying or absorbing reactive power at its connected feeders or controlling the active power flow between the feeders. According to (5-18) and (5-19), using either reactive or active control can achieve a desired voltage at the targeting bus. The corresponding impacts on network voltage profile and network operation (line losses) was tested in a simple MV network shown in Figure 5.9. The voltage operating limits of this test network was considered $\pm$5% of nominal. A 2.5 MW DG with unity power factor was assumed to be connected to bus 13 in feeder 1. The network parameters can be found in appendix A.

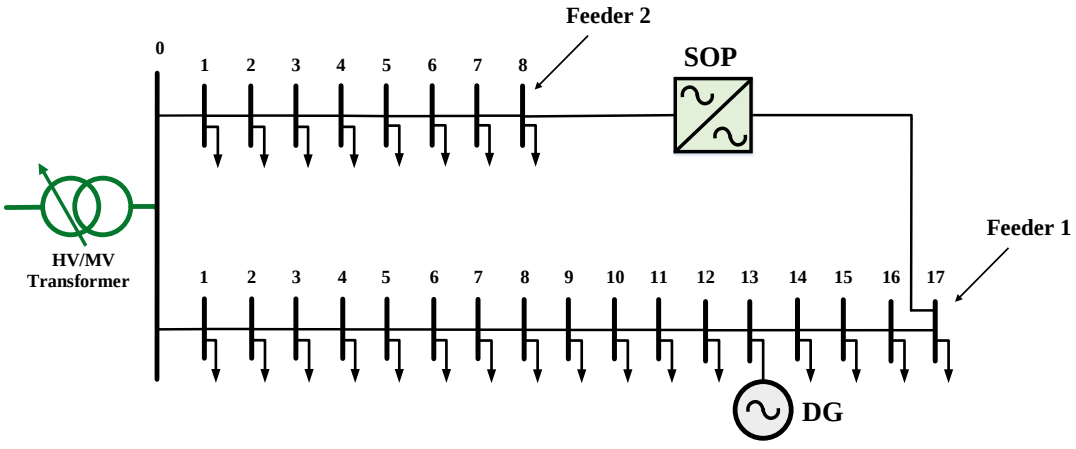

Figure 5.9: Two-feeder MV distribution network

Figure 5.10 shows the voltage profile of the two feeders before voltage control. The

voltages from bus 12 down to bus 17 violated the upper limit due to the DG connection, while the minimum voltage (on the other feeder) approached to the lower limit. The OLTC is infeasible for voltage control in such a case since the difference between the overall maximum and minimum voltages exceeded the gap between the upper and lower voltage limits and thus may cause improper settings and excessive tap operation [101]. Therefore, the SOP was used to reduce the voltages in feeder 1 by controlling either real or reactive power based on equation (5-18).

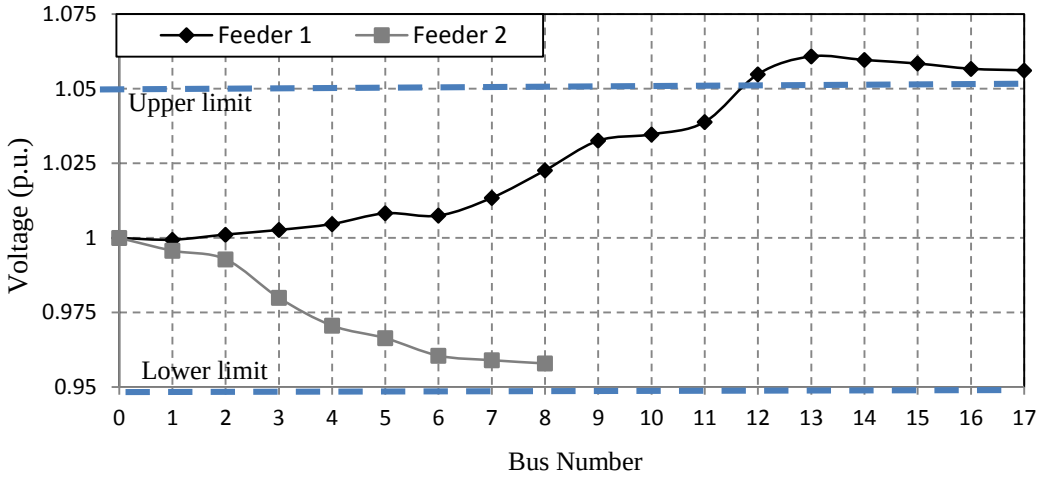

Figure 5.10: Voltage profiles of both feeder before voltage control

According to (5-18), it was assumed that the target bus is 13 and the desired voltage magnitude at the target bus, $V_{13}{}^{new}$ was set to be 1 p.u. Figure 5.11 shows the voltage profile with SOP control using different control methods. It is observed that both control methods achieved the control task, i.e., the voltages at bus 13 were close to the targeted value (1 p.u.).For active power control shown in Figure 5.11a, the voltage profile along feeder 2 rose while the voltage profile along feeder 1 dropped. This is due to the active power was transferred from feeder 1 to feeder 2. However, for the reactive control method, the reactive power was controlled independently on either side of the SOP and thus the voltage profile along the feeder 2 was not changed. In addition, it is shown that the closer to the SOP connecting bus, the bigger the increased (or decreased) voltage magnitude.. This can be explained by (5-19) where the sensitivity factors, $2 \cdot$

$\sum_{k=0}^{i-1} r_k$ and $2 \cdot \sum_{k=0}^{i-1} x_k$ increase with the distance between bus *i* and the substation bus increases.

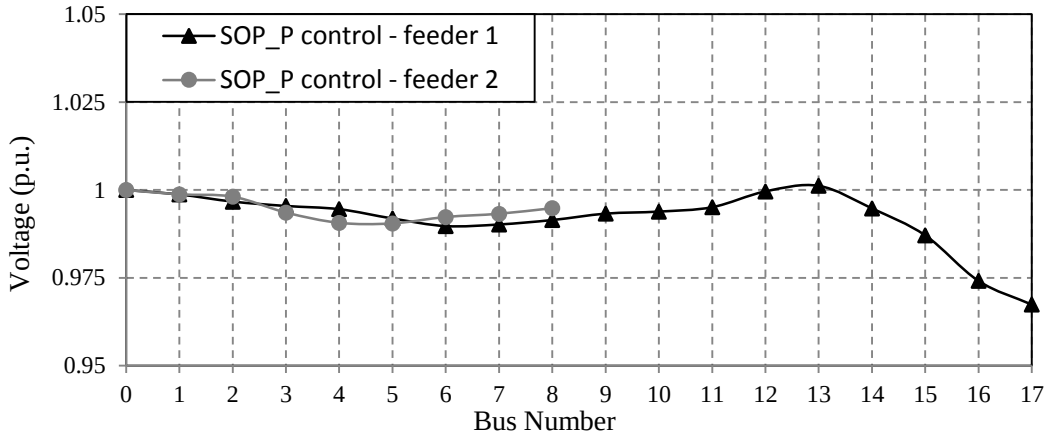

(a)

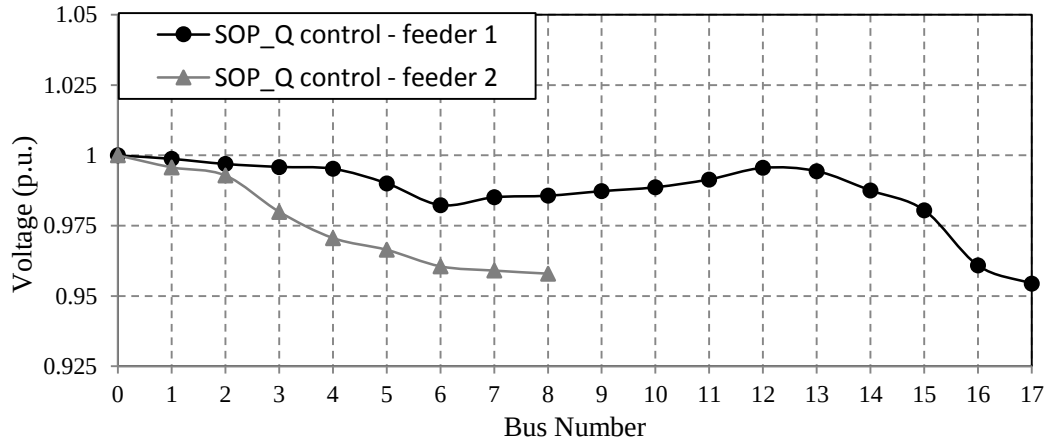

(b)

Figure 5.11: Voltage profiles with SOP voltage control: (a) active power control method; (b) reactive power control method

Figure 5.12 compares the network power losses before and after using SOP control. There was a significant increase of network power losses after using the reactive power control method. This is because the voltage improvement was achieved by absorbing excessive reactive power from the network, which caused an increased in feeder loading and consequently an increase in the line losses. On the contrary, the network power losses were decreased by using the active power control method which transferred active power between feeder 1 and feeder 2.

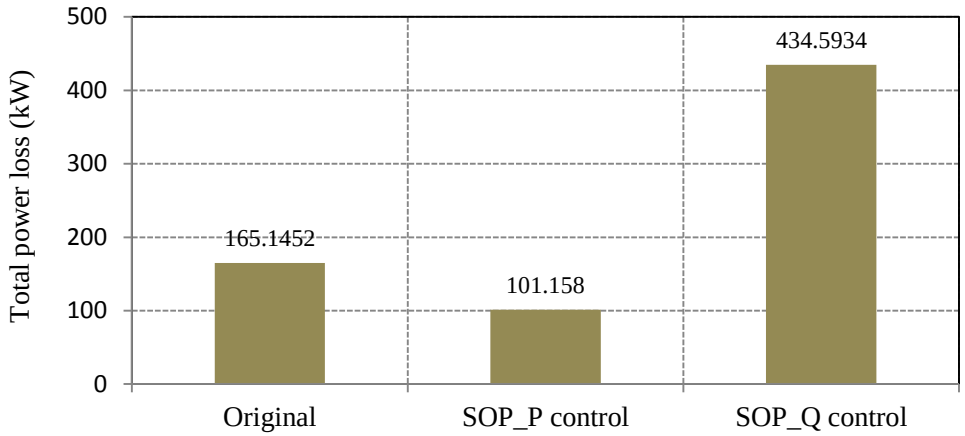

Figure 5.12: Comparison of the network active power losses

- **Discussion**

According to the above analysis, the following key findings of the SOP control are outlined:

- Either real or reactive power control of the SOP achieves the voltage control objective by using the sensitivity factors in (5-18). However, the voltage change is more sensitive to the active power control due to the fact that MV distribution networks have high line resistances and low X/R ratio [102]. This makes the active power control method more cost-effective considering the device capacity.
- For active power control method, the voltage profile on both feeders will be affected. A decrease in the voltage profile on one feeder leads to an increase in the voltage on the other feeder, and vice versa. Therefore, the voltage headroom of both connected feeders need to be considered when the active power control method is used. The main advantage of this control method compared with the reactive power control is that there will not be a significant change on network power losses using the active power control.
- The main advantage of the reactive power control method is that both sides of SOP supply and/or absorb reactive power independently. Therefore, it enables voltage control simultaneously and independently on both connected feeders. However, the voltage drop by absorbing excessive reactive power may cause a

significant increase in network power losses.

5.3.2 Priority-Based Coordination

Figure 5.13 shows a priority-based coordination among multiple agents, including the OLTC, the SOP and the DG units. Each of these agents is called a "local control agent" and each local control agent has multiple objectives. The first one (main objective) is identical to all agents and the remaining are called sub-objectives. The main objective used in this work is to keep the voltages within the allowable range. The sub-objectives are to reduce the number of tap operations, mitigate DG active power curtailment, and reduce network power losses.

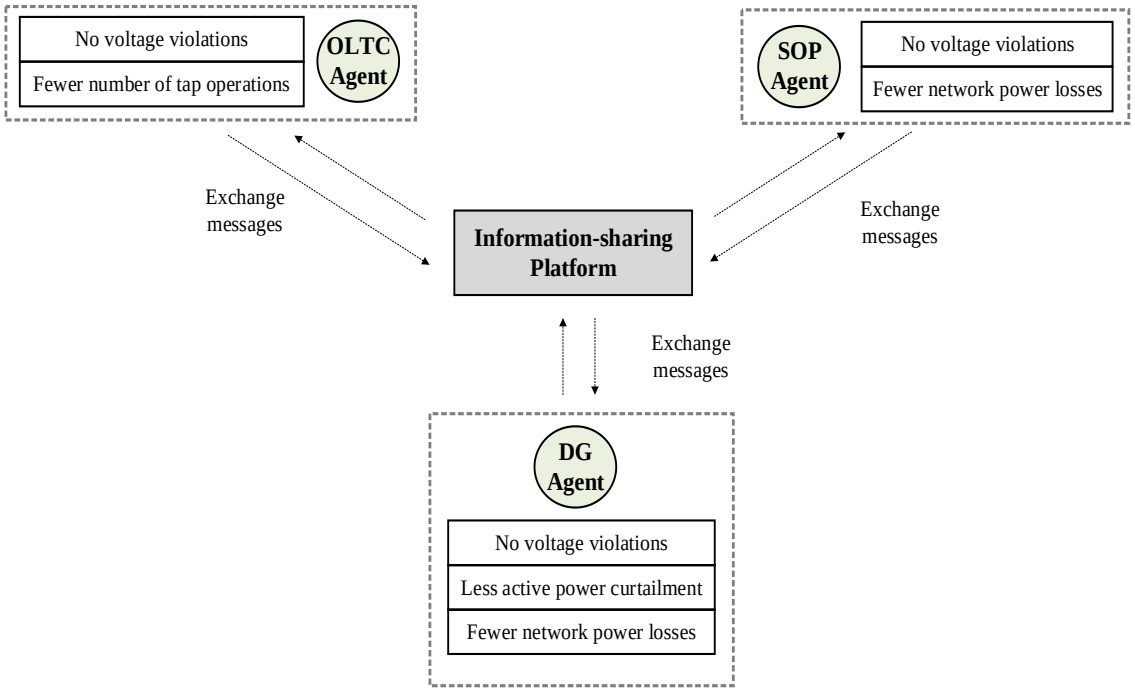

Figure 5.13: Priority-based coordination of the multiple local control agents

In order to achieve a trade-off among the aforementioned objectives, the objectives were grouped by defining the priority level, as shown in Figure 5.14.

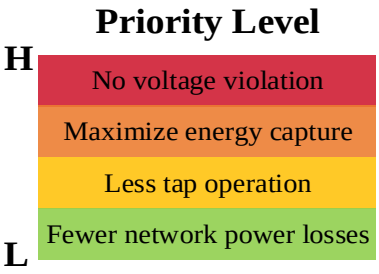

Figure 5.14: Prioritisation of the proposed objectives from high (H) to low (L)

A priority-based coordination is carried out to allow the local control agents to achieve their objectives in accordance with a specific sequence (i.e., the prioritisation). Figure 5.15 shows the flow chart of the priority-based coordination. Both DG and SOP control agents have two voltage control methods: real and reactive power control methods. The OLTC agent also has two control strategies to deal with both feasible and infeasible solutions. The main objective (no voltage violation) is considered each time before a control method to determine whether a control action is needed. All the control methods are coordinated in a pre-defined sequence based on the prioritisation of the sub-objectives. The higher the priority level, the later the corresponding control method will be activated.

Thus, as shown in the figure 5.15, the real and reactive power control of the SOP and the reactive control of the DG (green block) are the first considered methods. They are activated in a sequence that: 1) the active power control of the SOP agent is prior to the reactive power control methods due to the results obtained from Section 5.3.1, i.e., the active power control method is more sensitive to voltage change and results in reduced network power losses and 2) the reactive control method of the SOP agent is prior to that of the DG agent in order to allow more flexibility for the DG unit in case of an emergency [56]. All these real and reactive control methods are performed by solving an optimization problem to minimize the voltage deviation, and thus, reduce the number of tap operations. The second activated method is the OLTC control (yellow block). A double-check process (grey block) is introduced before activating the last control method in order to ensure that there is no feasible solutions to enable an OLTC

control (feasible solution strategy). The last activated control method is the active power curtailment by the DG, as the brown block shown.

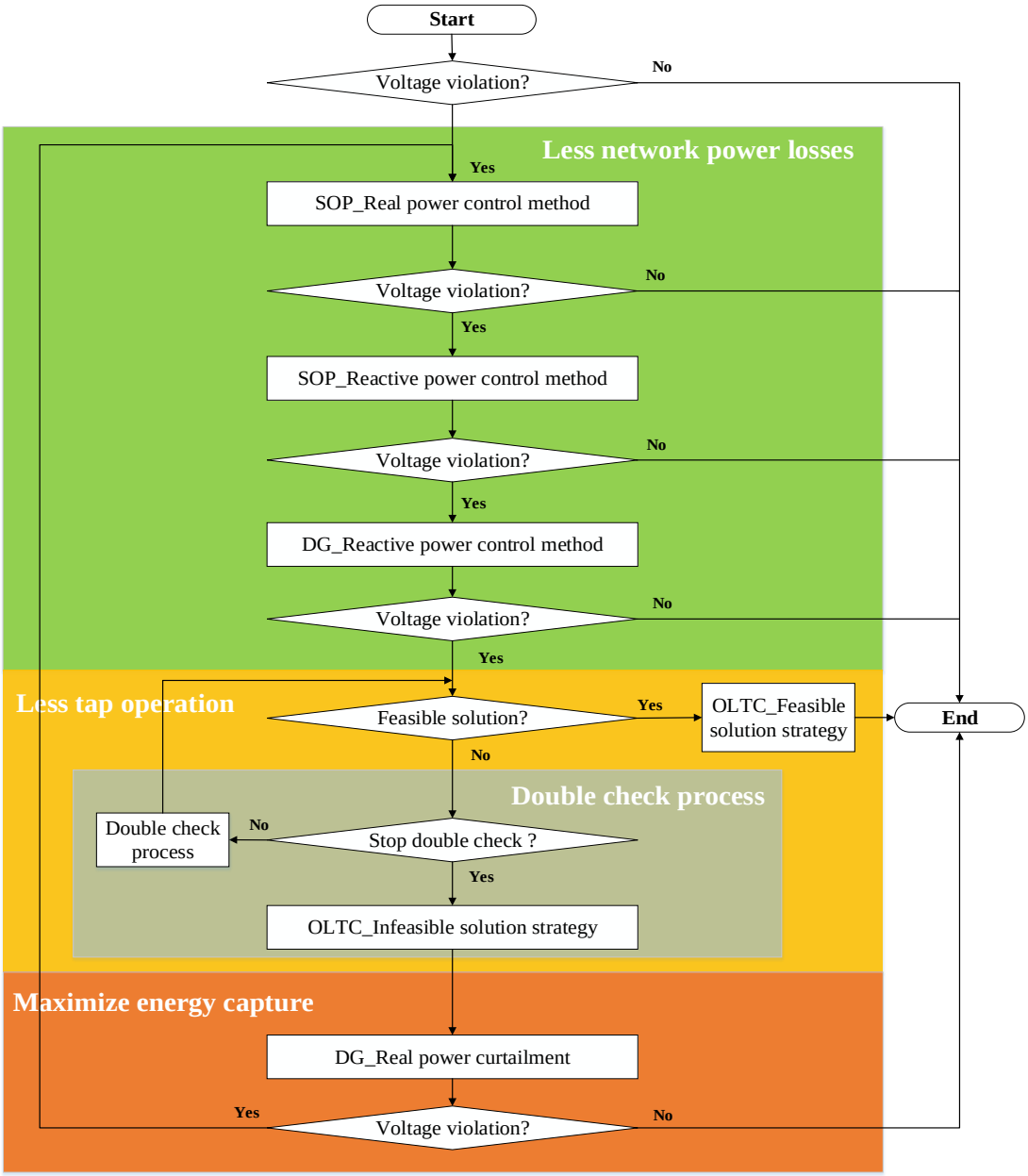

Figure 5.15: Flow chart of the proposed priority-based coordination

The details of the voltage control method for each agent and the double check process are given as follows.

- **Voltage control for the SOP agent**

A. Bidirectional interface

The SOP control agent receives data from the information-sharing platform. These data contains the action command, magnitudes and locations of all potential maximum and minimum voltages along the connected feeders. The action command specifies the method to be activated at current time step. The locations of all potential maximum and minimum voltage points are sent to the *knowledge based* to calculate the sensitivity factors.

After the *control algorithm module* determines the required real or reactive power for the SOP agent, two messages are sent out via the *interface*: the new real or reactive power set point to the actuator and the action confirmed message to the information-sharing platform.

B. Control algorithm module

The control algorithm module implements the control algorithm based on the action command, voltage data and the corresponding sensitivity factors.

1) Active power control algorithm

The active power control algorithm solves the optimization problem shown in (5-20)-(5-23). The objective function aims to minimize the voltage deviation of the maximum and minimum voltages along both connected feeders from the nominal value, V_{norm}:

$$Minimize \qquad F(P_{S\_inj}^{new}) = \sum_{i=1}^{N}(V_i - V_{norm})^2 \tag{5-20}$$

subject to

$$\left|P_{S\_inj}^{new}\right| \le P_{S\_inj}^{lim}, \quad P_{S\_inj}^{lim} = \sqrt{{S_{SOP}^{rate}}^2 - {Q_{S\_inj}}^2} \tag{5-21}$$

$$V_i^{new2} = V_i^{old2} - M_i \cdot (P_{S\_inj}^{new} - P_{S\_inj}^{old}) \quad (5\text{-}22)$$

$$V_{min}^{band} \leq V_i \leq V_{max}^{band} \quad (5\text{-}23)$$

where V_i is the voltage magnitude received from the *interface*; N is the total number of voltage points received from the *interface*; S_{SOP}^{lim} is the rating power of the SOP device; M_i is the sensitivity factor for the change of voltage V_i with respect to the change of active power; V_{min}^{band} and V_{max}^{band} are the acceptable limits of bandwidth for voltage control using the SOP agent. In this work, V_{norm} is assumed to be 1 p.u., i.e., a middle point between the upper and lower limits in order to leave headroom for both over- and under-voltage issues due to the future DG penetrations and increase of demands, e.g., electric vehicles and heat pumps.

Note that the defined bandwidth in (5-23) is wider than the specified limits to avoid the infeasible solution, which may occur due to the device power limits in (5-21). This wider bandwidth is also applied to the reactive power method of the SOP and DG agent and is refined by using the OLTC agent to ensure that the network voltages within the statutory limits. The optimization algorithm used in this study was the Powell's Direct Set Method, which is described in Chapter 4.

2) Reactive power control algorithm

The aim of reactive power control is to minimize the voltage deviation from the nominal value and the amount of reactive power absorbed by the SOP to improve voltage control. The objective function is defined as

$$Minimize \quad J\left(Q_{S_{inj}}^{new}\right) = \sum_{i=1}^{N}(V_i - V_{norm})^2 - \omega_{absor} \cdot min\{0, Q_{S_{inj}}^{new}\} \quad (5\text{-}24)$$

subject to

$$\left|Q_{S_{inj}}^{new}\right| \leq Q_{S\_inj}^{lim}, \quad Q_{S\_inj}^{lim} = \sqrt{{S_{SOP}^{lim}}^2 - {P_{S\_inj}}^2} \tag{5-25}$$

$$V_i^{new\,2} = V_i^{old\,2} - K_i \cdot (Q_{S\_inj}^{new} - Q_{S\_inj}^{old}) \tag{5-26}$$

$$V_{min}^{band} \leq V_i \leq V_{max}^{band} \tag{5-27}$$

where $Q_{S_{inj}}^{new}$ is the reactive power supplied by the SOP, and it turns to be a negative value when the SOP absorbs reactive power from the connected feeder; ω_{absor} is the penalty factor for absorbing reactive power from the connected feeder in order to avoid the increase in the losses along the feeder, i.e., the term $-\omega_{absor} \cdot min\{0, Q_{S_{inj}}^{new}\}$ will turn to be a non-zero (positive) value and add to the objective function when the SOP absorbs reactive power from the network; K_i is the sensitivity factor for the change of voltage V_i with respect to the change of reactive power.

- **Voltage control for the DG agent**

In this work, the DG units are assumed to operate at the maximum power point tracking (MPPT) before receiving the voltage control command from the information-sharing platform. Once receiving a command, the DG agents will accept or refuse the command based on the assessment of the request, for instance, assessing the remaining capacity for voltage support.

A. Bidirectional interface

The DG agent receives data from the information-sharing platform. Similar to the SOP agent, these data contains the action command, magnitudes and locations of potential maximum and minimum voltages along the connected feeder. The action command specifies the control method to be activated at current time step, i.e., reactive power control or active power curtailment. The locations of potential maximum and minimum voltage points are sent to the *knowledge based* to calculate the sensitivity factors.

After the *control algorithm module* determines the required reactive power or active power curtailment from the DG agent, two messages are sent out via the *interface*: the new power set point to the actuator and the action confirmed message to the information-sharing platform

B. Control algorithm module

1) Reactive power control algorithm

The aim of reactive power control by the DG agent is similar to that of the SOP agent. The objective function is given as

$$Minimize \quad J\left(Q_g^{new}\right) = \sum_{i=1}^{N}(V_i - V_{norm})^2 + \omega_{absor} \cdot min\{0, Q_g^{new}\} \tag{5-28}$$

subject to

$$\left|Q_g^{new}\right| \le Q_{S\_inj}^{lim}, \quad Q_{S\_inj}^{lim} = \sqrt{{S_g^{rate}}^2 - {P_g}^2} \tag{5-29}$$

$${V_i^{new}}^2 = {V_i^{old}}^2 - K_i \cdot (Q_g^{new} - Q_g^{old}) \tag{5-30}$$

$$V_{min}^{band} \le V_i \le V_{max}^{band} \tag{5-31}$$

where Q_g^{new} is the reactive power supplied by the SOP, and it turns to be a negative value when the DG absorbs reactive power from the connected feeder; ω_{absor} is the weight for absorbing reactive power from the connected feeder; K_i is the sensitivity factor for the change of voltage V_i with respect to the change of reactive power.

2) Active power curtailment algorithm

The objective of this method is to determine the required active power curtailment that keeps the maximum voltage within the specified upper limits using

$${V_{Upper}}^2 - {V_{max}^{old}}^2 + M_{max} \cdot (P_g^{new} - P_g^{MPPT}) \ =0 \tag{5-32}$$

where M_{max} is the sensitivity factor of the maximum voltage point; P_g^{MPPT} is the active power generation of the DG units under MPPT mode.

C. Coordination among multiple DG agents

The aim of coordinating multiple DG agents for voltage control is to minimize the cost of reactive power control and active power curtailment for all participated DG agents. In this work, all DG agents are assumed to have equal weights of real and reactive power control for voltage control. Therefore, the cost is only determined by the amount of reactive power support or active power curtailment of the participated DG agents. The coordination schemes among DG agents for different control methods are summarized as follows.

1) Coordination for reactive power control

A prioritization of the DG agents for reactive power control is determined based on the sensitivity factors using the follows steps:

Step 1) If the information–sharing platform determines to activate the reactive power control from DG agents, the last downstream DG along the feeder (most sensitive to voltage change) is informed first to achieve the optimization purpose. The required reactive power is calculated using (5-28) and the new reference is updated.

Step 2) If there is still voltage violations after activating the last downstream DG agent, the next *upstream* DG agent (second most sensitive to voltage change) is activated.

Step 3) Step 1) and 2) are repeated until there is no voltage violation along the feeder or the fist upstream DG agent is reached.

2) Coordination for active power curtailment

For active power control, the DG agent where the connecting bus has an overvoltage is activated first. The next *downstream* DG agent is activated if there is still a voltage violation. This sequence is due to the factors that 1) any DG agent connecting to the

downstream feeder of the overvoltage bus has the same while maximum sensitivity factor to the overvoltage bus; and 2) the further the downstream DG is to the substation, the more sensitive to voltage change it will be thus has a higher possibility to cause the voltage at any other bus exceeding the lower limit due to the active power curtailment.

- **Voltage control for the OLTC agent**

It was assumed in this study that the substation transformer has an on-load tap changer on the primary winding and the voltage on the primary side remains constant.

A. Bidirectional interface

The OLTC agent receives the action command and the overall maximum and minimum voltages of the network from the information-sharing platform. The action command specifies the control strategy required: feasible solution strategy or infeasible solution strategy. After the *control algorithm module* determines the new tap setting of the OLTC agent, two messages are sent out via the *interface*: the new reference to the actuator and the task confirmed message to the information-sharing platform

B. Control algorithm module

The control algorithm module receives the voltage data and action command from the *interface* and then implements the relevant control strategy described below.

1) Feasible solution strategy

When the agent receives a feasible solution message, i.e., $V_{max} - V_{min} \leq V_{upper} - V_{lower}$, the control algorithm module calculates the number of required taps at each time step *i* using

$$\begin{cases} T^i = T^{i-1} + \text{round}\left(\frac{V_{min} - V_{lower}}{\Delta V}\right), & \text{if } V_{lower} > V_{min} \\ T^i = T^{i-1} + \text{round}\left(\frac{V_{upper} - V_{max}}{\Delta V}\right), & \text{if } V_{upper} < V_{max} \end{cases} \tag{5-33}$$

subject to

$$V_s = V_p + T \cdot \Delta V \tag{5-34}$$

$$T_{\mathrm{upp}er} \le T^i \le T_{\mathrm{Lower}} \tag{5-35}$$

Where T^i and T^{i-1} is the tap position at time step *i* and *i-1*; V_{max} and V_{min} are the overall maximum and minimum voltage of the network; V_{upper} and V_{lower} are the standard upper and lower voltage limits; T^{old} is current tap position; ΔV is the step voltage of each tap; V_s is the secondary voltage of the substation; V_p is primary voltage of the substation; $T_{\mathrm{upp}er}$ and T_{Lower} are the upper and lower boundary of the OLTC.

2) Infeasible solution strategy

The infeasible solution strategy is required after the double check process while the infeasible solution still exists. The aim of this strategy is to keep the minimum voltage, V_{min} at the specified lower limit. Thus the maximum voltage though still violates the upper limit but is as low as possible, which in turn minimize the required curtailment of the DG active power. Thus the new tap setting is obtained using

$$T^i = T^{i-1} + \mathrm{round}\left(\frac{V_{min} - V_{lower}}{\Delta V}\right) \tag{5-36}$$

subject to

$$T_{\mathrm{upp}er} \le T^i \le T_{\mathrm{Lower}} \tag{5-37}$$

- **Voltage control for the double check process**

The purpose of the double check process is to avoid unnecessary DG active power curtailment. It is achieved by enabling a feasible solution for the OLTC control by either controlling the violated extreme voltage or controlling the other extreme voltage. The whole process is performed within the information-sharing platform as follows:

Step 1) Check for the condition of an infeasible solution before activating the

OLTC agent using

$$V_{upper} - V_{lower} < V_{max} - V_{min} \quad (5\text{-}38)$$

Step 2) If the infeasible solution is raised, allocate the feeders where V_{max} and V_{min} happen and then initiate the double check process. Otherwise, send an action command to the OLTC agent to activate the feasible solution strategy.

Step 3) If the double check process is initiated, activate the control agent (or method) that is connected to the feeder where V_{max} or V_{min} happens. The control method that has already been activated is not involved in this process.

Step 4) If there are multiple candidates, repeat step 1) - 3) until there is a feasible solution or all the candidates have been activated. The sequence of activating a candidate at each time step is based on the proposed coordination law shown in Figure 5.13, i.e., SOP active power control, SOP reactive control and finally DG reactive power control.

5.3.3 Implementation procedures of the information-sharing platform

The overall implementation procedures of the information-sharing platform are summarized below.

Step 1) Update the voltage information after receiving segment voltage data from the local control agents.

Step 2) Determine the maximum and minimum voltages in each feeder. Then, check the condition of voltage violation.

Step 3) If there is no voltage violation, go to step 1. Otherwise, allocate the feeders at which the voltage exceeds the specified limit and then initiate the coordinated control on these feeders.

Step 4) Send an action command to activate the relevant agent based on the

coordination law described in Section 5.3.2.

Step 5) Each time after receiving the action confirmed message from the agent, update voltage information by repeating step 1) and 2). If there is no voltage violation or all available control methods have been activated, go to step 1). Otherwise, go to step 4).

5.4 Discussion: Benefits of the Proposed Control Strategy

The main advantages of the coordinated voltage control strategy are summarized below.

- The proposed voltage control framework allows for required coordination between multiple agents (devices) while independent real-time control by each local control agent. Moreover, it is easy to modify and upgrade each local control agent or implement expansion (e.g. more DG connections) without interrupting other parts of control framework.
- Further flexibility is provided by the SOP when the over- and under-voltage issues exist simultaneously within a network that cannot be solved by the OLTC. The use of SOP also reduces network power losses compared to reactive power control (e.g. capacitor banks). Moreover, the power electronic based device provides fast enough voltage control compared with the tap changing devices (e.g., OLTC, capacitor banks), which may be needed for DGs to ride through the voltage sags during emergency conditions.
- A trade-off of the objectives, according to their prioritisation, is achieved by using the proposed priority-based coordination method. This method performed by an information-sharing platform is in line with the distributed control concept while unnecessary negotiation process among agents is eliminated and data communications are reduced.

- The computational burden is reduced because 1) a distributed voltage control is achieved by the local control agent, instead of doing a centralised calculation/optimisation using all data together, and 2) with the use of the simplified estimation method, the knowledge of the network voltage profile is obtained by each agent that find their respective maximum voltage and minimum voltages (within its corresponding segments) simultaneously. In addition, the numerical convergence problems of running the power flow algorithm is eliminated since there is no need for running the power flow algorithm in each time step, especially in the case of high R/X ratio networks.
- The communication investments are reduced since the meters and sensors are placed at the OLTC, DG and SOP connecting points and only the critical data are exchanged via the information-sharing platform.

5.5 Case Study

The effectiveness of the coordinated voltage control strategy was verified on an MV distribution network obtained from [55], as shown in Figure 5.16. This network is a 33-bus 11-kV distribution system with four feeders. The four feeders have different lengths, ratings and load types. Intermittent DG units with different characteristics were connected to different buses to simulate the unbalance in load/generation diversity between feeders. Table 5.1 shows a summary of the loads and DGs data. Figure 5.17 depicts the normalized profiles for different load types (commercial, residential and industrial) and for different DG types within two days (a weekday and a weekend). These normalized profiles (half-hourly per step) were multiplied by the rated power of each load or DG (shown in Table 5.1) to have the power daily profile of each bus. All these data were obtained from [55]. More detailed network data can be found in the Appendix B. The voltage limits of this test network are 11 kV $\pm$5%. The OLTC was assumed to have 32 taps with 0.00625 p.u. per step. An SOP was assumed to be installed between feeder 2 and 3. The capacity limit of the SOP is 1 MVA. This study

was programmed in Java and C. Balanced three-phase feeders were considered.

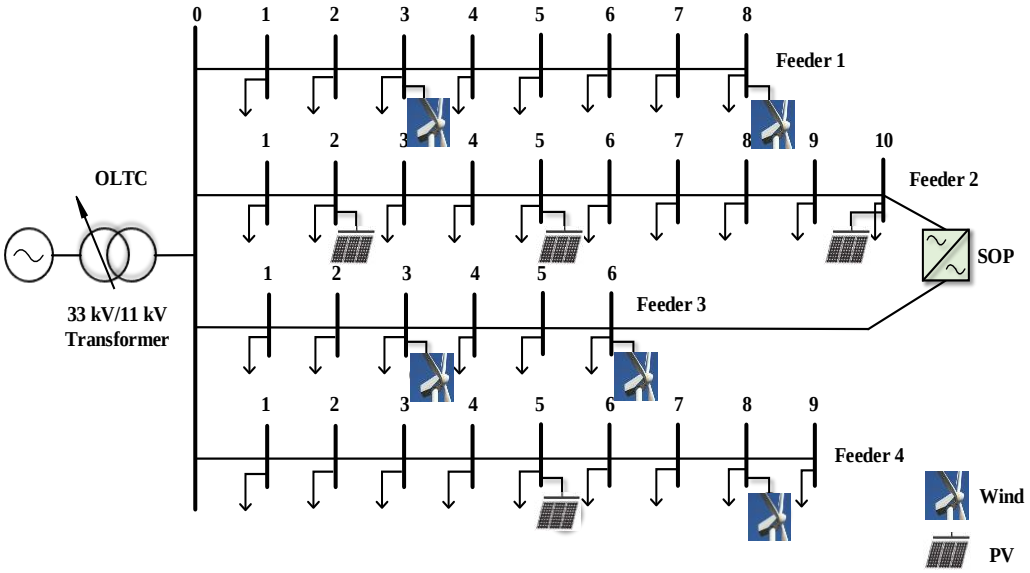

Figure 5.16: The four-feeder MV test network

Table 5.1: Data of the Load and DG

Feeder number	*Load profile*		*DG profile*		
	Types	Total rated loading (MVA)	Types	Locations	Ratings (MVA)
1	Commercial	4	Wind	3, 8	2, 0.5
2	Residential	5	PV	2, 5, 10	5, 2, 1
3	Industrial	3	Wind	3, 6	0.5, 2.5
4	Residential	4.5	PV, wind	5, 8	0.5, 0.5

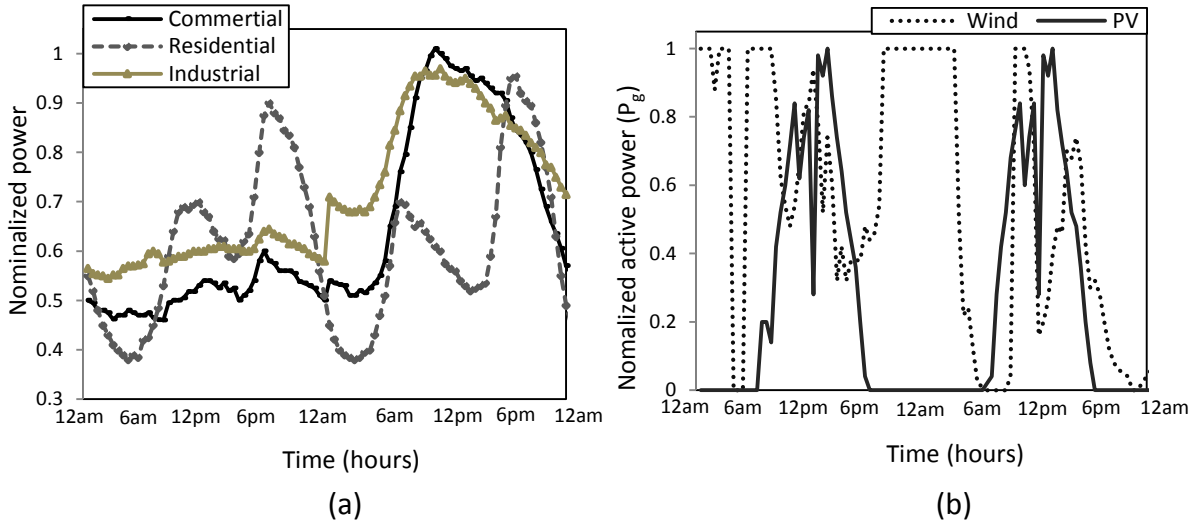

(a) (b)

Figure 5.17: Normalized profiles of a weekend and weekday: (a) loads; (b) DGs

5.5.1 Voltage Profile Estimation

The voltage profile generated by the estimation method proposed in section 5.2.1 was compared with the actual voltage profile (calculated by power flow analysis). Figure 5.18 shows the overall maximum and minimum voltages along each feeder during the studied two days before voltage control. The maximum voltage was read from meters thus the same. It can be seen that the estimated minimum voltages were close to the actual values (the maximum difference is 0.004 p.u). For the minimum voltages, lower voltage bounds were generated by the proposed simplified estimation method (see the red curves). Therefore, more conservative voltage references will be used for voltage control using the proposed estimation method.

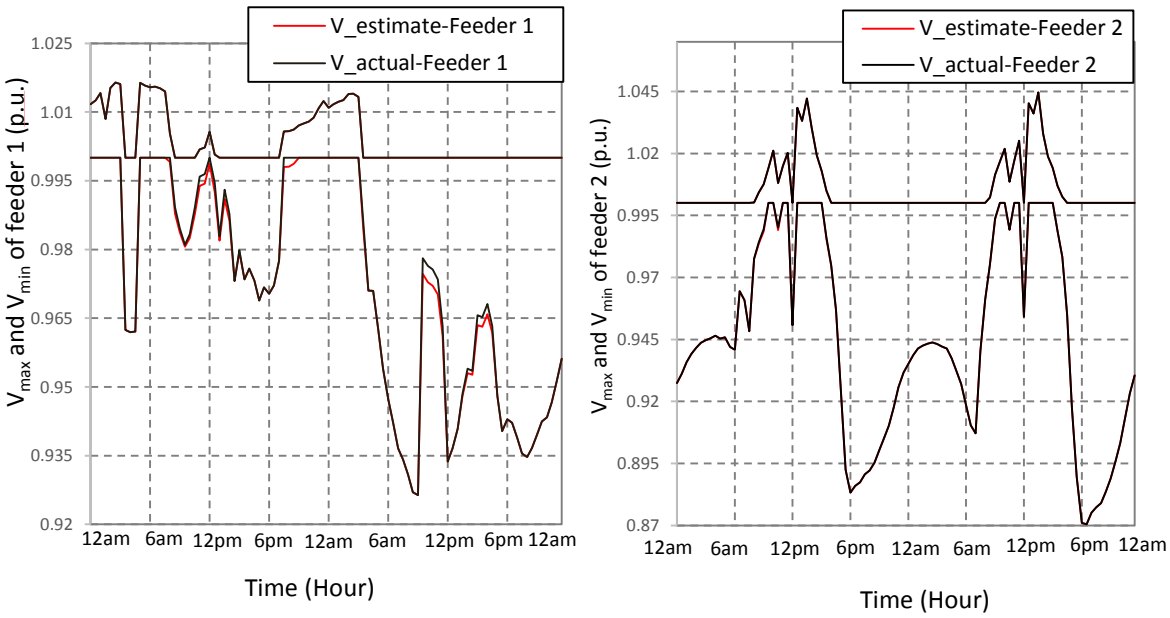

(a) (b)

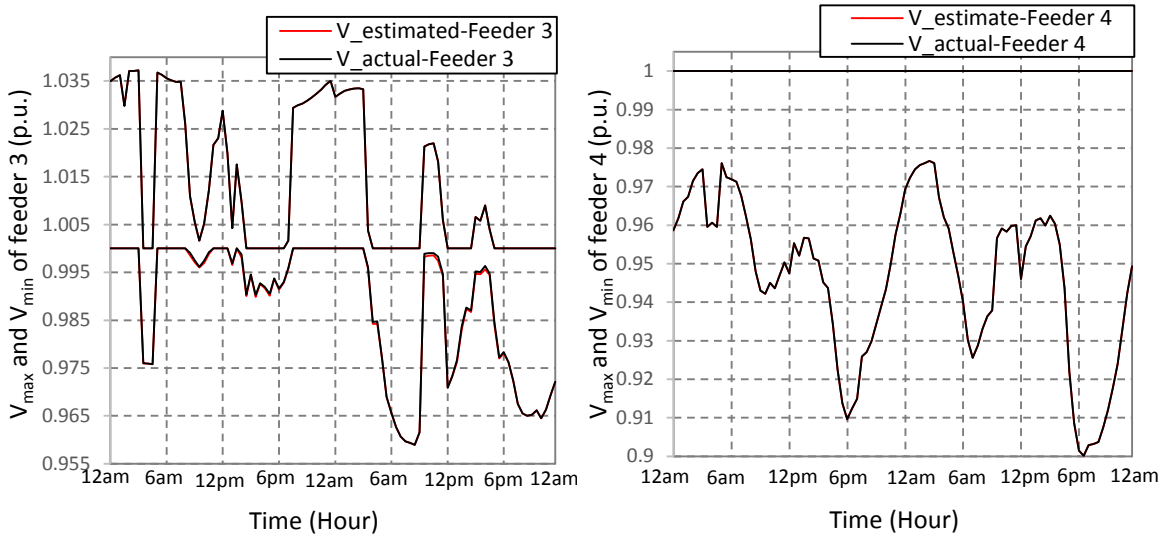

(c) (d)

Figure 5.18: Per unit maximum and minimum voltage profile over the studied period at (a) feeder 1; (b) feeder 2; (c) feeder 3; (d) feeder 4

Figure 5.19 shows the snapshot voltage profiles of all buses along each of the four feeders at 11 am in the first studied day. The voltage profile by the proposed method were generated by connecting the critical voltage points, i.e., the measured voltages (at the substation busbar, SOP and DG connecting buses) and the estimated minimum voltage within each segment using the segment estimation method. It is clear that all the maximum and minimum voltage points were captured as expected.

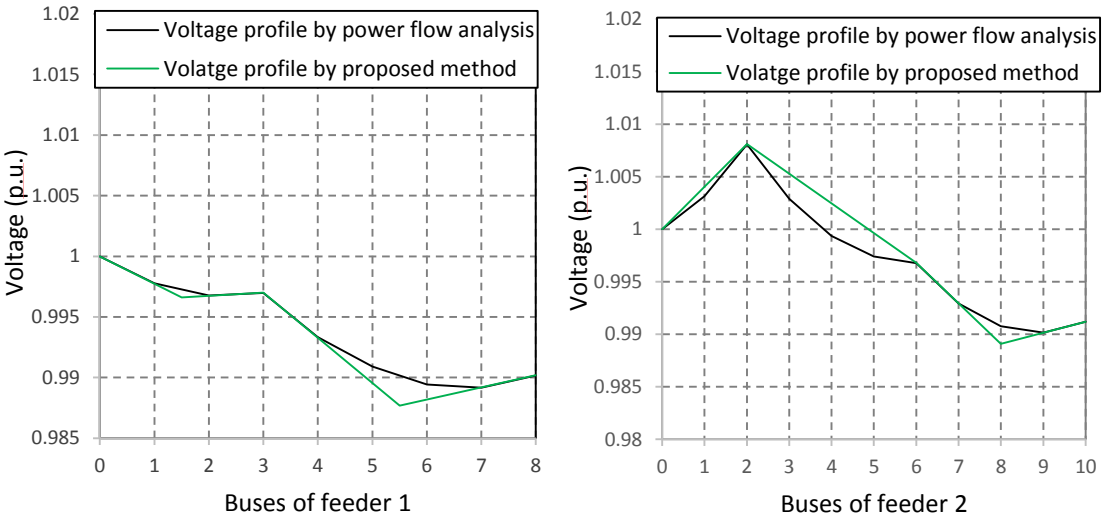

(a) (b)

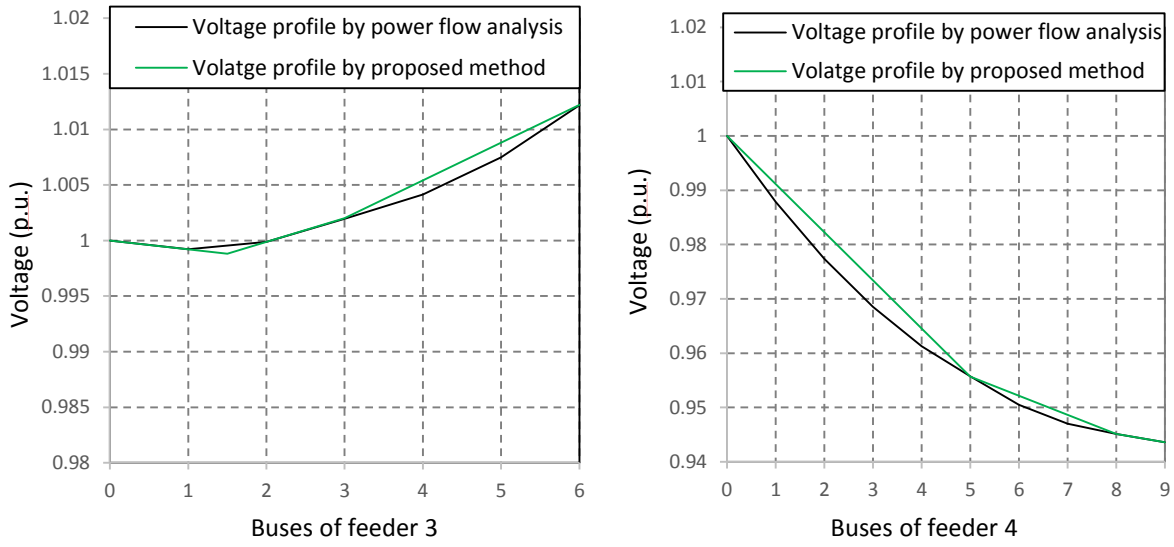

(c) (d)

Figure 5.19: Per unit voltage profile at 11am in the first studied day along (a) feeder 1; (2) feeder 2; (3) feeder 3; (4) feeder 4

5.5.2 Coordinated voltage control using OLTC and SOP

Most utilities prefer DG units to operate close to the unity power factor and do not allow regulating the voltage actively at the Point of Common Coupling [103]. In this context, the coordinated control merely considering the OLTC and SOP was conducted to investigate the performance of the proposed control strategy. All the DG units were assumed to operate in maximum power point tracking (MPPT) with unity power factor. Four control schemes were carried out for comparisons:

Scheme I: Voltage control using the OLTC;

Scheme II: Coordinated control between the OLTC and the SOP assuming only active power control;

Scheme III: Coordinated control between the OLTC and the SOP assuming only reactive power control;

Scheme IV: Coordinated control between the OLTC and the SOP assuming both real and reactive power control based on the proposed priority-based coordination.

The performance of the control schemes were evaluated in terms of the network voltage profile, the number of tap operations, total network power losses and the required size for the SOP to achieve voltage control.

- **Network voltage profile**

Figure 5.20 shows the overall maximum and minimum voltages of the network during the studied period when different control schemes are used. As shown in the figure, the network voltage profiles were within the specified limits for most of the time by using the OLTC, i.e., Scheme I. However, it could not solve the areas of infeasible solutions shown in the figure. These areas of infeasible solutions were mitigated when the SOP was coordinated with the OLTC, i.e., using Scheme II, III and IV.

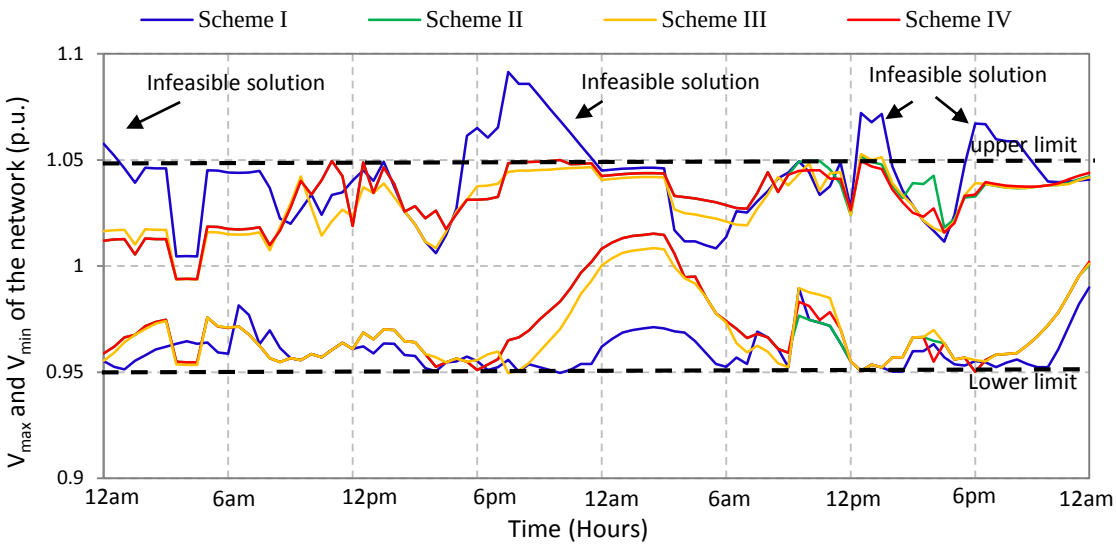

Figure 5.20: maximum and minimum voltage profiles at different control schemes

- **Tap operation**

Figure 5.21 compares the number of tap changes during the studies period when different control schemes are used. As shown in the figure, the number of tap operations was reduced significantly when the SOP was coordinated with the OLTC, i.e., using Scheme II, III and IV. The highest reduction was achieved by using Scheme

IV, which was reduced from 46 to 16 taps compared with Scheme I.

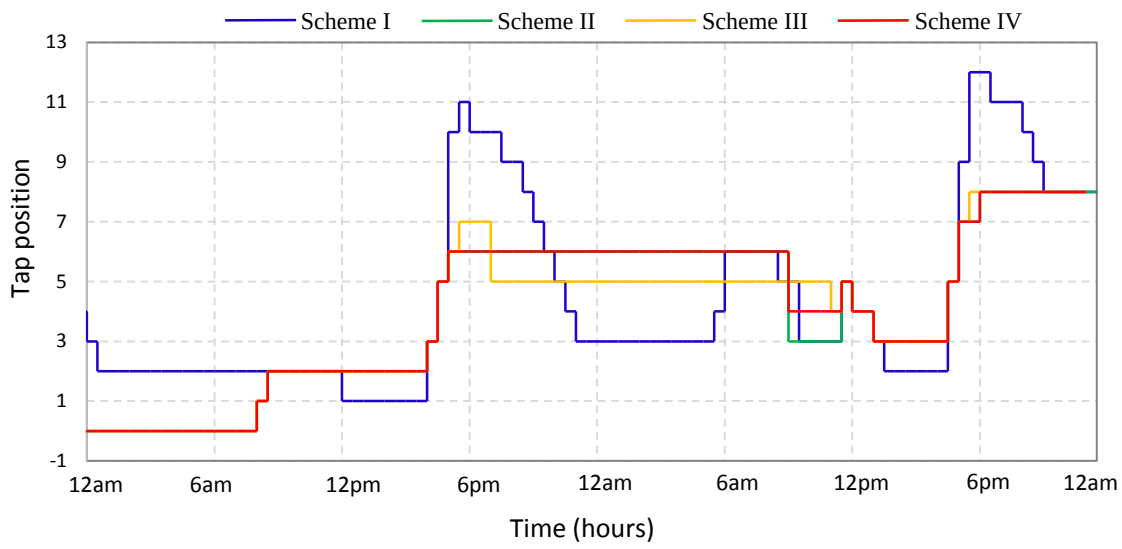

Figure 5.21: Change of the tap operation at different control schemes

- **Network power losses**

Figure 5.22 compares the total network losses at different control schemes. It can be seen that the total network losses were reduced when Scheme II and IV were used. The highest loss reduction (by 21.93%) was achieved when the active power control of the SOP was merely considered (Scheme II). Such loss reduction benefit was slightly lessened by 19.41% when Scheme IV was used due to the participation of reactive power control. However, on the contrary, the total network power losses were increased by 11.60% when the reactive power control of the SOP was merely considered (Scheme III). This is due to the excessive absorption of reactive power from the network, which is in line with the previous results obtained in Section 5.3.1.

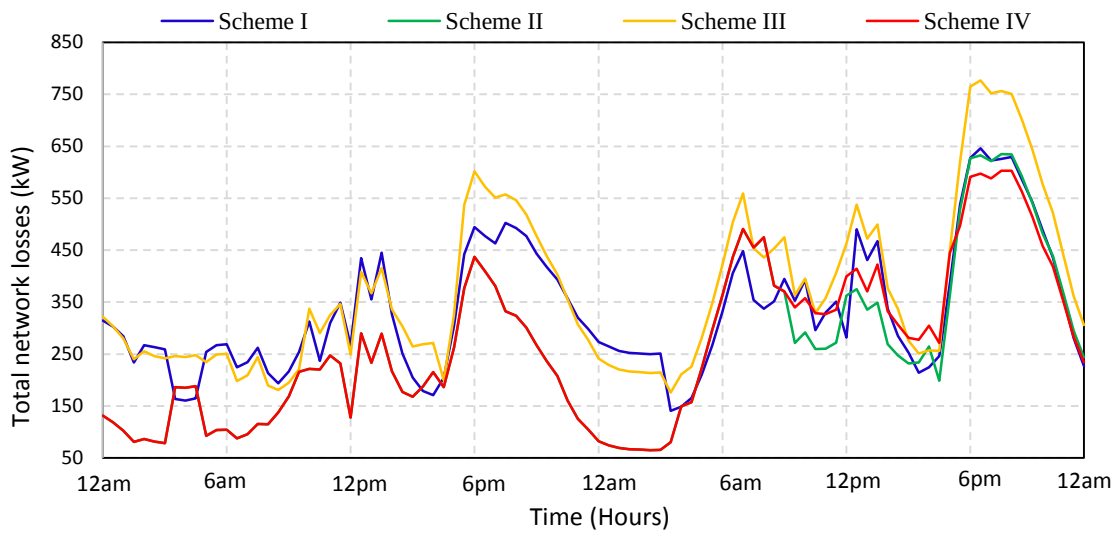

Figure 5.22: Total network losses at different control schemes

- **Required size of the SOP**

Figure 5.23 shows the required size (in apparent power) of the SOP for the corresponding control schemes. All the three control schemes considering SOP compensate the changes of the load demands and DG productions which, in turn, reduces the dynamic changes of the voltage profiles and hence the number of tap operations. However, the SOP operated at its rated power for most of the time when only controls reactive power (Scheme III). When controls active power (Scheme II), the SOP operated at its rated power for only a few hours. The total hours, operating at rated power using the coordinated real and reactive power control (Scheme IV), was in between the other two.

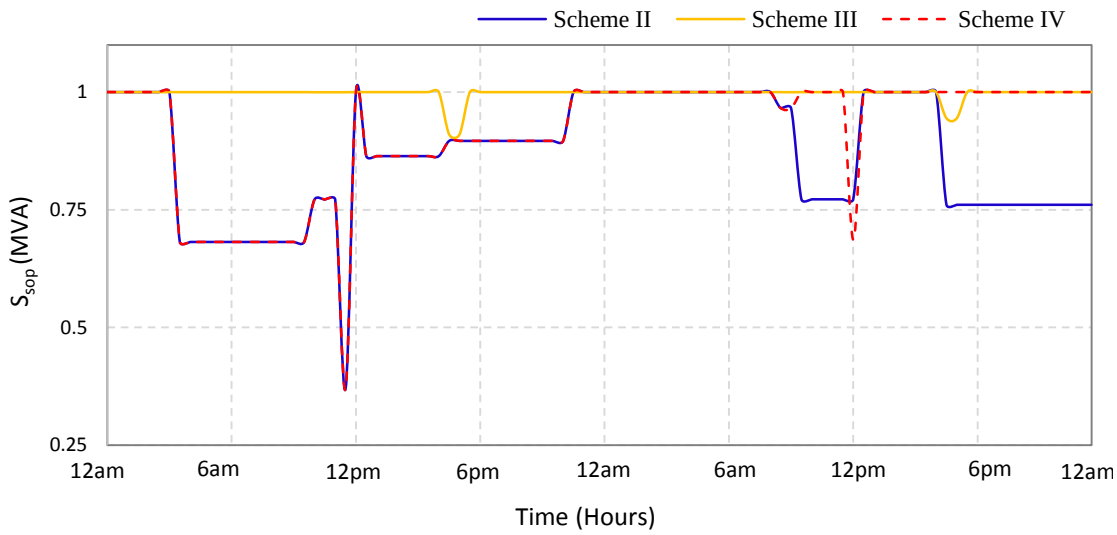

Figure 5.23: Apparent power requirements for different SOP control schemes

From the above results, it is concluded that the coordination between the OLTC and the SOP is essential when the OLTC is infeasible to solve the voltage problems. In addition, the proposed priority-based coordination of the OLTC and SOP achieves the best compromise of the sub-objectives (in accordance with the prioritisation of the objectives). It enables smaller number of tap operations comparing to the scheme of only using the active power control and fewer power losses comparing with only using the reactive power control.

5.5.3 Coordinated voltage control using OLTC, SOP and DG

Increasing the DG penetration in the distribution network brings more difficulties in controlling network voltages. The previous control using the OLTC and the SOP may not be able to control the voltage within the specified limits in such a case. Figure 5.24 shows the overall maximum and minimum voltages of the network during the studied period when the capacity (rated power shown in Table 5.1) of the DG units (connected in feeder 2) were enlarged by 10%. It is shown that an overvoltage problem still exist during the peak PV generation when the coordinated control between OLTC and SOP was used.

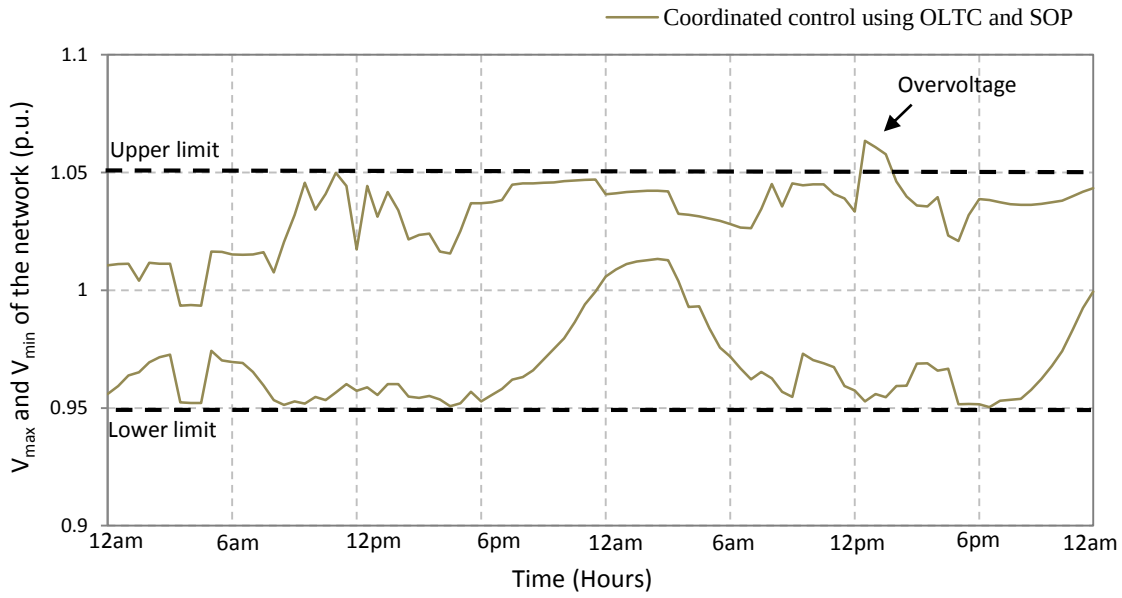

Figure 5.24: maximum and minimum voltage profiles when increase DG penetration

The coordinated control using the OLTC, SOP and DG units was conducted in this part. It was assumed that DG units installed at bus 9 in feeder 1, bus 5 in feeder 2, bus 6 in feeder 3 and bus 8 in feeder 4 were inverter-based DG unit and thus had the reactive power control capability. All DG owners were obligated to respond to the active power curtailment request.

Two different cases were carried out for comparison purposes, which are the coordinated control using OLTC and DG units and the coordinated control using OLTC, SOP and DG units. The performance of these two cases were evaluated in terms of the network voltage profile, the total active power generated by DGs, the number of tap operations, total network power losses and the power settings of the SOP and DG unit.

- **Network voltage profile and total active power generated by DGs**

Figure 5.25 shows the maximum and minimum voltages of the network during the studied period. It can be seen that the overvoltage problem was solved for both cases when the DG units were involved in voltage control. However, DG active power curtailment was required for the case without involving the SOP control, as shown in

Figure 5.26. There was no curtailed DG active power when OLTC, SOP and DG units were coordinated for voltage control.

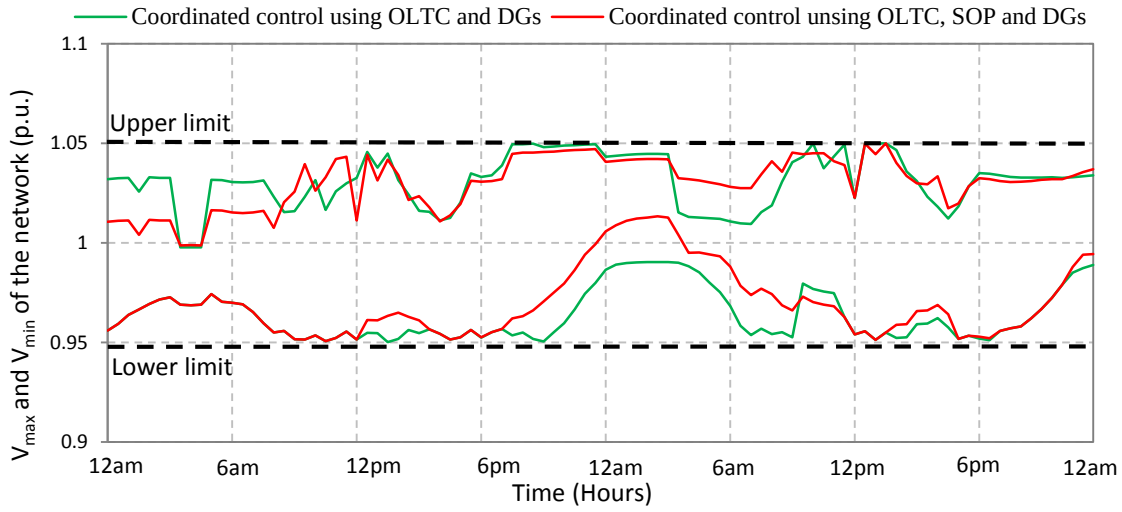

Figure 5.25: maximum and minimum voltage profiles with increased DG penetration by coordinated control with and without involving SOP

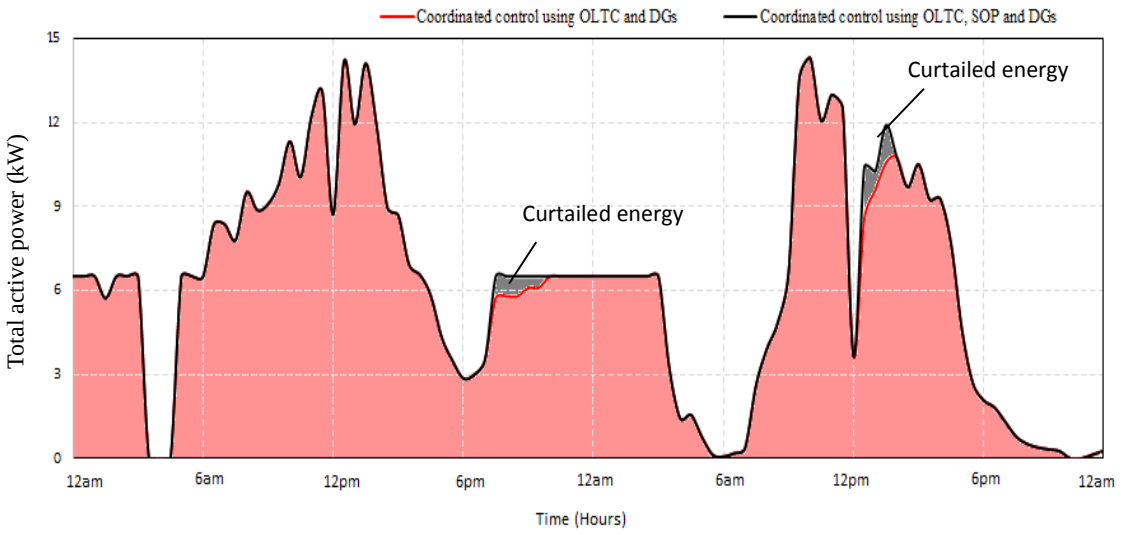

Figure 5.26: Total active power generated with increased DG penetration by coordinated control with and without involving SOP

- **Tap operation**

Figure 5.27 compares the number of tap changes during the studied period at different cases. As shown in the figure, a smaller number of tap operation was required when the OLTC, SOP and DG units were coordinated. The tap operation was reduced from 21 to

15 taps.

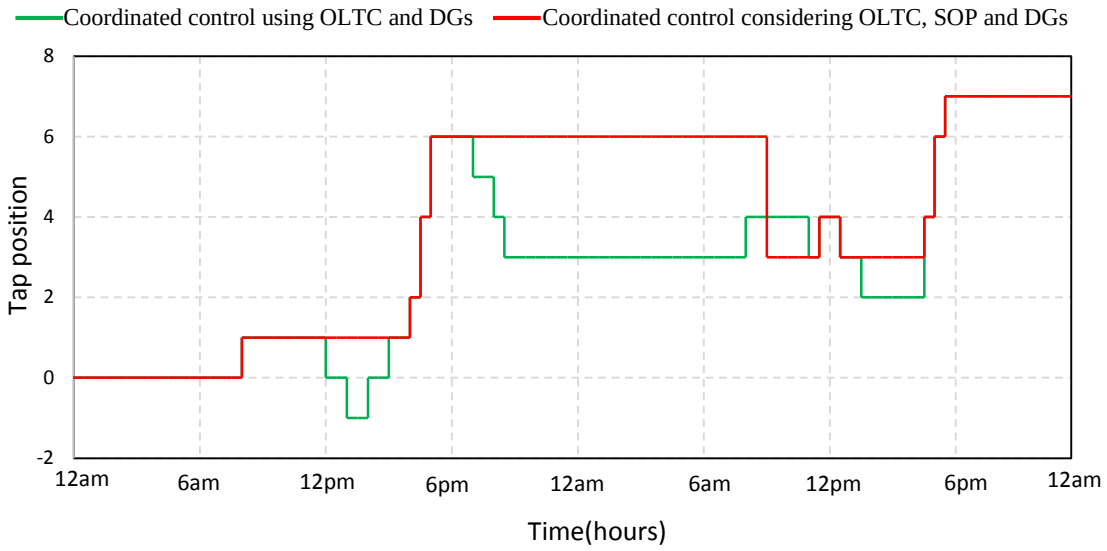

Figure 5.27: Change of the tap operation with increased DG penetration at different cases.

- **Network power losses**

Figure 5.28 compares the total network losses during the studied period at difference cases. It can be seen that the total network losses were reduced by 18.98% when the SOP were involved in the coordinated voltage control.

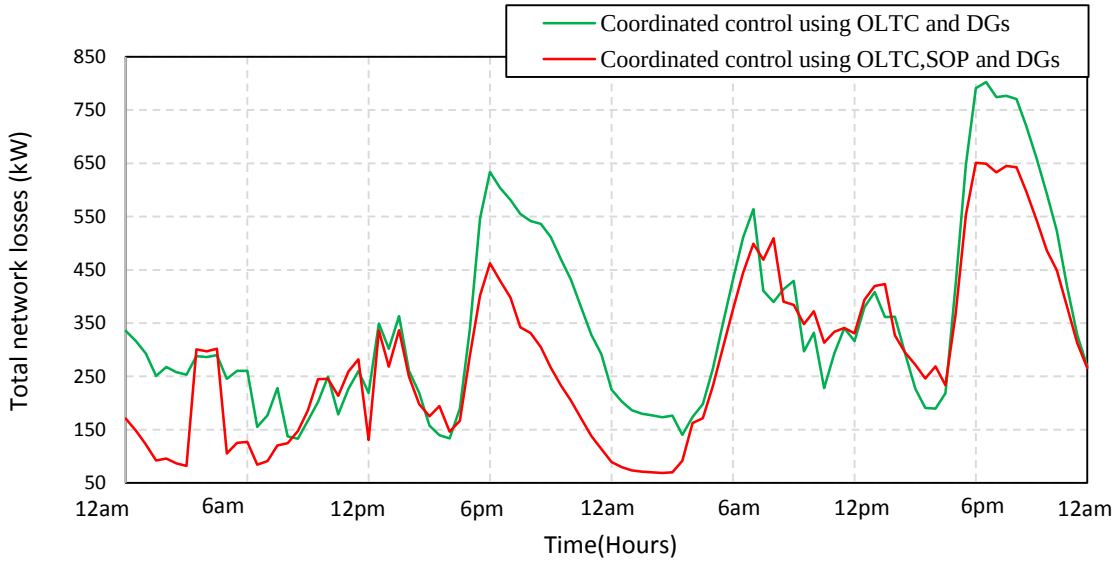

Figure 5.28: Total network losses with increased DG penetration

- **Power settings of the SOP and DG unit**

Figure 5.29 shows the required size (in apparent power) for the SOP and the reactive power for the PV DG units at bus 5 in feeder 2 during the studied period. As shown in Figure 5.29a, the SOP operates at its rated power for most of the time. For the PV DG unit, as shown in Figure 5.29b, it was operated under its rated power for most of the time when the SOP was not involved in the voltage control. However, the amount of reactive power support from the DG unit was reduced significantly when OLTC, SOP and DG were coordinated for voltage control.

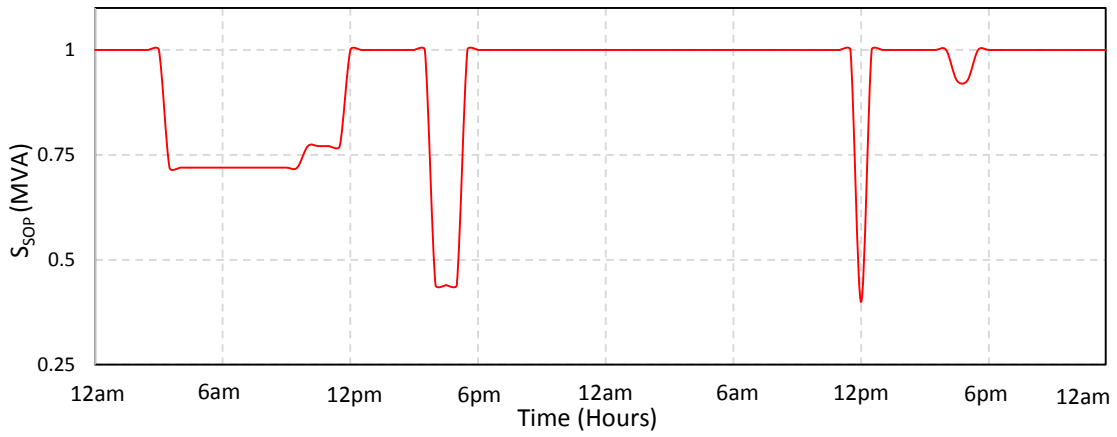

(a)

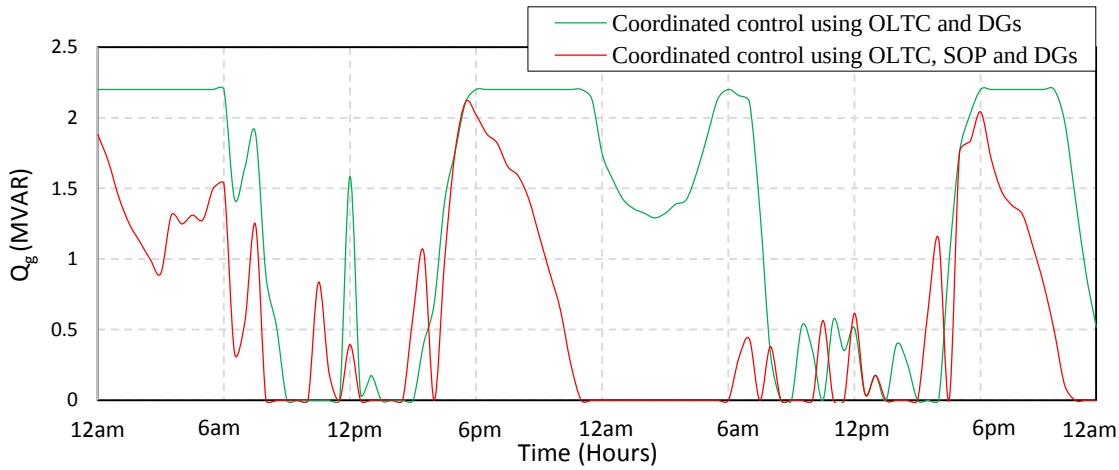

(b)

Figure 5.29: Power settings with increased DG penetration: (a) apparent power settings of the SOP, (b) reactive power settings of the PV DG unit

From the above results, it is concluded that the proposed coordination using the OLTC DG units and SOP is desirable in solving the voltage violation problem under high DG penetration while satisfying the sub-objectives, i.e., less active power curtailment, reduced number of tap operations and network power losses. The use of the proposed SOP control also reduces the amount of reactive power support from DG units for voltage control.

5.6 Summary

A novel coordinated voltage control strategy was proposed to maintain the network voltages within the specified limits whilst mitigating DG active power curtailment, reducing tap operations and network power losses. The OLTC, the SOP and multiple DG units were considered as the voltage control devices in this study.

A coordinated but distributed voltage control framework was developed which uses a simplified voltage profile estimation method. The simplified voltage profile estimation method obtain the maximum and minimum voltages of each feeder based on the measurements at the substation substation busbar, the DG and SOP locations and thus without having to measure the voltage at each network node. The voltage control framework is based on a distributed coordination where the OLTC, the SOP and the DG units are considered as the local control agents. These agents operate independently based on the local measurements and achieve the coordination via data exchange through an information-sharing platform.

Followed by an elaborated analysis of using SOP for distribution network voltage control, a priority-based coordination using the proposed voltage control framework was developed. This coordination allows the local control agents to be activated in a predefined sequence to achieve a trade-off among the objectives according to their prioritisation while remaining the independence of each agent.

Simulations verified the effectiveness of the proposed coordinated control strategy under various load and generation conditions as well as high DG penetration. The results showed that the proposed coordinated strategy has the capability to control network voltage while also mitigating DG active power curtailment, reduce the tap operations and avoid unnecessary increase in power losses in accordance with their prioritisation. Simulation results also illuminated the role and importance of the SOP for distribution network voltage control. It was found that the SOP is capable of compensating the OLTC control, avoiding unnecessary DG curtailment, reducing the number of tap operations and the network power losses as well as reducing the amount of reactive power support from DG units for voltage control.

Chapter 6

Conclusions and Future Work

THIS chapter outlines the major contributions and findings from the research. It also presents further work around the research areas in this thesis.

6.1 Conclusions

Soft Open Points are power electronic devices installed in place of normally-open points in electrical power distribution networks. They are able to provide active power flow control, reactive power compensation and voltage regulation under normal network operating conditions, as well as fast fault isolation and post-fault supply restoration under abnormal conditions. The use of SOPs for the operation of MV distribution networks was investigated from different perspectives including the control of a back-to-back VSC based SOP, the benefits analysis of using SOPs and distribution network voltage control with SOPs.

6.1.1 Control of a Back-to-Back VSC based SOP

Two control modes were developed for the operation of an SOP based on back-to-back VSCs. The power flow control mode regulates both active and reactive power flows on the connected feeders using a dual closed-loop current-controlled strategy. The supply restoration mode provides fast post-fault supply restoration to the isolated loads using a voltage and frequency control strategy. The operational principle and performance of the back-to-back VSC based SOP with these two control modes were analysed under both normal and abnormal network operating conditions:

- Under normal conditions, the proposed SOP controller is able to provide both instantaneous and longer duration power flow regulation between the connected feeders as well as dynamic Volt/VAR control on both interface terminals.

- During fault conditions, the SOP controller (power flow control mode) is able to isolate both balanced and unbalanced network fault between the connected feeders. Thus the fault propagation on the network can be limited and the short-circuit current can be maintained as same as the radial network operation without the SOP, which is important from a practical point of view as there is little impact on the existing protection schemes.

- Under post-fault supply restoration conditions, fast supply restoration (cold load pickup) can be achieved through a smooth transition between the power flow control mode and the supply restoration mode. For the transition from the power flow control mode to the supply restoration mode, a soft cold load pickup process was found preferred than a direct mode switching in order to avoid DC offset and inrush issues of current which may trigger unexpected protection operations. For the transition from the supply restoration mode to the power flow control mode, the undesirable current impulse and voltage drop can be reduced after using the voltage synchronization procedure and resetting the PI controllers.

6.1.2 Benefit Analysis of SOPs for MV Distribution Network Operation

The operational benefits of using SOPs in MV distribution networks were investigated focusing on power loss reduction, feeder load balancing and voltage profile improvement. A steady state analysis framework was developed to quantify the benefits of using SOPs. A generic power injection model of an SOP that is suitable for steady state analysis was developed. Both physical limits and internal power losses of a typical SOP device: back to back VSCs were considered in the model. The optimal SOP operation was obtained using improved Powell's Direction Set method. A combined method considering both SOP and network reconfiguration were also proposed to identify the benefits.

Based on the proposed framework, quantitative and sensitive analysis were conducted and the key findings are listed as follows:

- SOPs can contribute to significant power loss reduction, feeder load balancing and voltage profile improvement. In the case study, using only one SOP achieved similar improvement on network power loss reduction and feeder load balancing compared to the case of using network reconfiguration with all branches

equipped with remotely controlled switches. By combining SOP and network reconfiguration, the greatest improvements were obtained and smaller SOP sizes were required.

- When a large capacity of DGs were connected to the distribution network, SOPs were found be able to significantly reduce the peak currents in feeders and alleviate undesirable voltage excursions induced by the connection of DG and demand. Therefore, SOPs can be used as an alternative to infrastructure upgrades in accommodating distributed energy resources.

- When the device efficiency (at rated power) decreased, the economic benefit of SOP obtained from reducing total network power losses were lowered. However, a greater positive impact were obtained when the system loading increased. The requirements on SOP device efficiency for network loss reduction were reduced when the system loading increased.

6.1.3 Voltage Control in Active Distribution Networks with SOPs

A novel coordinated voltage control strategy was proposed, in which OLTC, SOP and DG units were considered as the controllable devices. The objective of the control strategy was to maintain the network voltage within the specified limits whilst avoiding unnecessary DG active power curtailment, reducing tap operations and network power losses.

A coordinated but distributed voltage control framework was developed which uses a simplified voltage profile estimation method. The simplified voltage profile estimation method obtains the maximum and minimum voltages of each feeder based on the measurements at the substation busbar, the DG and SOP locations and thus without having to measure the voltage at each network node, which is able to reduce the investment cost. The voltage control framework is based on a distributed control scheme where the OLTC, the SOP and the DG units are considered as the local control

agents. These agents operate independently based on the local measurements and achieve the coordination via data exchange through an information-sharing platform.

Followed by an analysis of using SOP for distribution network voltage control, a priority-based coordination using the proposed control framework was developed. This coordination, without affecting the independence of each agent, allows the local control agents to be activated in a predefined sequence that can achieve a trade-off among the objectives according to their prioritisation.

The results presented prove the capability of the proposed coordinated strategy to achieve a trade-off among objectives in accordance with their prioritisation. Simulation results also illuminated the role and importance of the SOP for distribution network voltage control. It was found that the SOP is capable of compensating the OLTC control, avoiding unnecessary DG active power curtailment, reducing the number of tap operations and the network power losses as well as reducing the amount of reactive power support from DG units for voltage control.

6.2 Future Work

The following future work was identified to extend the work reported in this thesis:

6.2.1 Use of other control strategies for the operation of the back-to-back VSC based SOP

In this study, when a fault occurs on a feeder, a voltage and frequency control strategy was used for the SOP to support isolated loads due to fault isolation. However, this control strategy cannot limit the overcurrent on the interfacing VSC when a further fault occurs on the isolated area. Hence additional protection of the interfacing VSC needs to be considered. Therefore, control strategies that can provide the function of limiting overcurrent should be investigated. One possible solution is to add an inner

current control loop to the current control strategy to limit the fault current.

A mode switching method were used to achieve a transition between the two control modes of the SOP. The parameters of the PI controllers need to be determined carefully upon the switching of the control modes in order to avoid unexpected transient oscillations on the output voltage and current. Control strategies of the SOP that can avoid the mode switching process should be investigated to improve the reliability.

6.2.2 Performances of the back-to-back VSC based SOP considering different load types

The performances of a back-to-back VSC based SOP in MV distribution networks have been investigated considering passive loads with constant impedances. However, induction and/or synchronous machines (e.g., induction motor, synchronous generator) are usually connected to distribution networks. These types of loads have different load characteristics and, hence, may lead to different transient behaviours. Therefore, further investigations on the performance of the proposed SOP device with different types of network loads should be undertaken as future work.

6.2.3 Impacts of SOPs on feeder automation

Feeder automation is realized through automatic detection, isolation and reconfiguration of faulted segments on distribution feeders. In this study, the capability of the back-to-back VSC based SOP for fault isolation and post-fault supply restoration was investigated. However, the interactions between the SOP and existing feeder automation schemes were not considered.

For example, a simple form of feeder automation is achieved by deploying combinations of reclosers and sectionalizers in a radial feeder. NOPs are used to allow the radial feeders operating as an ‘open ring’. These devices (reclosers, sectionalizers and NOPs) are coordinated to minimize the interruption of supply to customers under

fault conditions. When the NOPs are replaced with SOPs, the impact of the SOP on the existing feeder automation scheme should be assessed. Additionally, the coordination between the SOP and existing feeder automation scheme to avoid incoherent control actions and approaches to obtain an optimal solution should be investigated.

6.2.4 Use of SOPs in unbalanced three-phase distribution networks

In this thesis, the use of SOPs in balanced three-phase distribution networks was investigated. However, the domestic and some commercial customers connected to the distribution network usually have single-phase connections. Therefore, the load in distribution networks cannot be perfectly balanced. The imbalance in the three-phase equipment needs to be reduced.

The SOP contains a common DC bus and hence enabling exchange of instantaneous power between phases, which can be used to rebalance the power flows on the connected feeders. Hence, new controllers should be investigated for the operation of the SOP to address unbalanced three-phase conditions. In addition, the benefits of using SOPs for the operation of unbalanced three-phase distribution networks should be quantified and evaluated. Single phase power flow and optimization are suggested as possible solution methods for the benefit analysis. New voltage control strategy to address the voltage imbalance among the three phases should also be investigated.

6.2.5 Economic analysis of SOPs in MV distribution networks

This thesis investigated the technical benefits of SOPs in MV distribution networks. However, a purely economic evaluation will give a better idea of weather the SOP implementation is feasible, and where costs must be reduced to make it feasible. Hence, further study on the economic analysis of SOPs should be undertake as future work.

The life cycle costs of SOPs should be quantified. The optimal amount, locations and sizes of SOPs should also be determined considering the capital cost of SOPs. In

addition, the power loss reduction benefit of SOPs was performed in this thesis. In order to further quantify the loss reduction benefit of SOPs, this study should be extended to the study of quantifying energy power losses during a period.

Reference

[1] National Aeronautics and Space Administration, "The Current and Future Consequences of Global Change", 08-Aug-2015. [Online]. Available: http://climate.nasa.gov/effects/. [Accessed: 11-Sep-2015]

[2] T. Overbye et al., "The Electric Power Industry and Climate Change: Power Systems Research Possibilities", Jun-2007. [Online]. Available: http://pserc.wisc.edu/documents/publications/reports/2007_reports/pserc_climate_change_final_rpt_june07.pdf. [Accessed: 11-Sep-2015]

[3] European Commission, "EU action on climate", 15-July-2015. [Online]. Available: http://ec.europa.eu/clima/policies/brief/eu/index_en.htm. [Accessed: 11-Sep-2015]

[4] Department of Energy and Climate Change, UK, "2010 to 2015 government policy: greenhouse gas emissions", 08-May-2015. [Online]. Available: https://www.gov.uk/government/publications/2010-to-2015-government-policy-greenhouse-gas-emissions/2010-to-2015-government-policy-greenhouse-gas-emissions. [Accessed: 11-Sep-2015]

[5] Her Majesty's Goverment, UK, "The UK Renewable Energy Strategy", Jul-2009. [Online]. Available: http://www.biomassenergycentre.org.uk/pls/portal/docs/PAGE/RESOURCES/REF_LIB_RES/PUBLICATIONS/THEUKRENEWABLEENERGYSTRATEGY2009.PDF. [Accessed: 11-Sep-2015]

[6] K. Qian, "Modelling of electrical distribution systems with high penetration level of distributed generation and electric vehicles," Ph.D thesis, Glasgow Caledonian University, 2000.

[7] C. L. Masters *et al.*, "Statistical evaluation of voltages in distribution systems with embedded wind generation," *IEE Proc. Gener. Transm. Distrib.*, vol. 147, no.4, pp. 207-212, Jul. 2000.

[8] I. P. D. Povh, D. Retzmann, and M. G. Weinhold, "Future Developments in Power Industry," presented at the 4th IERE General Meeting and IERE Cental and Eastern Europe Forum, Poland, 2014.

[9] International Energy Agency, "World Energy Outlook" 2009 [Online]. Available: www.worldenergyoutlook.org/media/weowebsite/2009/WEO2009.pdf. [Accessed: 11-Sep-2015]

[10] Electricity North West, UK, "Capacity and carbon challenges", 2014. [Online]. Available: http://www.enwl.co.uk/c2c/future-challenges/capacity-and-carbon-challenges

[11] Electricity North West, UK, "Impact of low carbon future", 2014. [Online]. Available: http://www.enwl.co.uk/c2c/future-challenges/impact-of-a-low-carbon-future. [Accessed: 11-Sep-2015]

[12] Ofgem, "Project Discovery Energy Market Scenarios", consultation document, 09-Oct-2009. [Online]. Available:

https://www.ofgem.gov.uk/ofgem-publications/40361/discoveryscenarioscondocfinal.pdf. [Accessed: 11-Sep-2015]

[13] H. Farhangi, "The path of the smart grid," *Power and Energy Magazine, IEEE,* vol. 8, pp. 18-28, 2010.

[14] J. Zhu, *Power System Operation Optimization*, Second ed., Wiley-IEEE Press, 2008.

[15] U.S. Department of Energy, "Smart Grid System Report", Jul- 2009, [Online]. Available: http://www.oe.energy.gov/sites/prod/files/oeprod/DocumentsandMedia/SGSRMain_090707_lowres.pdf. [Accessed: 11-Sep-2015]

[16] Department of Energy and Climate Change, UK, "Smart Grid Vision and Routemap Smart", 27-Feb-2014. [Online]. Available: https://www.gov.uk/.../Smart_Grid_Vision_and_RoutemapFINAL.pdf. [Accessed: 11-Sep-2015]

[17] Electricity Networks Strategy Group, UK, "'A Smart Grid Routemap' Executive Summary", Feb-2010. [Online]. Available: http://webarchive.nationalarchives.gov.uk/20100919181607/http:/www.ensg.gov.uk/assets/smartgrid_routemap_executive_summary_final.pdf. [Accessed: 11-Sep-2015]

[18] T. G. Richard Silversides, Tom Luth. "Power Electronics in Distribution System Management", HubNet Position Paper, 05-Jan-2015. [Online]. Available: www.hubnet.org.uk/filebyid/633/PE_Distribution.pdf. [Accessed: 11-Sep-2015]

[19] J. Ekanayake, N. Jenkins, K. Liyanage, J. Wu, and A. Yokoyama, *Smart Grid: Technology and Applications*, Wiley Press, 2012.

[20] B. A. Robbins, C. N. Hadjicostis, and A. D. Dominguez-Garcia, "A Two-Stage Distributed Architecture for Voltage Control in Power Distribution Systems," *Power Systems, IEEE Transactions on,* vol. 28, pp. 1470-1482, 2013.

[21] European Network of Transmission System Operators, "Network Code on Operational Security", 24-Sep-2013 [Online]. Available: http://www.acer.europa.eu/Official_documents/Acts_of_the_Agency/Annexes%20to%20ACER%20Recommendation%20092013%20on%20the%20NC%20on/The%20amended%20Network%20Code%20on%20Operational%20Security%20resubmitted%20on%2024%20September.pdf. [Accessed: 11-Oct-2015].

[22] G. Strbac and J. Mutale, "Framework and Methodology for Pricing of Distribution Networks with Distributed Generation - A report to OFGEM", Mar-2005 [Online]. Available: https://www.ofgem.gov.uk/ofgem-publications/44458/10147-strbacmutale.pdf. [Accessed: 11-Oct-2015].

[23] N. Hodge, "Power trip", 2010. [Online]. Available: http://www.agcs.allianz.com/assets/PDFs/GRD/GRD%20individual%20articles/Power_blackout_risks_article.pdf. [Accessed: 11-Oct-2015].

[24] T. Green et al., "Issues for Distribution System Operation at 2030", HubNet Position Paper, 11-May-2014. [Online]. Available: http://www.hubnet.org.uk/filebyid/523/2030GridOperation.pdf. [Accessed: 11-Oct-2015].

[25] OFGEM, UK, "Losses Incentive Mechanism", 2015. [Online]. Available: https://www.ofgem.gov.uk/electricity/distribution-networks/losses-incentive-mechanism. [Accessed: 11-Oct-2015].

[26] OFGEM, UK, "Decision on restatement of 2009-10 data and closing out the DPCR4 losses incentive mechanism", 21-Mar-2014. [Online]. Available: https://www.ofgem.gov.uk/ofgem-publications/86757/decisiononclosingoutdprc4lossesmechanism-mar-14.pdf. [Accessed: 11-Oct-2015].

[27] S. Civanlar, J. J. Grainger, H. Yin, and S. S. H. Lee, "Distribution feeder reconfiguration for loss reduction," *Power Delivery, IEEE Transactions on,* vol. 3, pp. 1217-1223, 1988.

[28] I. Roytelman and V. Ganesan, "Coordinated local and centralized control in distribution management systems," *Power Delivery, IEEE Transactions on,* vol. 15, pp. 718-724, 2000.

[29] R. S. Rao, K. Ravindra, K. Satish, and S. V. L. Narasimham, "Power Loss Minimization in Distribution System Using Network Reconfiguration in the Presence of Distributed Generation," *Power Systems, IEEE Transactions on,* vol. 28, pp. 317-325, 2013.

[30] A. Merlin and H. Back, "Search for a minimal-loss operating spanning tree configuration in an urban power distribution system," presented at the Proc. 5th Power System Computation Conference, Cambridge, 1975.

[31] K. Nara, A. Shiose, M. Kitagawa, and T. Ishihara, "Implementation of genetic algorithm for distribution systems loss minimum re-configuration," *Power Systems, IEEE Transactions on,* vol. 7, pp. 1044-1051, 1992.

[32] D. Das, "A fuzzy multiobjective approach for network reconfiguration of distribution systems," *Power Delivery, IEEE Transactions on,* vol. 21, pp. 202-209, 2006.

[33] J. Young-Jae, K. Jae-Chul, O. K. Jin, S. Joong-Rin, and K. Y. Lee, "An efficient simulated annealing algorithm for network reconfiguration in large-scale distribution systems," *Power Delivery, IEEE Transactions on,* vol. 17, pp. 1070-1078, 2002.

[34] Y. Yu and J. Wu, "Loads combination method based core schema genetic shortest-path algorithm for distribution network reconfiguration," in *Proceedings of Power System Technology Conference*, 2002, pp. 1729-1733, vol 3.

[35] A. Ahuja, S. Das, and A. Pahwa, "An AIS-ACO Hybrid Approach for Multi-Objective Distribution System Reconfiguration," *Power Systems, IEEE Transactions on,* vol. 22, pp. 1101-1111, 2007.

[36] C. Chao-Shun, T. Cheng-Ta, L. Chia-Hung, H. Wei-Lin, and K. Te-Tien, "Loading Balance of Distribution Feeders With Loop Power Controllers Considering Photovoltaic Generation," *Power Systems, IEEE Transactions on,* vol. 26, pp. 1762-1768, 2011.

[37] W. Cao, J. Wu, and N. Jenkins. "Feeder Load Balancing in MV Distribution Networks Using Soft Normally-Open Points,"in *IEEE Innovative Smart Grid Technologies Conference Europe,* 2014, PP 1-6.

[38] S. K. Bhattacharya and S. K. Goswami, "Distribution Network Reconfiguration Considering Protection Coordination Constraints," *Electric Power Components and*

Systems, vol. 36, pp. 1150-1165, 2008.

[39] S. Rahimi, M. Marinelli, and F. Silvestro, "Evaluation of requirements for Volt/Var control and optimization function in distribution management systems," in *IEEE International Energy Conference and Exhibition (ENERGYCON)*, 2012, pp. 331-336.

[40] F. A. Viawan and D. Karlsson, "Voltage and Reactive Power Control in Systems With Synchronous Machine-Based Distributed Generation," *Power Delivery, IEEE Transactions on*, vol. 23, pp. 1079-1087, 2008.

[41] H. E. Z. Farag, E. F. El-Saadany, and R. Seethapathy, "A Two Ways Communication-Based Distributed Control for Voltage Regulation in Smart Distribution Feeders," *Smart Grid, IEEE Transactions on*, vol. 3, pp. 271-281, 2012.

[42] L. Xiaohu, A. Aichhorn, L. Liming, and L. Hui, "Coordinated Control of Distributed Energy Storage System With Tap Changer Transformers for Voltage Rise Mitigation Under High Photovoltaic Penetration," *Smart Grid, IEEE Transactions on*, vol. 3, pp. 897-906, 2012.

[43] M. J. E. Alam, K. M. Muttaqi, and D. Sutanto, "A Multi-Mode Control Strategy for VAr Support by Solar PV Inverters in Distribution Networks," *Power Systems, IEEE Transactions on*, vol. 30, pp. 1316-1326, 2015.

[44] C. Joon-Ho and K. Jae-Chul, "Advanced voltage regulation method of power distribution systems interconnected with dispersed storage and generation systems," *Power Delivery, IEEE Transactions on*, vol. 16, pp. 329-334, 2001.

[45] F. Shahnia, M. T. Wishart, and A. Ghosh, "Voltage regulation, power balancing and battery storage discharge control by smart demand side management and multi-objective decision making," in *Power Engineering Conference (AUPEC), 2013 Australasian Universities*, 2013, pp. 1-5.

[46] N. Yorino, Y. Zoka, M. Watanabe, and T. Kurushima, "An Optimal Autonomous Decentralized Control Method for Voltage Control Devices by Using a Multi-Agent System," *Power Systems, IEEE Transactions on*, vol. 30, pp. 2225-2233, 2015.

[47] P. M. S. Carvalho, P. F. Correia, and L. A. F. Ferreira, "Distributed Reactive Power Generation Control for Voltage Rise Mitigation in Distribution Networks," *Power Systems, IEEE Transactions on*, vol. 23, pp. 766-772, 2008.

[48] A. Kulmala, S. Repo, Ja, x, and P. rventausta, "Coordinated Voltage Control in Distribution Networks Including Several Distributed Energy Resources," *Smart Grid, IEEE Transactions on*, vol. 5, pp. 2010-2020, 2014.

[49] P. N. Vovos, A. E. Kiprakis, A. R. Wallace, and G. P. Harrison, "Centralized and Distributed Voltage Control: Impact on Distributed Generation Penetration," *Power Systems, IEEE Transactions on*, vol. 22, pp. 476-483, 2007.

[50] M. R. Kleinberg, K. Miu, N. Segal, H. Lehmann, and T. R. Figura, "A Partitioning Method for Distributed Capacitor Control of Electric Power Distribution Systems," *Power Systems, IEEE Transactions on*, vol. 29, pp. 637-644, 2014.

[51] M. B. Liu, C. A. Canizares, and W. Huang, "Reactive Power and Voltage Control in Distribution Systems With Limited Switching Operations," *Power Systems, IEEE Transactions on*, vol. 24, pp. 889-899, 2009.

[52] M. A. Azzouz, M. F. Shaaban, and E. F. El-Saadany, "Real-Time Optimal Voltage

Regulation for Distribution Networks Incorporating High Penetration of PEVs," *Power Systems, IEEE Transactions on,* vol. 30, pp. 3234-3245, 2015.

[53] T. Senjyu, Y. Miyazato, A. Yona, N. Urasaki, and T. Funabashi, "Optimal Distribution Voltage Control and Coordination With Distributed Generation," *Power Delivery, IEEE Transactions on,* vol. 23, pp. 1236-1242, 2008.

[54] K. Young-Jin, A. Seon-Ju, H. Pyeong-Ik, P. Gi-Chan, and M. Seung-Il, "Coordinated Control of a DG and Voltage Control Devices Using a Dynamic Programming Algorithm," *Power Systems, IEEE Transactions on,* vol. 28, pp. 42-51, 2013.

[55] H. E. Z. Farag and E. F. El-Saadany, "A Novel Cooperative Protocol for Distributed Voltage Control in Active Distribution Systems," *Power Systems, IEEE Transactions on,* vol. 28, pp. 1645-1656, 2013.

[56] M. E. Baran and I. M. El-Markabi, "A Multiagent-Based Dispatching Scheme for Distributed Generators for Voltage Support on Distribution Feeders," *Power Systems, IEEE Transactions on,* vol. 22, pp. 52-59, 2007.

[57] M. E. Elkhatib, R. El-Shatshat, and M. M. A. Salama, "Novel Coordinated Voltage Control for Smart Distribution Networks With DG," *Smart Grid, IEEE Transactions on,* vol. 2, pp. 598-605, 2011.

[58] D. Divan, R. Moghe, and A. Prasai, "Power Electronics at the Grid Edge : The key to unlocking value from the smart grid," *Power Electronics Magazine, IEEE,* vol. 1, pp. 16-22, 2014.

[59] Scottish and Southern Energy, "technical Appendix 12 - Making Innovation Happen ", 2013. [Online]. Available: http://www.energyinnovationcentre.com/wp-content/uploads/SSEPD-Innovation-Strategy.pdf. [Accessed: 11-Oct-2015].

[60] C. Goodhand. "Ofgem - LCNF Tier 1 project: 33kV Superconducting Fault Current Limiter", 2015. [Online]. Available: https://www.ofgem.gov.uk/ofgem-publications/94151/33kvsfclfinalclosedownreportver10final-pdf. [Accessed: 11-Oct-2015].

[61] UK Power Networks, " Ofgem - LCNF Tier 2 project: Flexible Urban Networks Low Voltage", 2014 [Online]. Available: http://innovation.ukpowernetworks.co.uk/innovation/en/Projects/tier-2-projects/Flexible-Urban-Networks-Low-Voltage/Project-Documents/Overview+Flexible+Urban+Networks+Low+Voltage-+Jan+2014.pdf. [Accessed: 11-Oct-2015].

[62] M. McGranaghan, "Intelligent Universal Transformer Design and Applications", Jun-2009. [Online]. Available: http://www.cired.net/publications/cired2009/main_sessions/Session%201/Main%20Session%201%20pdfs/Block%201/S1%201032.pdf. [Accessed: 11-Oct-2015].

[63] D. J. Rogers and T. C. Green, "An Active-Shunt Diverter for On-load Tap Changers," *Power Delivery, IEEE Transactions on,* vol. 28, pp. 649-657, 2013.

[64] G. L. A. Ghosh, *Power Quality Enhancement Using Custom Power Devices*: Springer, 2002.

[65] Y. Pal, A. Swarup, and B. Singh, "A Review of Compensating Type Custom Power Devices for Power Quality Improvement," in *Power System Technology and IEEE*

Power India Conference, 2008, pp. 1-8.

[66] Scottish and Southern Energy, "OFGEM - LCNF Tier 1 Close-Down Report", 28-Feb-2013. [Online]. Available: https://www.ofgem.gov.uk/ofgem-publications/45826/sset1002-lv-monitoring-lcnf-t1-close-down-report-130228.pdf. [Accessed: 11-Oct-2015].

[67] J. M. Bloemink and T. C. Green, "Increasing distributed generation penetration using soft normally-open points," in *IEEE Power and Energy Society General Meeting*, 2010, pp. 1-8.

[68] J. M. Bloemink and T. C. Green, "Increasing photovoltaic penetration with local energy storage and soft normally-open points," in *IEEE Power and Energy Society General Meeting*, 2011, pp. 1-8.

[69] E. Romero-Ramos, *et al.*, "Assessing the loadability of active distribution networks in the presence of DC controllable links," *Generation, Transmission & Distribution, IET*, vol. 5, pp. 1105-1113, 2011.

[70] J. M. Bloemink and T. C. Green, "Benefits of Distribution-Level Power Electronics for Supporting Distributed Generation Growth," *Power Delivery, IEEE Transactions on*, vol. 28, pp. 911-919, 2013.

[71] N. Okada, M. Takasaki, H. Sakai, and S. Katoh, "Development of a 6.6 kV - 1 MVA Transformerless Loop Balance Controller," in *IEEE Power Electronics Specialists Conference*, 2007, pp. 1087-1091.

[72] M. Noroozian, L. Angquist, M. Ghandhari, and G. Andersson, "Use of UPFC for optimal power flow control," *Power Delivery, IEEE Transactions on*, vol. 12, pp. 1629-1634, 1997.

[73] M. Takeshita and H. Sugihara, "Effect of fault current limiting of UPFC for power flow control in loop transmission," in *IEEE Transmission and Distribution Conference and Exhibition 2002: Asia Pacific.*, 2002, pp. 2032-2036.

[74] M. Barragan, *et al.*, "Operational benefits of multiterminal DC-links in active distribution networks," in *IEEE Power and Energy Society General Meeting*, 2012, pp. 1-6.

[75] G. Fang and M. R. Iravani, "A Control Strategy for a Distributed Generation Unit in Grid-Connected and Autonomous Modes of Operation," *Power Delivery, IEEE Transactions on*, vol. 23, pp. 850-859, 2008.

[76] N. Okada, "Verification of Control Method for a Loop Distribution System using Loop Power Flow Controller," in *IEEE Power Systems Conference and Exposition*, 2006, pp. 2116-2123.

[77] A. Marano-Marcolini, E. Romero-Ramos, A. Gomez-Exposito, J. M. Maza-Ortega, and J. L. Martinez-Ramos, "Enhancing the integration of renewable sources in distribution systems using DC-links," in *IEEE Sustainable Alternative Energy (SAE) Conference*, 2009, pp. 1-5.

[78] M. A. Sayed and T. Takeshita, "All Nodes Voltage Regulation and Line Loss Minimization in Loop Distribution Systems Using UPFC," *Power Electronics, IEEE Transactions on*, vol. 26, pp. 1694-1703, 2011.

[79] J. M. Maza-Ortega, *et al.*, "Voltage source converter-based topologies to further

integrate renewable energy sources in distribution systems," *Renewable Power Generation, IET,* vol. 6, pp. 435-445, 2012.

[80] R. A. A. de Graaff, J. M. Myrzik, W. L. Kling, and J. H. R. Enslin, "Series Controllers in Distribution Systems - Facilitating Increased Loading and Higher DG Penetration," in *IEEE Power Systems Conference and Exposition*, 2006, pp. 1926-1930.

[81] R. A. A. de Graaff, J. M. A. Myrzik, W. L. Kling, and J. H. R. Enslin, "Intelligent Nodes in Distribution Systems - Optimizing Steady State Settings," in *Power Tech, 2007 IEEE Lausanne*, 2007, pp. 391-395.

[82] N. Flourentzou, V. G. Agelidis, and G. D. Demetriades, "VSC-Based HVDC Power Transmission Systems: An Overview," *Power Electronics, IEEE Transactions on,* vol. 24, pp. 592-602, 2009.

[83] S. G. Johansson., G. A. Splund., R. Jansson., and E. A. Rudervall., "Power system stability benefits with VSC dc-transmission systems," in *CIGRE* Paris, 2004, pp. 1-8.

[84] B. Jacobson, Y. Jiang-Hafner, G. A. P. Rey, M. Jeroense, A. Gustafsson, and M. Bergkvist, "HVDC with Voltage Source Converters and Extruded cables for up to +/- 300 kV and 1000 MW," in *CIGRE Sessions*, Paris, 2006, pp. 1-8.

[85] N. R. Chaudhuri, R. Majumder, B. Chaudhuri, and P. Jiuping, "Stability Analysis of VSC MTDC Grids Connected to Multimachine AC Systems," *Power Delivery, IEEE Transactions on*, vol. 26, pp. 2774-2784, 2011.

[86] J. M. Espi Huerta, J. Castello-Moreno, J. R. Fischer, and R. Garcia-Gil, "A Synchronous Reference Frame Robust Predictive Current Control for Three-Phase Grid-Connected Inverters," *Industrial Electronics, IEEE Transactions on,* vol. 57, pp. 954-962, 2010.

[87] I. J. Balaguer, L. Qin, Y. Shuitao, U. Supatti, and P. Fang Zheng, "Control for Grid-Connected and Intentional Islanding Operations of Distributed Power Generation," *Industrial Electronics, IEEE Transactions on,* vol. 58, pp. 147-157, 2011.

[88] L. G. B. Rolim, D. R. da Costa, and M. Aredes, "Analysis and Software Implementation of a Robust Synchronizing PLL Circuit Based on the pq Theory," *Industrial Electronics, IEEE Transactions on,* vol. 53, pp. 1919-1926, 2006.

[89] S. Cole, J. Beerten, and R. Belmans, "Generalized Dynamic VSC MTDC Model for Power System Stability Studies," *Power Systems, IEEE Transactions on*, vol. 25, pp. 1655-1662, 2010.

[90] B. Silva, C. L. Moreira, H. Leite, and J. A. Lopes, "Control Strategies for AC Fault Ride Through in Multiterminal HVDC Grids," *Power Delivery, IEEE Transactions on,* vol. 29, pp. 395-405, 2014.

[91] H. Nikkhajoei and R. H. Lasseter, "Microgrid Protection," in *IEEE Power Engineering Society General Meeting*, 2007, pp. 1-6.

[92] N. T. Stringer, "The effect of DC offset on current-operated relays," *Industry Applications, IEEE Transactions on,* vol. 34, pp. 30-34, 1998.

[93] M. E. Baran and F. F. Wu, "Optimal sizing of capacitors placed on a radial distribution system," *Power Delivery, IEEE Transactions on*, vol. 4, pp. 735-743, 1989.

[94] G. Daelemans, K. Srivastava, M. Reza, S. Cole, and R. Belmans, "Minimization of steady-state losses in meshed networks using VSC HVDC," in *IEEE Power & Energy*

Society General Meeting, 2009, pp. 1-5.

[95] M. J. D. Powell, "An efficient method for finding the minimum of a function of several variables without calculating derivatives," *The Computer Journal*, vol. 7, pp. 155-162, 1964.

[96] L. Cheng-Ling, C. Tai-Ning, L. Yuan-Yao, H. Pin, and R.-K. Lee, "Powell's method for designing optical multilayer thin-film filters," in *15th OptoeElectronics and Communications Conference*, 2010, pp. 388-389.

[97] S. Lazarou, V. Vita, and L. Ekonomou, "Application of powell's optimisation method for the optimal number of wind turbines in a wind farm," *Science, Measurement & Technology, IET*, vol. 5, pp. 77-80, 2011.

[98] H. Cho, A. D. Smith, and P. Mago, "Combined cooling, heating and power: A review of performance improvement and optimization," *Applied Energy*, vol. 136, pp. 168-185, 2014.

[99] M. E. Baran and F. F. Wu, "Network reconfiguration in distribution systems for loss reduction and load balancing," *Power Delivery, IEEE Transactions on*, vol. 4, pp. 1401-1407, 1989.

[100] UK Statutory Instruments, No. 2665, "The Electricity Safety, Quality and Continuity Regulations," 2002.

[101] M. A. Azzouz, M. F. Shaaban, and E. F. El-Saadany, "Real-Time Optimal Voltage Regulation for Distribution Networks Incorporating High Penetration of PEVs," *Power Systems, IEEE Transactions on*, vol. PP, pp. 1-12, 2015.

[102] A. E. Kiprakis and A. R. Wallace, "Maximising energy capture from distributed generators in weak networks," *Generation, Transmission and Distribution, IEE Proceedings-*, vol. 151, pp. 611-618, 2004.

[103] "IEEE Application Guide for IEEE Std 1547(TM), IEEE Standard for Interconnecting Distributed Resources with Electric Power Systems," *IEEE Std 1547.2-2008*, pp. 1-217,

Publications

Journal Paper:

[1] **W. Cao,** J. Wu, C. Wang, T. Green and N. Jenkins, “Operating Principle of Soft Open Points for Electrical Distribution Network Operation” *Applied Energy,* Vol. 164, pp 245-247, Feb. 2016. 10.1016/j.apenergy.2015.12.005

[2] **W. Cao**, J. Wu, C. Wang, T. Green and N. Jenkins, “Benefits Analysis of Soft Open Points for Electrical Distribution Network Operation” *Applied Energy,* Vol. 165, pp 36-47, Mar. 2016. 10.1016/j.apenergy.2015.12.022

Conference Paper:

[1] **W. Cao,** J. Wu, and N. Jenkins, “Feeder Load Balancing in MV Distribution Networks Using Soft Normally-Open Points," in IEEE PES Innovative Smart Grid Technologies (ISGT), Europe, 2014, PP 1-6.

[2] **W. Cao,** J. Wu, and Z. Huang, “Soft Open Points for Supply Restoration in Medium Voltage Distribution Networks” accepted for publication in IEEE PES Asia-Pacific Power and Energy Engineering Conference (APPEEC), Australia, 2015.

[3] A. Aithal, C. Long, **W. Cao**, J. Wu, “Impact of Soft Open Point on Feeder Automation” accepted for publication in IEEE ENERGYCON, Europe, 2016.

Appendix A: Data for the Two-Feeder Test Network

Table A.2 Network Parameters for the SOP study in Chapter 5

Feeder No.	From bus	To bus	Line Impedance parameters		Length (km)	load parameters at receiving buses	
			r (ohm/km)	x (ohm/km)		P (kW)	Q (kVar)
2	0	1	0.203	0.1034	1	60	25
2	1	2	0.2842	0.1447	1	60	25
2	2	3	1.059	0.9337	1	60	20
2	3	4	0.8042	0.7006	1	120	70
2	4	5	0.5075	0.2585	1	200	600
2	5	6	0.9744	0.963	1	150	70
2	6	7	0.3105	0.3619	1	210	100
2	7	8	0.341	0.5302	1	60	40
1	0	1	0.0922	0.047	1	100	60
1	1	2	0.493	0.2511	1	90	40
1	2	3	0.366	0.1864	1	120	80
1	3	4	0.3811	0.1941	1	60	30
1	4	5	0.819	0.707	1	60	20
1	5	6	0.1872	0.6188	1	200	100
1	6	7	0.7114	0.2351	1	200	100
1	7	8	1.03	0.74	1	60	20
1	8	9	1.044	0.74	1	60	20
1	9	10	0.1966	0.065	1	45	30
1	10	11	0.3744	0.1238	1	60	35
1	11	12	1.468	1.155	1	60	35
1	12	13	0.5416	0.7129	1	120	80

1	13	14	0.591	0.526	1	60	10
1	14	15	0.7463	0.545	1	60	20
1	15	16	1.289	1.721	1	60	20
1	16	17	0.732	0.574	1	90	40

Appendix B: Data for the Four-Feeder Test Network

Table B.3 Network Parameters for the Case study in Chapter 5

Feeder No.	From bus	To bus	Line Impedance parameters		Length (km)	Rated loading at receiving buses	
			r (ohm/km)	x (ohm/km)		P (kw)	Q (kvar)
1	0	1	0.55	0.4	1	228	171
1	1	2	0.55	0.4	1	273.6	79.8
1	2	3	0.55	0.4	1	112.5	124.26
1	3	4	0.55	0.4	1	171	228
1	4	5	0.55	0.4	1	79.8	273.6
1	5	6	0.55	0.4	1	256.5	124.26
1	6	7	0.55	0.4	1	228	171
1	7	8	0.55	0.4	1	163.2	68.6
2	0	1	0.55	0.4	1	196	147
2	1	2	0.55	0.4	1	235.2	68.6
2	2	3	0.55	0.4	1	220.5	106.82
2	3	4	0.55	0.4	1	147	196
2	4	5	0.55	0.4	1	68.6	235.2
2	5	6	0.55	0.4	1	235.2	68.6
2	6	7	0.55	0.4	1	196	147
2	7	8	0.55	0.4	1	235.2	68.6
2	8	9	0.55	0.4	1	196	147
2	9	10	0.55	0.4	1	343.2	100.1
3	0	1	0.55	0.4	1	286	214.5
3	1	2	0.55	0.4	1	321.75	155.87
3	2	3	0.55	0.4	1	307.2	100.1

3	3	4	0.55	0.4	1	100.1	343.2
3	4	5	0.55	0.4	1	214.5	286
3	5	6	0.55	0.4	1	55.2	68.6
4	0	1	0.55	0.4	1	196	147
4	1	2	0.55	0.4	1	235.2	68.6
4	2	3	0.55	0.4	1	220.5	106.82
4	3	4	0.55	0.4	1	147	196
4	4	5	0.55	0.4	1	235.2	68.6
4	5	6	0.55	0.4	1	220.5	106.82
4	6	7	0.55	0.4	1	235.2	68.6
4	7	8	0.55	0.4	1	111	196
4	8	9	0.55	0.4	1	106.82	220.5